

REVIEW

[View Article Online](#)  
[View Journal](#) | [View Issue](#)



Cite this: *Inorg. Chem. Front.*, 2020, 7, 3735

## Advances in ligand-unsupported argentophilic interactions in crystal engineering: an emerging platform for supramolecular architectures

Amanpreet Kaur Jassal <sup>a,b</sup>

Functionality of silver metal ions in coordination chemistry and in crystal engineering is one of the most important research topics. These compounds have been extensively examined thanks to their distinctive properties and various arrangements of structural designs, with the presence of important argentophilic interactions. Various compounds are useful both in the absence and presence of ligand-supported interactions, which are established to obtain appreciably diverse molecular/structural and physical/physicochemical characteristics from silver core-based compounds. In some cases, weak interactions have been seen to be useful for Ag–Ag contacts and in some cases, Ag–Ag contacts cooperate in the erection of a variety of interactions and result in topological variations in molecular structures. The outcomes of various developmental studies are appraised herein, focusing on molecular structural systems in which more than two silver cores are accessible at a close distance, supporting the required structural characterization. This review describes examples of various ligand-unsupported argentophilic interactions, emphasizing reticular design methods, synthetic approaches, and characterization techniques for these materials.

Received 21st April 2020,  
Accepted 24th June 2020

DOI: 10.1039/d0qi00447b  
[rsc.li/frontiers-inorganic](http://rsc.li/frontiers-inorganic)

<sup>a</sup>Schulich Faculty of Chemistry, Technion–Israel Institute of Technology, Haifa, Israel  
<sup>b</sup>Chemistry Department, Indian Institute of Technology Delhi, New Delhi, India.  
E-mail: amanpreetkaurjassal@gmail.com



Amanpreet Kaur Jassal

(DST-WOSA) at IIT Delhi. Her research interests include crystal engineering, polyoxometalates, metal–organic frameworks, and organometallic compounds. She has published more than 45 peer-reviewed international articles, with a h-factor of 13 and 433 citations.

## Introduction

In the last couple of decades, the study of argentophilic interactions<sup>1–8</sup> in silver chemistry is one of the most rapidly growing fields in crystal engineering and supramolecular chemistry.<sup>9–14</sup> Silver ions can participate in argentophilic interactions, even at distances little more than the sum of their van der Waals radii (3.44 Å),<sup>15</sup> maintaining angular specificities. From the literature survey, it has been found that weak argentophilic interactions are speculated to result in double bonds within a distance of 4.2 Å.<sup>16</sup> Strongly bridging counter anions, like carboxylate ions,<sup>17–22</sup> bridge silver atoms very strongly, with observed Ag–Ag distances as short as 2.778 Å.

Amid the weak bridging ions,  $\text{NO}_3^-$  ions<sup>2,23,24</sup> have shown more enhanced bridging capabilities than  $\text{ClO}_4^-$ ,  $\text{PF}_6^-$ , and  $\text{BF}_4^-$  anions.<sup>12,25–28</sup> These interactions can be manipulated by various types of ligands used for the construction of compounds with  $\text{Ag}^+$  ions. The nature of the ligand<sup>29</sup> has a noteworthy influence on the distance between silver atoms and the robustness of the argentophilic interactions. The role of the ligand in favoring and enforcing argentophilicity is vital, as shown by the large number of compounds containing “ligand-supported” interactions<sup>20,30–32</sup> in comparison with the rare “ligand-unsupported” examples (Table 1).<sup>33–37</sup> The above-mentioned interactions are distinguished in earlier reported data as either unsupported or supported, depending on the pres-

**Table 1** A description of coordination compounds with ligand-unsupported argentophilic interactions

No.	Compound	Geometry around Ag(I)	Ag...Ag (Å) (ligand-unsupported)	Description	Ref.
1.	$[\text{Ag(imid)}_2][\text{ClO}_4]$	Linear	3.051(1), 3.493(1)	—	1
2.	$[\text{Ag(pyrazole)}_3]$	Linear	3.414(5), 3.431(4)	—	10
3.	$[\text{Ag}_3(\text{INA})_2]\text{BF}_4$	—	2.969(5)–3.236(5)	—	11
4.	$[\text{Ag}_3(2-(3(5)-pz)\text{py})_3]_2\cdot 2\text{py}$	—	3.227, 3.655, 3.702	1D polymer	13
5.	$\text{Tl}[\text{Ag}(\text{CN})_2]$	Distorted square planar	3.110(3)	—	14
6.	$[\text{Ag}(2,4'\text{-bpy})]\text{ClO}_4$	Trigonal	3.153(6)	—	32
7.	$[\text{Ag}_2(\text{bsdab})_3]_n(\text{NO}_3)_2n$	Trigonal	2.934(2)	—	25
8.	$[\text{Ag}_2(\text{bsdab})_3]_n(\text{ClO}_4)_2n$	Trigonal	2.946(2)	3D network	25
9.	$[\text{Ag}(4,4'\text{-bpy})(\text{NO}_3)]$	Trigonal	2.977(1)	3D network	23
10.	$[\text{NBu}_4]_4[\text{Ag}_2\{\text{Mo}_5\text{O}_{13}(\text{OMe})_4(\text{NO})\}_2]$	—	2.873(2)	3D polymer	24
11.	$[\text{Ag}_2(\text{NH}_3)_2(\text{ntp})]_n$	—	3.110(7), 3.434(8)	2D sheet	17
12.	$[\text{Ag}_2(\text{NH}_3)(\text{ntp})]_n$	—	3.205	2D $4^4$ -sq1 net	17
13.	$[\text{Ag}_4(\text{NH}_3)_4(\text{ntp})_2\cdot \text{H}_2\text{O}]_n$	—	2.948(8)–3.301(10)	2D network	17
14.	$[\text{Ag}(4,4'\text{-bpy})]_n[\text{H}_2\text{PO}_4]_n\cdot [\text{H}_3\text{PO}_4]_n$	T-shaped	3.286(2)	3D network	47
15.	$[\text{Ag}_4(\text{tren}(\text{mim})_3)_2](\text{CF}_3\text{SO}_3)_4\cdot 2\text{H}_2\text{O}$	Distorted T-shaped	3.117(2)	1D polymer	57
16.	$[\text{Ag}_2(\mu\text{-dcpm})_2]\text{X}_2$ ( $\text{X} = \text{CF}_3\text{SO}_3^-$ , $\text{PF}_6^-$ )	T-shaped	2.907(1)–2.960(1)	Dimeric	12
17.	$[\text{Ag}_3(\text{py-hep})_2](\text{ClO}_4)_3\cdot 0.5\text{CH}_3\text{CN}$	T-shaped	3.179(1)	2D brick wall	65
18.	$[\text{Ag}(\text{bpp})]\text{ClO}_4$ , $[\text{Ag}(\text{bpp})]\text{PF}_6$	Linear	3.221(10), 3.085(9)	2D layer	26
19.	$\text{Ag}_2\text{C}_2\cdot 6\text{CF}_3\text{CO}_2\text{Ag}\cdot 3\text{CH}_3\text{CN}$	—	2.917(4)	2D network	48
20.	$[\text{Ag}_2(\text{ppa})_2\cdot(\text{ox})]\cdot 9\text{H}_2\text{O}$	T-shaped	3.202(1)	2D $\beta$ -sheet	3
21.	$[\{\text{Ag}(\text{H}_2\text{btc})_2\}\cdot\{\text{Ag}_2(\text{Hbtc})\}]_n$	Distorted trigonal	2.963(12)–3.278(8)	3D polymer	18
22.	$[\text{Ag}_4(3\text{-CP})_8(\text{SiF}_6)_2(\text{H}_2\text{O})_2]_n$	Distorted square planar	3.307(5), 3.024(6)	2D network	67
23.	$[\text{Ag}(\text{L})_2]\text{X}_2$ ( $\text{X}^- = \text{NO}_3^-$ , $\text{ClO}_4^-$ , $\text{PF}_6^-$ )	T-shaped	3.200(1)–3.670(1)	Discrete	27
24.	$[\{\text{Ag}_3(\text{INA})_2\}\text{NO}_3]_n$	—	3.096(7)	—	19
25.	$[\text{Ag(en)}\text{Ag}(\text{dnbc})_2]_n\cdot 2n\text{H}_2\text{O}$	—	3.177(4)	2D layer	68
26.	$[\text{Ag}_3(\text{l-3,5-Ph}_2\text{pz})_3]_2$	T-shaped	2.971(14)	—	69
27.	$[\text{Ag}(\text{NO}_2)(\text{BPDMs})]$	—	3.002(2)	2D sheet	31
28.	$[\text{Ag}_2(\text{ophen})_2]_2\cdot 6\text{H}_2\text{O}$	—	3.199	Dimer	70
29.	$[\text{Ag}_2(\text{obpy})_2]_2\cdot 4.5\text{H}_2\text{O}\cdot 0.5\text{DMF}$	—	3.023, 3.092	Dimer	70
30.	$[\text{Ag}_2(\text{obpy})_2]_3\cdot 18\text{H}_2\text{O}$	—	3.171, 3.173	Trimer	70
31.	$\{\{\text{Ag}_2(\text{BMIMB})_3\}(\text{BF}_4)_2\}$	Trigonal planar	3.062(4)	—	28
32.	$[\text{Ag}(2\text{-amp})_2(\text{tfa})]$	Trigonal-bipyramidal	3.007(4)	Dimer	71
		Square pyramidal			
33.	$[\text{Ag}(\text{rac-chxn})]\text{BF}_4$	T-shaped	3.110	2D network	72
34.	$\text{Ag(imidazolate)}$	T-shaped	3.159(5), 3.445(5)	2D network	4
35.	$\text{Ag(3-amp)OTf}$	T-shaped	3.182(4)	2D network	73
36.	$\text{Ag}_2(2,2'\text{-bpy})_2\cdot\mu\text{-}(3\text{-amp})(\text{tfa})_2$	Distorted square planar	3.058(3)	1D polymer	73
37.	$\text{Ag}_2(2,2'\text{-bpy})_2\cdot\mu\text{-}(3\text{-amp})(\text{OTf})_2$	T-shaped	3.085(3), 3.040(3)	Dimeric	73
38.	$\text{Ag}_2(5,5'\text{-bm-2,2'-bpy})_2(4\text{-amp})(\text{BF}_4)_2$	T-shaped	3.348(1)	Polymer	74
39.	$(\text{Ag(3-amp)}\text{BF}_4)_n$	—	3.289(1)	Polymer	30
40.	$\text{Ag}_2(2,2'\text{-bpy})_2\cdot\mu\text{-}(3\text{-amp})(\text{BF}_4)_2$	Trigonal pyramidal	2.988(4)	Dimeric	30
41.	$[\text{Ag(dach)}]_n(\text{NO}_3)_n$	T-shaped	3.233(4)	2D	75
42.	$[\text{Ag}_5(\text{CN})_5(2,2'\text{-bpy})_2]_n$	Distorted square planar	3.276(2)–3.342(2)	3D	46
43.	$[\{\text{Me}_4\text{N}\}\text{Ag}_3(\text{CN})_4]_n$	Distorted square planar	3.073(5), 3.149(5)	3D	46
44.	$[\text{Ag(pmtmb)}]_n$	—	3.336(11)	2D layer	20
45.	$\{\{\text{Ag}_2(\text{C}_{10}\text{H}_{14}\text{N}_4)\}_2\}(\text{ClO}_4)_2$	T-shaped	2.966(1)	1D	76
46.	$[\text{Ag(py)}_2]^+\text{X}^-$ ( $\text{X} = \text{ClO}_4^-$ , $\text{BF}_4^-$ , $\text{PF}_6^-$ )	Distorted square planar	2.960–3.000	1D	77
47.	$[\text{Ag}(\text{PCPA})(\text{PCPAH})(4,4'\text{-bpy})\text{H}_2\text{O}]_n$	T-shaped	3.209(13)	1D ladder	78
48.	$\{\{\text{Ag}(4,4'\text{-bpy})\}[\text{Ag}(\text{HSIP})\cdot(4,4'\text{-bpy})](\text{H}_2\text{O})_2\}_n$	—	3.473	2D network	79
49.	$[\text{Ag}_2(\text{H}_2\text{L}_3)_2(\text{HL}_4)_2]$	Distorted square planar	3.040(1)	Dimeric	80
50.	$\{\{\text{Ag}_2(\text{bpdc})(\text{bpp})(\text{H}_2\text{O})\}\cdot 2\text{H}_2\text{O}\}_n$	—	3.080, 3.170	3D network	21
51.	$\text{Ag}_2(4,4'\text{-py})_{1.5}\cdot(\text{dpa})(\text{H}_2\text{O})$	—	2.880	3D	82
52.	$[\text{Ag}(\text{SS-chxn})](\text{X})\cdot 1.5\text{H}_2\text{O}$	Trigonal pyramidal	3.002(8)	1D chain	83
53.	$[\text{Ag}_2(\text{dmt})_2(\text{suc})\text{H}_2\text{O}]_n$	Square planar, seesaw	3.106(15)	2D sheet	84
54.	$[\text{Ag}_2(\text{dmt})_2(\text{suc})(\text{H}_2\text{O})\cdot 0.5\text{H}_2\text{O}]$	Trigonal pyramidal	3.146(16)	2D polymer	84
55.	$[\text{Ag}(3\text{-PAH})_2]\cdot(\text{BF}_4)$	Distorted square planar	3.340	2D polymer	5
56.	$[\text{Ag}(3\text{-PAH})_2](\text{ClO}_4)\cdot\text{H}_2\text{O}$	Distorted square planar	3.340	2D polymer	5
57.	$[\text{Ag}(3\text{-PA})\cdot 1.5\text{H}_2\text{O}$	Square pyramidal	3.610	2D polymer	5
58.	$[\text{Ag}_2(\text{L}_1)_2\cdot\text{AgNO}_3]_\infty$	—	3.173(11)	2D network	6
59.	$[\text{Ag}_{1.5}(\text{apym})(\text{nta})_{0.5}]_n$	Trigonal pyramidal	3.020(3)	3D framework	7
60.	$\{\{\text{Ag}_4(\mu_4\text{-pzdc})_2(\mu\text{-en})_2\}\cdot\text{H}_2\text{O}\}_n$	—	3.096, 3.307	3D framework	8
61.	$\{\{\text{Ag}_3(\text{NMP})_6(\text{L}_1)_2\}\cdot 3(\text{ClO}_4)\}_\infty$	—	3.275(9)	3D	9

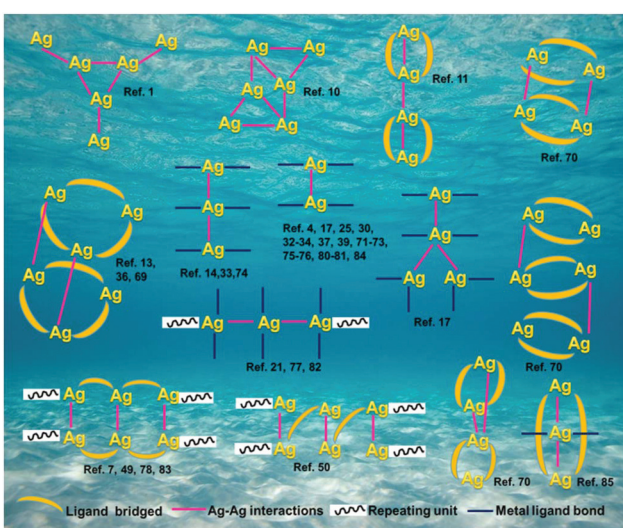
Table 1 (Contd.)

No.	Compound	Geometry around Ag <sup>+</sup>	Ag...Ag (Å) (ligand-unsupported)	Description	Ref.
62.	[Ag <sub>3</sub> (tbb) <sub>3</sub> (NH <sub>3</sub> ) <sub>2</sub> ] <sub>n</sub>	Square planar	3.028(14)–3.091(2)	1D chain	22
63.	Ag <sub>4</sub> L <sub>2</sub> (4,4'-bpy)(H <sub>2</sub> O) <sub>2</sub> ·6H <sub>2</sub> O	Square planar	3.087, 3.114	2D sheet	49
64.	[Ag(HL1)(OTf)] <sub>2</sub> ; [Ag(HL2)(OTf)] <sub>2</sub>	Square pyramidal	3.132(4)–3.263(7)	Dimer	39
65.	[Ag(Hdpma)][NO <sub>3</sub> ) <sub>2</sub> ·H <sub>2</sub> O	T-shaped	3.068(6)	2D polymer	50
66.	[Ag(dpma-NO)(NO <sub>2</sub> ) <sub>2</sub>	—	3.094(5)	1D chain	50
67.	[Ag(CH <sub>3</sub> CN) <sub>2</sub> CAg <sub>2</sub> (bis-MeOEtIm) <sub>2</sub> ][NO <sub>3</sub> ](BF <sub>4</sub> ) <sub>2</sub>	Trigonal pyramidal	2.823(4), 2.995(4)	Discrete	85
68.	[(AgL)ClO <sub>4</sub> ] & [(AgL)BF <sub>4</sub> ]	T-shaped	3.098(13)	2D and 3D	86
69.	[Ag <sub>2</sub> (Hssa)(daoc) <sub>n</sub>	—	3.131(11)	3D polymer	34
70.	[Ag(CF <sub>3</sub> SO <sub>3</sub> ) <sub>2</sub> OPPh <sub>2</sub> N(H)CMe <sub>3</sub> ] <sub>2</sub> {Ag(OPPh <sub>2</sub> N(H)CMe <sub>3</sub> ) <sub>2</sub> }SO <sub>3</sub> CF <sub>3</sub>	T-shaped and five coordinated	2.897(3)	Dimer	35
71.	[Ag <sub>6</sub> (HacacPz) <sub>6</sub> ]·2EtOH	T-shaped	2.906, 3.007	Dimer	36
72.	[Ag <sub>6</sub> (HacacPz) <sub>6</sub> ]·4EtOH	T-shaped	2.905	Dimer	36
73.	[Ag <sub>6</sub> (HacacPz) <sub>6</sub> ]·0.5DCM·1.5Et <sub>2</sub> O	T-shaped	2.912, 2.969	Dimer	36
74.	[(AgO <sub>2</sub> C <sub>2</sub> F <sub>3</sub> ) <sub>2</sub> ·L <sub>2</sub> ]	Trigonal pyramidal	2.943(2), 3.173(13)	Dimer	37
75.	[Cu(en) <sub>2</sub> ][Ag <sub>2</sub> (CN) <sub>3</sub> ][Ag(CN) <sub>2</sub> ]	Square planar	3.102	2D	33
76.	[Cu(dien)Ag(CN) <sub>2</sub> ] <sub>2</sub> [Ag <sub>2</sub> (CN) <sub>3</sub> ][Ag(CN) <sub>2</sub> ]	T-shaped	3.172	3D	33
77.	[AgNa(C <sub>5</sub> O <sub>5</sub> )(H <sub>2</sub> O) <sub>2</sub> ] <sub>n</sub>	—	3.170(2)	polymer	51
78.	{Fe(pmd)[Ag(CN) <sub>2</sub> ][Ag <sub>2</sub> (CN) <sub>3</sub> ]}	Square planar	2.980–3.020	3D	52
79.	{[Ni(f-rac-L)][Ag(CN) <sub>2</sub> ] <sub>n</sub>	T-shaped	3.048(1)	2D network	53
80.	[Ag <sub>5</sub> Zn <sub>2</sub> (tren) <sub>2</sub> (CN) <sub>9</sub> ]	Square planar	3.335(6)–3.376(7)	1D polymer	54
81.	[CuAg(CN) <sub>2</sub> (dien)] <sub>2</sub> [Ag(CN) <sub>2</sub> ][Ag <sub>2</sub> (CN) <sub>3</sub> ]	T-shaped	3.160–3.300	2D	87
82.	[Me <sub>4</sub> N] <sub>2</sub> [KAg <sub>3</sub> (CN) <sub>6</sub> ]	—	3.201(9)	2D network	88
83.	{[Ag <sub>7</sub> (H <sub>2</sub> biim) <sub>5</sub> ][PW <sub>11</sub> O <sub>39</sub> ]·Cl·H <sub>3</sub> O	Trigonal pyramidal	3.184(4)	2D network	55

ence or absence of any connectivity *via* ligands between the silver centers in the molecular system. In unsupported systems, the Ag–Ag contacts habitually signify a close approach between two or more independent molecular units and, therefore, the effects become less complicated to evaluate. By description, single and multiple systems of unsupported interactions are classified essentially as either self-regulating mono- or polynuclear entities (*i.e.*, intermolecular). Such ligand unsupported interactions (Scheme 1) are important in

supramolecular chemistry, even in the absence of other functionalities. The accumulation of the constituents could appear at first glance, to be solely examined based on intermolecular Ag–Ag contacts. This topic has been a matter of some debate thanks to the scarcity of unambiguous experimental evidence showing silver aggregates that are stable in the absence of stabilizing ligands.<sup>38</sup> It has been noticed that even in the absence of ligand bridging *via* conventional electron-pair bonding, the Ag<sup>+</sup>–Ag<sup>+</sup> interactions might not be “unsupported” in every condensed phase.

Numerous ubiquitous weak forces, like H-bonding,  $\pi$ – $\pi$  stacking, ion–ion, dipole–dipole, and ion–dipole attractive interactions, have been established to exist between ligands, distinctly manipulating the mode of aggregation and determining the Ag–Ag distance between components.<sup>39</sup> The construction of multidimensional frameworks with metal–metal interactions, especially within monovalent coinage metal (Ag, Au, and Cu) based systems, is a viable design approach for the rise of dimensionality or the enrichment of supramolecular topology, according to previous work. The strengths of the argentophilic interactions<sup>40–45</sup> have an order of magnitude comparable to that of H-bonding interactions, suggesting that they could be a useful tool for strengthening the intended frameworks.<sup>46</sup> In this review, the literature pertaining to ligand-unsupported homometallic<sup>47–50</sup> and bimetallic metallophilic contacts<sup>33,51–54</sup> between silver atoms and in polyoxometalate-based compounds<sup>55,56</sup> is decisively presented (Table 1). There is a wealth of data relating to discrete compounds,<sup>12</sup> and dimeric<sup>10,13</sup> and polymeric<sup>17,26,46,57</sup> structures, including diverse geometries around Ag<sup>+</sup> ions.



**Scheme 1** Various examples of ligand-unsupported argentophilic interactions reported in the literature relating to the crystal engineering of supramolecular coordination polymers.

The literature around polyoxometalate-cluster-based compounds containing ligand-unsupported argentophilic interactions has been summarized as a subtopic as part of a broader review. This review aims to give a concise overview focused on recent developments relating to advanced synthetic strategies for noncovalent interactions, highlighting weak to strong interactions and other aspects for improving the qualities of these compounds. The last part of this article will address theoretical evidence, the spectroscopic characterization of relevant compounds, and the roles of other supporting interactions in the formation of extended networks.

## Early observations

Earlier, the 1984 edition of “Structural Inorganic Chemistry” divulged fewer than half a dozen compounds where astonishingly close Ag–Ag contact exists had been scrutinized, suggesting that “some metal–metal interaction” studies had been published.<sup>58</sup> Martin Jansen, in 1987, published the first review explaining the influence of  $d^{10}$ – $d^{10}$  interactions on the structures and properties of compounds and recapitulated the experimental support for plausible metal–metal bonding interactions with a “closed-shell” electronic configuration.<sup>59</sup> Later, Pyykko *et al.*, in 1994,<sup>60</sup> introduced the term “metalophilicity” for metal–metal interactions in a broad sense, involving silver, gold, mercury, copper, platinum, palladium, *etc.* Progress in silver coordination chemistry research incited the introduction of descriptive terminology for Ag–Ag interactions.<sup>61–63</sup> The terms ‘argentophilicity’ and ‘argentophilic bonding or interactions’ were proposed, based on the Latin word “argentum” and not the Greek word “argyros”, to describe various kinds of Ag–Ag interactions within silver compounds. In the current literature, it has emerged as a general concurrence that argentophilic interactions must be considered as present in all molecular and crystal structures where two or more low-coordinated silver metal ions appear in groups with van der Waals radii between two silver atoms shorter than *ca.* 3.44 Å. In the last few decades, argentophilic interactions have been differentiated on the basis of the absence or presence of any ligand connectivity between silver metal ions. In unsupported cases, the Ag–Ag interactions habitually represent the closest approach between independent molecular units and, therefore, it is easier to appraise their existence in terms of short Ag–Ag contacts between two atoms in molecules within multi-dimensional systems, as compared to ligand-supported compounds. The appraisal of the significance of any supported argentophilic contacts made only on the basis of distance is more difficult because the structural requirements of the ligand may enforce either shortened or elongated Ag–Ag contacts. Wherever possible, most of the time, experimental or theoretical attempts to estimate the structural and energy characteristics of argentophilic interactions have tried to rely on cases of unsupported contacts. These unsupported interactions are particularly relevant in the area of supramolecular chemistry, where other functionalities are absent and the

aggregation of components may seem at first glance to be solely determined by intermolecular Ag–Ag contacts.

In the early eighties, Symons, Russell, and coworkers<sup>1</sup> successfully synthesized the silver-imidazole perchlorate **1**. The basic structural unit has crystallographic  $D_3$  symmetry and consists of six linear  $[\text{Ag(imid)}_2]^{2+}$  cations and six  $[\text{ClO}_4]^-$  anions. The crystal structure reveals the presence of a planar  $(\text{Ag}^+)_6$  cluster, in which three radiating pairs of  $\text{Ag}^+$  ions, 3.051(1) Å apart, are located at the corners of an equilateral triangle, with the inner  $\text{Ag}^+$  ions being 3.493(1) Å apart (Fig. 1). There are two of these hexameric units in the rhombohedral unit cell, but there are no other Ag–Ag contacts with distances of less than 5 Å.

In 1994, Sironi and coworkers synthesized the trimeric compound  $[\text{Ag(pyrazole)}]_3$  (pz = pyrazole), **2**, which was solved about the crystallographic 2-fold axis in the  $Pbcn$  space group and acquires idealized  $D_{3h}$  symmetry. It consists of an almost regular triangle (Fig. 2) of non-bonded silver atoms ( $\text{Ag1–Ag2} = 3.414(5)$  Å and  $\text{Ag2–Ag2F} = 3.431(4)$  Å), whose sides are bridged by pyrazolato groups, in a plane running parallel to the crystallographic  $c$  direction.<sup>10</sup>

In 1998, Burrows and coworkers performed the reaction of  $\text{AgBF}_4$  with isonicotinic acid (HINA), leading to the formation

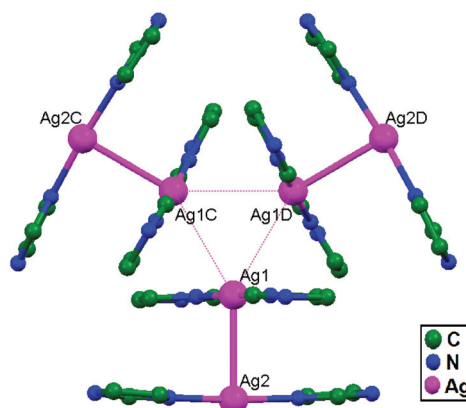


Fig. 1 The hexamer unit made of  $[\text{Ag(imid)}_2]^{2+}$  cations in **1**, viewed along the crystallographic three-fold axis. There is a two-fold axis along each  $\text{Ag}^+-\text{Ag}^+$  vector, and hydrogen atoms are removed for clarity.

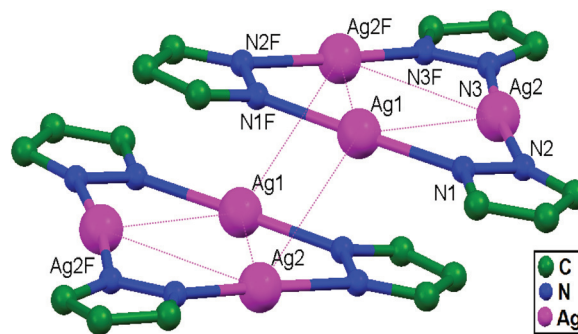


Fig. 2 The structure of  $[\text{Ag(pz)}]_3$ , **2**; two adjacent units are shown, and the hydrogen atoms are removed.

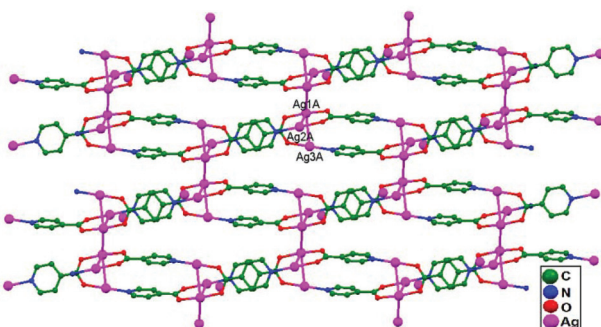


Fig. 3 A polymeric chain of **3** with Ag–Ag contacts; hydrogen atoms and tetrafluoroborate anions are omitted for clarity.

of an unusual polymeric structure  $[\text{Ag}_3(\text{INA})_2]\text{BF}_4$ , **3**, consisting of  $\text{Ag}_3$  triangles ( $\text{Ag}-\text{Ag} = 2.969(5)$ – $3.236(5)$  Å) linked together *via* two isonicotinic ligands (Fig. 3). This coordination polymer consists of both bridged and unbridged short Ag–Ag contacts. The fact that the two unsupported contacts are longer than those supported by bridged carboxylate suggests that the ligands do have a significant effect on  $\text{Ag}^+$ – $\text{Ag}^+$  separation.<sup>11</sup>

In the year 1997, the reaction between  $\text{Ag}(\text{O}_3\text{SCF}_3)$  and 2-[3(5)-pyrazolyl]pyridine anions was performed by Stavropoulos and coworkers, yielding colorless, light-sensitive rods of  $[\text{Ag}_3(2-(3(5)-\text{pz})\text{py})_3]_2\text{2py}$  (where pz = pyrazolyl; and py = pyridine), **4**. With the help of this compound, the authors succeeded in presenting strong evidence of Ag–Ag contacts that have possibly managed to survive without any supportive bridging ligand. The  $\text{Ag1-Ag3}$  (3.227 Å),  $\text{Ag1-Ag2}$  (3.655 Å), and  $\text{Ag2B-Ag3}$  (3.702 Å) interactions (Fig. 4) demonstrate the existence of 1D chain structures through unsupported Ag–Ag contacts, which are somewhat masked by the existing coulombic interactions.<sup>13</sup>

In 1998, Patterson and coworkers synthesized  $\text{Tl}[\text{Ag}(\text{CN})_2]$ , **5**, which consists of three crystallographically inequivalent Ag sites in the unit cell (Fig. 5) with a Ag–Ag distance of 3.110 Å. The  $\text{Ag}(\text{CN})_2^-$  ions are stacked in two patterns throughout the crystal structure, in which Ag1 is present on the inversion center of one pattern and Ag2 is present on the inversion center of other pattern. The stacking in the Ag1 environment

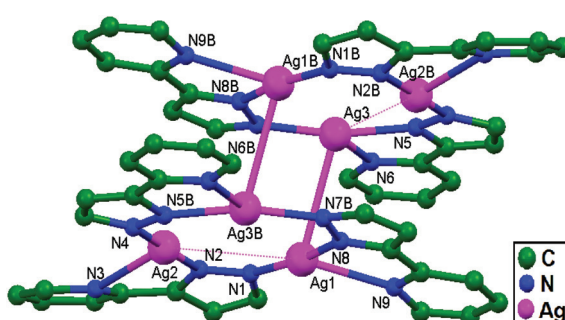


Fig. 4 A molecular pair from  $[\text{Ag}_3(2-(3(5)-\text{pz})\text{py})_3]_2\text{2py}$ , **4**, in which ligand-unsupported Ag–Ag contacts are clearly shown. Hydrogen atoms and pyridine molecules in the lattice are omitted.

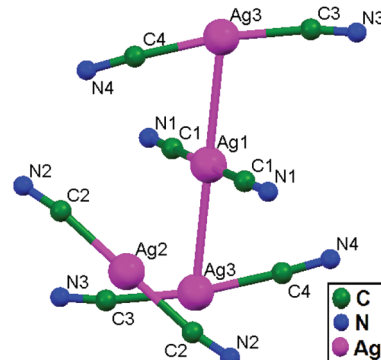


Fig. 5 The compound  $\text{Tl}[\text{Ag}(\text{CN})_2]$ , **5**, showing three crystallographically distinct silver atom sites with ligand-unsupported argentophilic interactions.

results in a trimer of interacting  $\text{Ag}(\text{CN})_2^-$  ions with a linear arrangement of the three silver atoms. The Ag1 atom is surrounded by two opposite images of Ag3 in this environment, with an Ag1–Ag3 contact distance of 3.110(3) Å. The other stacking pattern is observed in the Ag2 environment and can be described as a pentamer of  $\text{Ag}(\text{CN})_2^-$  ions with distorted square planar geometry. Ag–Ag contact distances of 3.528(3) and 3.899(1) Å are present between the central Ag2 atom and each of the opposite images of Ag3 and Ag1 terminal atoms, respectively. The Ag–Ag interactions in  $\text{Tl}[\text{Ag}(\text{CN})_2]$  are ligand-unsupported, suggesting that argentophilicity is likely important in coordination compounds of  $\text{Ag}^+$  ions, in a similar way to aurophilicity in  $\text{Au}^+$ -based compounds.<sup>14</sup>

In 1998, Chen and coworkers prepared the compound  $[\text{Ag}(2,4'\text{-bpy})]\text{ClO}_4$  (where 2,4'-bpy = 2,4'-bipyridine), **6**, in which the helical  $[\text{Ag}(2,4'\text{-bpy})]_{\infty}$  chains are racemic, surrounded by perchlorate counter ions. The  $\text{Ag}^+$  ion is linked to two nitrogen atoms from 2,4'-bpy groups from two different ligands in addition to the oxygen atom of the counter ion. Adjacent helical chains (Fig. 6) are linked *via* weak ligand-unsupported

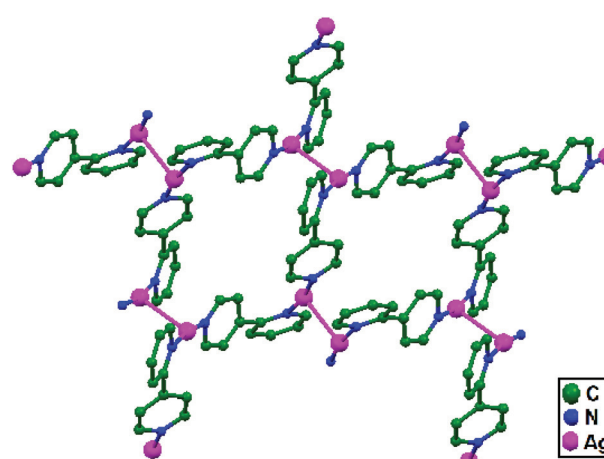


Fig. 6 Ligand-unsupported argentophilic interactions forming helical chains in **6**, resulting in a 2D network; perchlorate counter ions and hydrogen atoms are removed.

Ag–Ag (3.153(6) Å) interactions, resulting in an open 2D network with compressed hexagons as building units. This symbolizes a structural example of the presence of asymmetric cavities in a non-interpenetrating network. The  $\text{Ag}^+–\text{ClO}_4^-$  bond is a relatively weak bond, but its weak nature probably contributes to the strength of the Ag–Ag interaction, which presumably stabilizes the crystal structure.<sup>32</sup>

In 1999, Chen and coworkers synthesized the novel 3D non-interpenetrating networks  $[\text{Ag}_2(\text{bsdab})_3]_n(\text{NO}_3)_{2n}$ , **7**, and  $[\text{Ag}_2(\text{bsdab})_3]_n(\text{ClO}_4)_{2n}$ , **8**, ( $\text{bsdab} = N,N'$ -bis(salicylidene)-1,4-diaminobutane) in which bis-monodentate phenol groups of a Schiff base ligand serve as bridging units.<sup>25</sup> Each silver atom is coordinated by three phenol groups from three bsdab ligands in an unusual perfect trigonal arrangement (Fig. 7). Each pair of adjacent centrosymmetrically related  $\text{Ag}^+$  ions is joined by a ligand-unsupported Ag–Ag bond (2.934(2) Å); this bond lies on a crystallographic threefold axis and the 3D network consists of rhombohedral building blocks. In the rhombohedron, each top site is occupied by a pair of ligand-unsupported  $\text{Ag}^+$  ions, which is surrounded by six phenol groups.

Network **8** is isomorphous to **7**, and the structural parameters are very similar. The Ag–Ag distances (2.934(2) Å in **7** and 2.946(2) Å in **8**) are similar to the ligand-unsupported Ag–Ag distance (2.977(1) Å) in the 3D polymer  $[\text{Ag}(4,4'-\text{bpy})(\text{NO}_3)]$ .<sup>23,24</sup> These distances are well below the summation of the van der Waals radii of two silver atoms (3.44 Å) and are very close to the Ag–Ag separation in silver metal (2.89 Å),<sup>2</sup> which suggests significant Ag–Ag bonding. In the compound  $[\text{NBU}_4]_4[\text{Ag}_2\{\text{Mo}_5\text{O}_{13}(\text{OMe})_4(\text{NO})\}_2]$ , a shorter ligand-unsupported Ag–Ag bond (2.873(2) Å) is reported, where the bridging polyoxoanions most probably play a role in fixing the Ag–Ag separation.<sup>24</sup> It is noteworthy that, neglecting the Ag–Ag interactions, the frames of **7** and **8** are formed by 2D highly undulated simple layers of (6,3) topology that catenate in a parallel fashion to give a 3D overall network, instead of the usual 2D one.

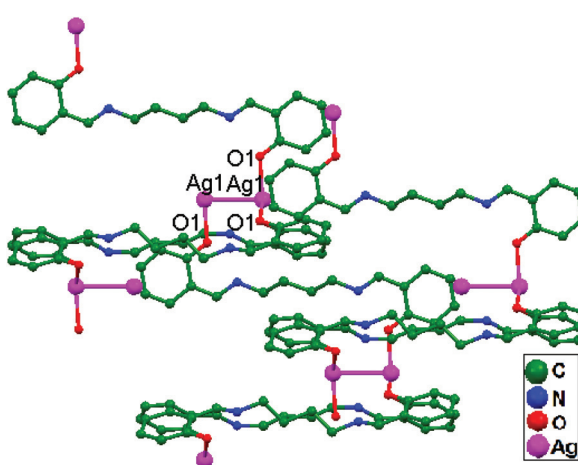


Fig. 7 The coordination environment of silver atoms in  $[\text{Ag}_2(\text{bsdab})_3]_n(\text{NO}_3)_{2n}$ , **7**; ligand-unsupported argentophilic interactions form a 3D network consisting of rhombohedral building blocks.

## Ligand-unsupported argentophilic interactions in homometallic compounds

In conventional chemistry relating to crystals, simple unsupported examples of  $[\text{H}_3\text{N}-\text{Ag}-\text{NH}_3]^+\text{X}^-$  salts have originated, with a variety of examples. In all related cases identified to date, with different  $\text{X}^-$  anions, the cations combine to form chains *via* Ag–Ag contacts (distances in the range of 2.910 to 3.110 Å) with linearity for Ag–Ag–Ag assembly.  $[\text{H}_3\text{N}-\text{Ag}-\text{NH}_3]^+$  cations have also been found to attach *via* argentophilic contacts to  $\text{Ag}^+$  ions engaged with other sets of ligands. Sun and coworkers, in 2013, synthesized and structurally characterized new  $\text{Ag}^+$ -ion-based coordination polymers based on 3-nitrophthalic acid ( $\text{H}_2\text{npt}$ ), namely  $[\text{Ag}_2(\text{NH}_3)_2(\text{npt})]_n$ , **9**,  $[\text{Ag}_2(\text{NH}_3)(\text{npt})]_n$ , **10**, and  $[\text{Ag}_4(\text{NH}_3)_4(\text{npt})_2\cdot\text{H}_2\text{O}]_n$ , **11**.<sup>17</sup> Compound **9** shows a 1D chain of binuclear silver atom based secondary building units, in which  $[\text{Ag}(\text{NH}_3)_2]^+$  is connected on two sides of this chain (Fig. 8a) through ligand-unsupported argentophilic interactions ( $\text{Ag1–Ag2} = 3.110(7)$  Å). Another ligand-unsupported weak Ag–Ag interaction ( $\text{Ag2–Ag2} = 3.434(8)$  Å) extends the 1D chain into a 2D sheet-like structure. The interesting point about this compound is the existence of a silver wire of  $-\text{Ag1–Ag1–Ag2–Ag2–}$  repeating units in a 2D sheet with an alternating arrangement of diverse Ag–Ag inter-

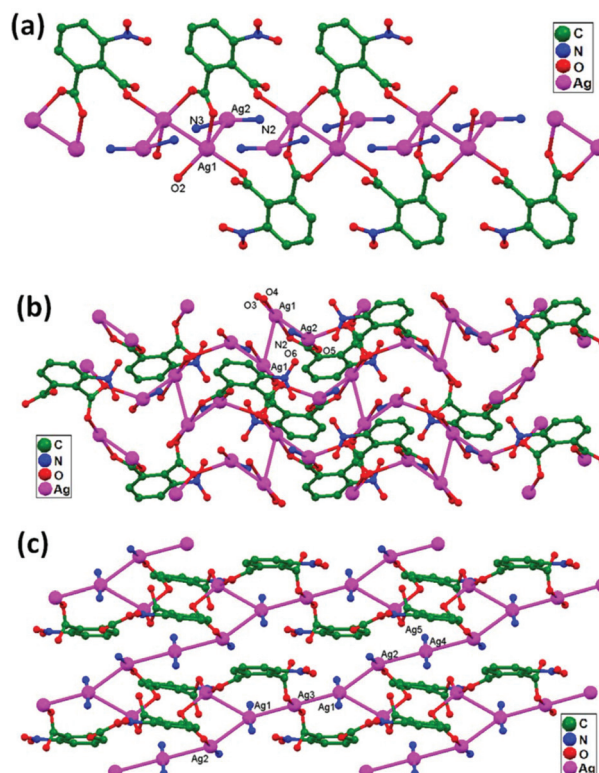


Fig. 8 (a) The formation of a 1D chain in **9** and the ligand-unsupported argentophilic interactions between  $\text{Ag1}$  and  $\text{Ag2}$  atoms, (b) the 2D  $4^4$ -sq net in **10**, and (c) the 2D silver net in **11**, formed from purely ligand-unsupported Ag–Ag contacts.

actions. Compound **10** is a 2D 4<sup>4</sup>-sql net constructed from npt ligand bridged centrosymmetric Ag<sub>4</sub> rhombus secondary building units, in which the Ag–Ag contact (3.205 Å) is a ligand-unsupported interaction (Fig. 8b). In compound **11**, all neighboring two-coordinated Ag<sup>+</sup> ions propagate to form an infinite 1D silver wire with the arrangement of –Ag3–Ag1–Ag2–Ag2–Ag2–Ag1–Ag3– through purely ligand-unsupported Ag–Ag interactions (Ag1–Ag2 = 3.019(11) Å, Ag1–Ag3 = 2.948(8) Å, and Ag4–Ag2 = 3.092(8) Å). Moreover, Ag5 is established between adjacent 1D silver wires and furnishes another three ligand-unsupported argentophilic interactions, with Ag–Ag contact distances in the range of 3.128(12)–3.301(10) Å, extending the 1D silver wires to a 2D silver net (Fig. 8c).

Kraus and coworkers gave examples of novel compounds with unsupported Ag–Ag interactions between silver atoms with higher coordination numbers. Ag–Ag contacts with smaller distances are established between silver atoms of the [Ag<sub>2</sub>(NH<sub>3</sub>)<sub>8</sub>]<sup>2+</sup> units in [ZrF<sub>6</sub>]<sup>2-</sup> and [HfF<sub>6</sub>]<sup>2-</sup>-ion-based salts. Two quasi-tetrahedral [Ag(NH<sub>3</sub>)<sub>4</sub>]<sup>+</sup> units are highly flattened in this compound and mutual approach between these two units gave Ag–Ag distances of 3.122(5)–3.141(9) Å.<sup>64</sup> Chen and coworkers, in the year 2000, reported a ladder motif of [Ag(4,4'-bpy)]<sub>nfinity</sub> (4,4'-bpy = 4,4'-bipyridine) side pieces that were crystallographically documented in [Ag(4,4'-bpy)]<sub>n</sub>[H<sub>2</sub>PO<sub>4</sub>]<sub>n</sub>·[H<sub>3</sub>PO<sub>4</sub>]<sub>n</sub>, **12**, synthesized from the self-assembly of silver(I) salt with 4,4'-bpy.<sup>47</sup> The crystal structure consists of molecular ladders with [Ag(4,4'-bpy)]<sub>nfinity</sub> and ligand-unsupported Ag–Ag contacts, H<sub>2</sub>PO<sub>4</sub><sup>-</sup> counter ions, and H<sub>3</sub>PO<sub>4</sub> molecules. Each Ag<sup>+</sup> ion in T-shaped coordination geometry is coordinated with two 4,4'-bpy units; each pair of [Ag(4,4'-bpy)]<sub>nfinity</sub> chains is linked into a 1D molecular ladder *via* ligand-supported Ag–Ag interactions with a separation of 3.286 (2) Å (Fig. 9). These 1D ladders are gathered into a layered structure, which is organized in an auxiliary fashion by a H-bonded 3D network with the help of counter ions (H<sub>3</sub>PO<sub>4</sub>) and water molecules.

In the year 2000, Chen and coworkers prepared the compound [Ag<sub>4</sub>(tren(mim)<sub>3</sub>)<sub>2</sub>](CF<sub>3</sub>SO<sub>3</sub>)<sub>4</sub>·2H<sub>2</sub>O (where tren(mim)<sub>3</sub> = tris{2-[2-(1-methyl)imidazolyl] methyliminoethyl}amine), **13**, which consists of discrete tetranuclear [Ag<sub>4</sub>(tren(mim)<sub>3</sub>)<sub>2</sub>]<sup>4+</sup> cations, trifluoromethanesulfonate anions, and water molecules, where two ligands encapsulate four Ag<sup>+</sup> ions in an interlocking fashion.<sup>57</sup> One arm of each tren(mim)<sub>3</sub> component

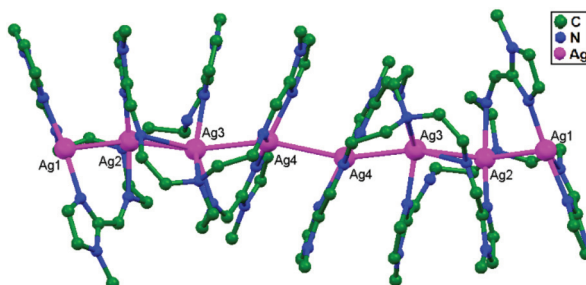


Fig. 10 A perspective view showing a dimeric form of [Ag<sub>4</sub>(tren(mim)<sub>3</sub>)<sub>2</sub>]<sup>4+</sup> cations in **13** connected by weak ligand-unsupported Ag–Ag interactions.

uses its imine and imidazole nitrogen atoms to bind Ag1 (or Ag4) in bidentate chelate mode; the second arm bridges Ag1 and Ag2 using its imidazole and imine nitrogen atoms; and the third arm links to Ag3 using its imidazole nitrogen atom as a unique donor. A couple of tetranuclear cations unite to form an octanuclear cation *via* ligand-unsupported contacts between two Ag<sup>+</sup> ions (Ag4–Ag4 = 3.117(2) Å) belonging to different tetranuclear cations. Although the Ag4–Ag4a distance is relatively long, it is comparable to other ligand-supported metallophilic separations.<sup>20,30–32</sup> Since the four imidazole rings ligated to Ag4 and Ag4 are arranged in an off-set fashion, there are no significant  $\pi$ – $\pi$  interactions between imidazole groups from different tetramers (Fig. 10). Each Ag<sup>+</sup> ion is coordinated in distorted T-shaped geometry, connected with a five-membered chelate ring; the metallic chain thus adopts a zigzag fashion with Ag–Ag–Ag angles in the range of 116.44(3)–156.83(4)°.

Che, Phillips, and coworkers performed a reaction between stoichiometric amounts of Ag(O<sub>2</sub>CCF<sub>3</sub>) and tricyclohexylphosphine (PCy<sub>3</sub>) in dichloromethane to afford crystals of [Ag<sub>2</sub>( $\mu$ -dcpm)<sub>2</sub>]X<sub>2</sub> (X = CF<sub>3</sub>SO<sub>3</sub>: **14**, PF<sub>6</sub>: **15**; dcpm = bis(dicyclohexylphosphino)methane) upon recrystallization from dichloromethane/*n*-hexane. Ag<sub>2</sub>P<sub>4</sub>C<sub>2</sub> cores are present in the molecular structures of **14** and **15** (Fig. 11), adopting chair conformations; ligand-unsupported Ag–Ag separations of 2.936(1) and 2.960(1) Å are observed in **14** and separations of 2.907(1) and 2.938(1) Å are observed in **15**.<sup>12</sup>

In 2001, Sun and coworkers reported the assembly of a flexible tetradentate ligand, namely 1,7-bis(4'-pyridyl)-2,6-diazaheptane (py-hep), with AgClO<sub>4</sub>·H<sub>2</sub>O, giving rise to a fascinating 2D brick-wall network of the compound [Ag<sub>3</sub>(py-hep)<sub>2</sub>](ClO<sub>4</sub>)<sub>3</sub>·0.5CH<sub>3</sub>CN, **16**. The network comprises Ag<sup>+</sup> ions with trigonal and linearly coordinated geometries. In the cationic part of the structure, three Ag<sup>+</sup> ions and two ligands are present in the repeating unit, and dissimilar coordination behaviors have shown around the two- and three-coordinate Ag<sup>+</sup> ions. Both Ag1 and Ag2 are coordinated three-fold by two NH groups from py-hep and one pyridine group from another py-hep, with Ag–N distances in the range of 2.234(5)–2.374(5) Å. The atom Ag3 is coordinated two-fold by two nitrogen atoms from pyridine, with an Ag–N distance of 2.108(6) Å. It is clear that each Ag<sup>+</sup> ion is coordinated by two different py-hep

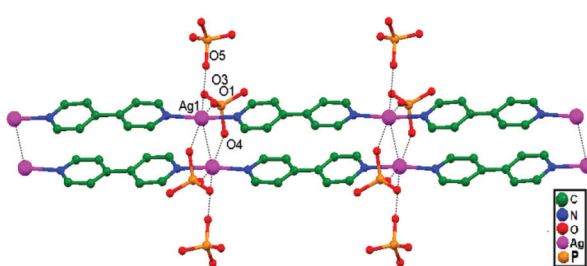


Fig. 9 The rectangular unit in **12**; hydrogen atoms and lattice water molecules are omitted.

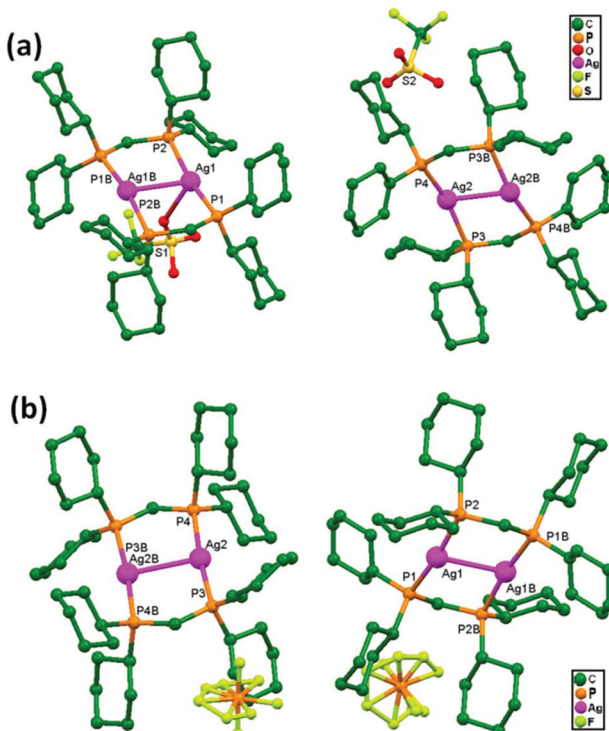


Fig. 11 Perspective views of  $[\text{Ag}_2(\mu\text{-dcpm})_2]\text{X}_2$  (where  $\text{X} = \text{CF}_3\text{SO}_3$  for (a) and  $\text{PF}_6$  for (b)); the anions  $\text{CF}_3\text{SO}_3$  and  $\text{PF}_6$  are present in the lattices of compounds **14** and **15**, respectively.

entities and, in turn, each py-hep ligand connects three  $\text{Ag}^+$  ions (Fig. 12). The distance of  $3.179(1)$  Å between  $\text{Ag}3$  and  $\text{Ag}3\text{B}$  indicates the existence of weak ligand-unsupported  $\text{Ag}-\text{Ag}$  metal interactions, which are responsible for the generation of a polymeric network.<sup>65</sup>

Wang and coworkers, in the same year, reported the assembly of  $[\text{Ag}(\text{bpp})]\text{ClO}_4$ , **17**, and  $[\text{Ag}(\text{bpp})]\text{PF}_6$ , **18** (where bpp = 1,3-bis(4-pyridyl)propane), two coordination polymers with novel and distinct cationic network structures. In their research paper, the authors described well the irreversible conversion of **17** into **18** upon treatment with  $\text{NaPF}_6$ . This conversion is unique because it is driven by the formation of stronger  $\text{Ag}-\text{Ag}$  bonds in the polymeric cation, which are absent in the silver(I)-based coordination polymers described above. In both

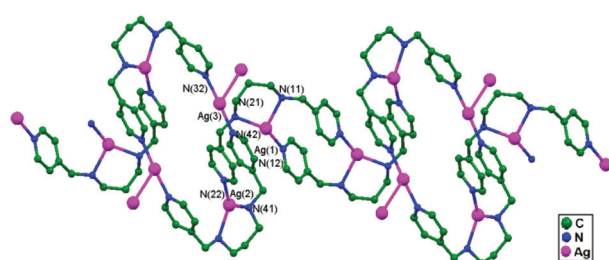


Fig. 12 The coordination environment of two-coordinate  $\text{Ag}^+$  ions in  $[\text{Ag}_3(\text{py-hep})_2](\text{ClO}_4)_3 \cdot 0.5\text{CH}_3\text{CN}$ , **16**, and the formation of a brick-wall network via weak ligand-unsupported  $\text{Ag}-\text{Ag}$  interactions.

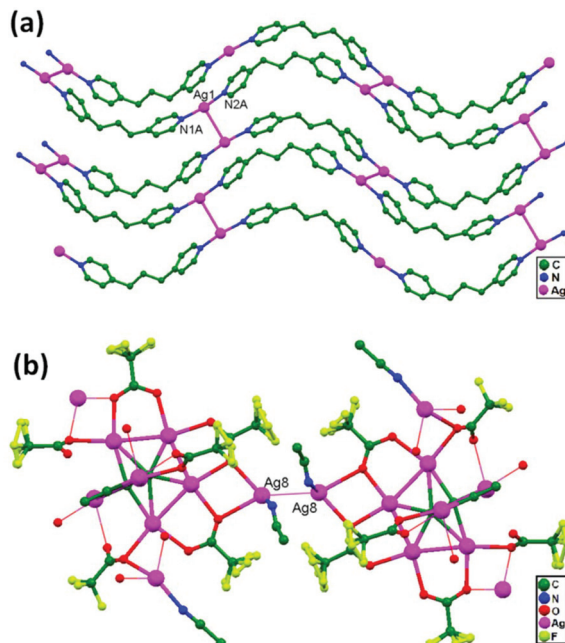


Fig. 13 (a) A 2D polymeric chain formed via  $\text{Ag}-\text{Ag}$  contacts in  $[\text{Ag}(\text{bpp})]\text{ClO}_4$ , **17**;  $\text{ClO}_4^-$  counter anions and hydrogen atoms are removed for clarity. (b) Strong ligand-unsupported  $\text{Ag}8-\text{Ag}8$  interactions in  $\text{Ag}_2\text{C}_2 \cdot 6\text{CF}_3\text{CO}_2\text{Ag} \cdot 3\text{CH}_3\text{CN}$ , **19**, resulting in the construction of a 2D network.

**17** and **18**, each  $\text{Ag}^+$  ion is coordinated by two pyridyl nitrogen atoms from different bpp units in approximately linear geometry (Fig. 13a). In the cationic network, there are two types of crystallographically and chemically equivalent  $\text{Ag}^+$  ions, both of which form 1D sinusoidal chains with the coordinated bpp molecules, where each  $-\text{CH}_2-\text{CH}_2-\text{CH}_2-$  spacer adopts TT conformation. Adjacent chains consist of one type of  $\text{Ag}^+$  ion, cross-linked through argentophilic bonding to form 2D layers, as evidenced by the  $\text{Ag}-\text{Ag}$  contact distances ( $3.221(10)$  Å in **17** and  $3.085(9)$  Å in **18**). Comparing the extended structures of **17** and **18**, it has been reasoned that the latter is more stable than the former, primarily because of the greater number and strength of  $\text{Ag}-\text{Ag}$  bonds.<sup>26</sup>

In 2001, Kristiansson reported a ligand-unsupported silver(I) aggregate, namely *catena*( $\mu_3\text{-O},\text{O}'\text{-N-4-aminobenzoato})(\mu_2\text{-O},\text{N-4-amino-benzoato})disilver(I)acetone solvate, with higher complexity and shorter  $\text{Ag}-\text{Ag}$  distances.<sup>38</sup> The crystals are assembled from rhombohedral  $\text{Ag}_4$  units, which are coordinated with eight *p*-aminobenzoate ligands (four oxygen atoms from carboxylate groups, and four nitrogen atoms from amino groups), and these rhombohedral units are exclusively linked via ligand unsupported  $\text{Ag}-\text{Ag}$  interactions. The  $\text{Ag}_4$  units are further linked to form infinite chains via  $\text{Ag}-\text{Ag}$  interactions supported by bis(carboxylato- $\text{O},\text{O}'$ ) bridges ( $\text{Ag}-\text{Ag} = 2.946(6)$  and  $3.025(4)$  Å). Polymeric chains interlinked via unsupported dimeric  $\text{Ag}-\text{Ag}$  interactions ( $3.161(4)$  Å) have previously been observed in silver imidazolate.<sup>66</sup>$

Mak and coworkers, in the same year, reported the compound  $\text{Ag}_2\text{C}_2 \cdot 6\text{CF}_3\text{CO}_2\text{Ag} \cdot 3\text{CH}_3\text{CN}$ , **19**, consisting of a zigzag

chain of edge-sharing triangulated dodecahedra, which can be regarded as arising from the fusion of two sets of tetrahedra. The dodecahedra share edges of the type Ag5–Ag6 to generate a chain-like structure. The silver atoms Ag5 and Ag6 help to assemble a virtually planar zigzag chain in which silver atoms Ag1 to Ag4 attached through binding with  $C_2^{2-}$  anions. The remaining silver atoms of type Ag7 and Ag8 are attached around the chain *via* trifluoroacetate bridges and are both four-coordinated, but the latter has its fourth coordination site saturated by an unsupported Ag8–Ag8 interaction with a distance of 2.917(4) Å (Fig. 13b). These composite chains are interlinked through such interactions to construct a 2D network.<sup>48</sup>

In 2002, Tong, Kitagawa, and coworkers reported a compound  $[\text{Ag}_2(\text{ppa})_2(\text{ox})] \cdot 9\text{H}_2\text{O}$  (ox = oxalate, ppa = *N*-(4-pyridinylmethyl)-4-pyridinecarboxamide), **20**, consisting of an open 3D neutral network of rectangular channels with lattice water molecules. The overall network consists of  $\beta$ -sheets with ox<sup>2-</sup> ligands as pillars. Each Ag<sup>+</sup> ion, in T-shaped coordination geometry, is ligated by two ppa units and one relatively weakly coordinated ox<sup>2-</sup> counterion; adjacent Ag–ppa chains are linked into interesting 2D  $\beta$ -sheet-like layers *via* weak ligand-unsupported Ag–Ag contacts (3.202(1) Å).<sup>3</sup> It is noteworthy that the ligand-unsupported Ag–Ag contacts and side-to-side interchain offset stacking interactions extend the 1D coordination chains into 2D sheets (Fig. 14).

Cao, Hong, and coworkers, in the same year,<sup>18</sup> constructed a luminescent polymer  $[\{\text{Ag}(\text{H}_2\text{btc})_2\}\{\text{Ag}_2(\text{Hbtc})\}]_n$  (H<sub>2</sub>btc = benzene-1,3,5-tricarboxylic acid), **21**, consisting of silver chains formed from ligand-unsupported Ag–Ag interactions and H<sub>2</sub>btc<sup>2-</sup> and Hbtc<sup>2-</sup> spacers (Fig. 15).

It comprises two independent building units, Ag<sub>2</sub>(H<sub>2</sub>btc)<sub>2</sub> (A) and Ag<sub>8</sub>(Hbtc)<sub>12/3</sub> (B). The two silver atoms in unit A are bridged by two deprotonated carboxyl groups with an Ag–Ag distance of 2.976(13) Å. Two A units in each case are connected through weak Ag–O<sub>(carbonyl)</sub> contacts; the geometry around the Ag<sup>+</sup> ion is distorted trigonal and a 1D chain-like structure is formed. Every two adjacent chains that are aligned in different directions are combined *via* ligand-unsupported Ag–Ag interactions (Ag1–Ag1: 2.963(12) Å), forming a 3D structure. Each B unit is arranged with four Ag<sub>2</sub> subunits, united *via* two car-

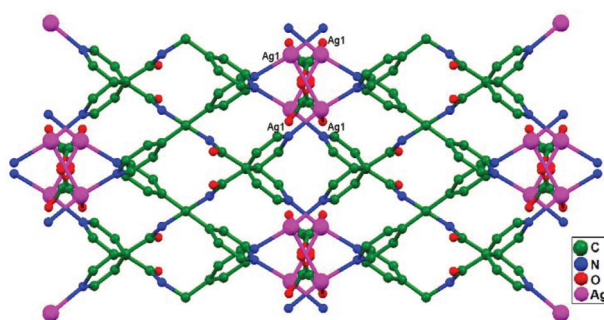


Fig. 14 The 2D sheet-like network of **20** constructed *via* Ag–Ag contacts, shown in the *ab* plane.

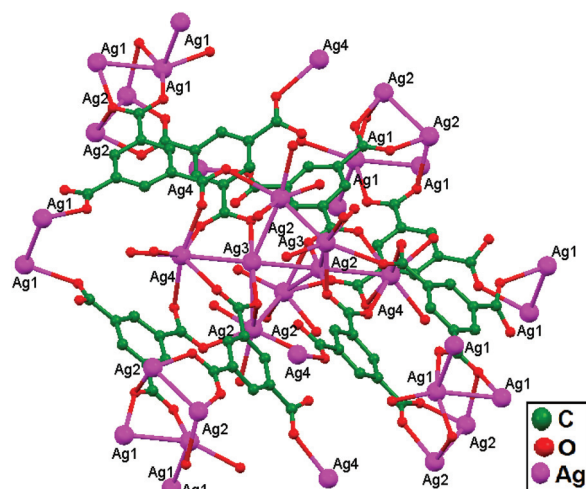


Fig. 15 The structure of the silver(i) chain formed *via* ligand-unsupported Ag–Ag interactions in  $[\{\text{Ag}(\text{H}_2\text{btc})_2\}\{\text{Ag}_2(\text{Hbtc})\}]_n$ , **21**.

boxyl groups from the ligand. Two Ag3–Ag4 subunits (Ag3–Ag4: 3.210(11) Å) are joined *via* ligand-unsupported Ag–Ag interactions (Ag3–Ag3: 3.092(16) Å), generating a linear Ag<sub>4</sub> chain, which connects two Ag2–Ag2 (2.989(13) Å) subunits through weak Ag–O bonding and ligand-unsupported Ag–Ag interactions (Ag2–Ag3: 3.185(6) Å). Owing to the ligand-unsupported Ag1–Ag2 (3.278(8) Å) interactions between the two kinds of 3D structures, they interpenetrate, producing linear distorted ladder-like silver(i) chains and the final condensed 3D structure.

In 2004, Henderson and coworkers prepared the compound  $[\text{Ag}_4(3\text{-CP})_8(\text{SiF}_6)_2(\text{H}_2\text{O})_2]_n$  (3-CP = 3-cyanopyridine), **22**, where  $[\text{Ag}_4(3\text{-CP})_8]^{4+}$  is essentially a centrosymmetric linear tetranuclear cationic cluster, containing four  $[\text{Ag}(3\text{-CP})_2]^+$  units connected *via* three Ag–Ag interactions and  $\pi$ – $\pi$  contacts between adjacent monocoordinated 3-CP ligands (Fig. 16). The three Ag–Ag bond lengths (3.307(5), 3.024(6), and 3.307(5) Å) in this centrosymmetric tetramer are shorter than the van der Waals

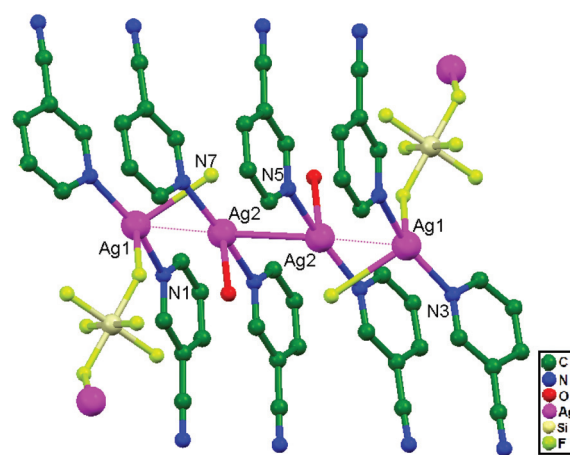


Fig. 16 The structure of the centrosymmetric  $[\text{Ag}_4(3\text{-CP})_8]^{4+}$  unit in compound **22**.

contact distance (3.40 Å). Each 3-CP ligand is terminally coordinated to an  $\text{Ag}^+$  ion *via* its pyridyl nitrogen and the nitrile group remains uncoordinated. The absence of coordination between  $\text{Ag}^+$  ions and these pendant nitrile groups highlights the significance of the  $\pi$ - $\pi$  stacking interactions between adjacent aromatic rings. The  $\text{Ag}_4$  skeleton is not quite linear, with  $\text{Ag}-\text{Ag}-\text{Ag}$  angles of 160.50(19)°. Neglecting this fact, this compound represents an unusual example of a 2D network based on discrete linear  $\text{Ag}_4$  clusters.<sup>67</sup>

In 2004, Jun and coworkers reported unique molecular rectangles of  $[\text{Ag}(\text{L})_2\text{X}_2]$  ( $\text{X}^- = \text{NO}_3^-$ : 23;  $\text{ClO}_4^-$ : 24;  $\text{PF}_6^-$ : 25;  $\text{CF}_3\text{SO}_3^-$ : 26) *via* the slow diffusion of  $\text{AgX}$  with  $\text{O}(\text{SiMe}_2(4\text{-Py}))_2$ . In these rectangular systems, transannular metallophilic interactions compete with the interactions between  $\text{Ag}^+$  ions and the anions (Fig. 17). The order of strength for argentophilic interactions is:  $\text{NO}_3^- > \text{ClO}_4^- > \text{PF}_6^- > \text{CF}_3\text{SO}_3^-$  based on the anion exchange distances, ranging from 3.20(1) to 3.81(1) Å without the demolition of the cyclic framework. It has been noted that a transannular  $\text{Ag}-\text{Ag}$  interaction (3.200(1) Å in 23) exists in the solid-state, and this distance is much shorter than the corresponding distance of ligand-unsupported  $\text{Ag}-\text{Ag}$  interactions recorded in the literature. All four structures are basically similar, but the argentophilic interaction distances (3.20(1) Å for 23, 3.41(1) Å for 24, 3.67(1) Å for 25, and 3.81(1) Å for 26) along with the related N- $\text{Ag}$ -N angles are very sensitive to the bite-size of each anion. The  $\text{Ag}-\text{Ag}$  interaction strengths are inversely proportional to the bite-sizes of the anions.  $\text{NO}_3^-$  (2.13(1) Å),  $\text{ClO}_4^-$  (2.36(1) Å), and  $\text{CF}_3\text{SO}_3^-$  (2.39(1) Å) anions exhibit substantial differences in the bite-size.<sup>27</sup>

In 2005, Liu and coworkers reported the assembly of isonicotinate acid (HINA) and  $\text{Ag}^+$  ions *via* a layer-separating diffusion method at ambient temperature, which gave rise to two structural coordination polymers, namely,  $[(\text{Ag}_4(\text{INA})_4)\cdot\text{H}_2\text{O}\cdot0.5\text{CH}_3\text{OH}]_n$ , 27, and  $[(\text{Ag}_3(\text{INA})_2)\text{NO}_3]_n$ , 28. Compound 27 is the primary example of a double-layered structural design, and it involves an unconventional stacking mode with  $\text{Ag}-\text{Ag}$ ,  $\text{Ag}-\text{O}$  contacts and  $\pi$ - $\pi$  interactions. The construction of double-layer network in 28 presents an opportunity to examine the functionality of counter anions in ligand-unsupported  $\text{Ag}-\text{Ag}$  interactions. Fascinatingly, ligand-unsupported  $\text{Ag}-\text{Ag}$  interactions (3.096(7) Å for  $\text{Ag}2$ - $\text{Ag}4$ ) are available only in the interlayers of the structural design. In

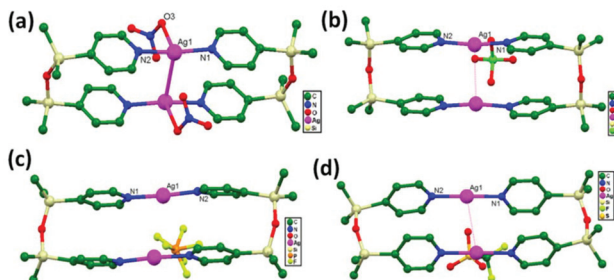


Fig. 17 The solid-state structures of (a) 23; (b) 24; (c) 25; (d) 26 showing transannular  $\text{Ag}-\text{Ag}$  interactions. The anions can be clearly observed, and hydrogen atoms are removed for clarity.

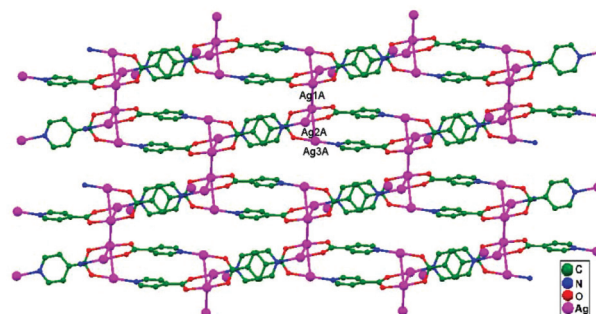


Fig. 18 The crystal structure of 29 shows weak ligand-unsupported argentophilic interactions, extending it into a 2D layered structure.

addition to the  $\text{Ag}-\text{Ag}$  contacts,  $\pi$ - $\pi$  interactions can only be obtained between pyridyl rings, and the interlayer connections are completed by them.<sup>19</sup> In 2005, Zhu and coworkers reported the polymeric compound  $[\text{Ag}(\text{en})\text{Ag}(\text{dnbc})_2]_n\cdot2n\text{H}_2\text{O}$  (en: ethylenediamine, dnbc: 3,5-dinitrobenzoic acid), 29, in which  $\text{Ag}1$  and  $\text{Ag}2$  atoms show ligand-unsupported weak argentophilic interactions ( $\text{Ag}-\text{Ag}$  distance = 3.177(4) Å). The amine ligands bridge  $\text{Ag}^+$  ions to form a coordination polymer chain with an  $\text{Ag}(\text{dnbc})_2$  coordination fragment attached *via*  $\text{Ag}-\text{Ag}$  interactions (Fig. 18), and this helps the extension into a 2D layered structure.<sup>68</sup>

A solution of sodium 3,5-diphenylpyrazolate  $[\text{Na}(\text{Ph}_2\text{pz})]$  with  $\text{Ag}(\text{tht})\text{NO}_3$  in dichloromethane reacts to afford an unsolvated and photostable dimer of trimers  $[\text{Ag}_3(\text{l-3,5-Ph}_2\text{pz})_3]_2$ , 30. These two trimers are rotated anti to each other (Fig. 19). Three silver atoms bridge through exobidentate pyrazolate groups to form a slightly puckered nine-membered ring with a shortest  $\text{Ag}-\text{Ag}$  intramolecular interaction distance in the metallocycle of 3.357(8) Å. The other two silver centers are weakly interacting, with an  $\text{Ag}3$ - $\text{Ag}1$  distance of 3.49 Å and  $\text{Ag}3$ - $\text{Ag}2$  distance of 3.52 Å. The  $\text{Ag}-\text{Ag}$  intermolecular interaction distance between the two trimers is 2.971(14) Å.<sup>69</sup>

In 2005, Jung and coworkers carried out the synthesis of the compound  $[\text{Ag}(\text{NO}_2)(\text{BPDMs})]$ , 31, with  $\text{AgNO}_2$  and bis(4-pyridyl)-dimethylsilane (BPDMs). The 1:1 adduct of  $\text{Ag}^+$ -

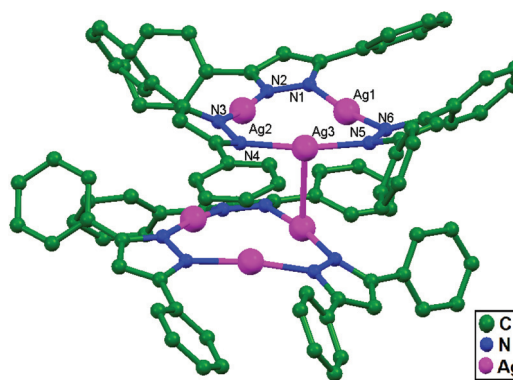
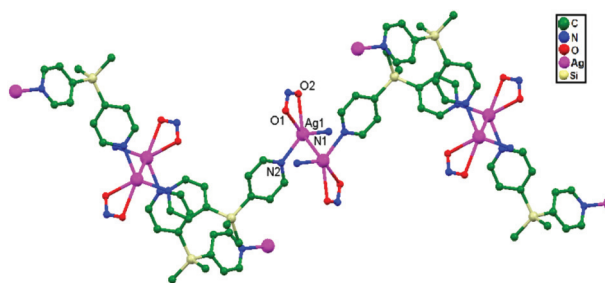


Fig. 19 The structure of  $[\text{Ag}_3(\text{Ph}_2\text{pz})_3]_2$ , 30, showing ligand-unsupported argentophilic interactions; hydrogen atoms have been omitted.



**Fig. 20** The coordination environment around  $\text{Ag}^+$  ions, with ligand-unsupported argentophilic interactions forming a zigzag chain in  $[\text{Ag}(\text{NO}_2)(\text{BPDMS})]$ , **31**.

BPDMs and  $\text{NO}_2^-$  was been obtained and a linear relationship between the ligand to metal ratio and anion coordinating ability was observed. This compound has a unique sheet-like structure containing double helices that are joined to each other into a unique sheet through  $\text{Ag}-\text{Ag}$  ( $3.002(2)$  Å) contacts (Fig. 20). It has been demonstrated that the silicon atom based bipyridine ligand is a mesmerizing structural forming unit, exhibiting minute strain in the manufacture of diverse skeletons, like a double-helical sheet with ligand-unsupported  $\text{Ag}-\text{Ag}$  contacts in a five-coordinated  $\text{Ag}^+$  ion based compound, a sheet consisting of nano-tubes, ladder-type tubes, and 2D sheets.<sup>31</sup>

Chen and coworkers, in 2005, successfully designed the compounds  $[\text{Ag}_2(\text{ophen})_2]_2 \cdot 6\text{H}_2\text{O}$ , **32**,  $[\text{Ag}_2(\text{obpy})_2]_2 \cdot 4.5\text{H}_2\text{O} \cdot 0.5\text{DMF}$ , **33**, and  $[\text{Ag}_2(\text{obpy})_2]_3 \cdot 18\text{H}_2\text{O}$ , **34** (Hophen =  $1\text{H}-[1,10]\text{phenanthrolin}-2\text{-one}$ , and Hobpy =  $1\text{H}-[2,2']\text{bipyridinyl}-6\text{-one}$ ), in which all compounds consist of the desired  $[\text{Ag}_2\text{L}_2]$  ( $\text{L}$  = ophen or obpy) structural unit.<sup>70</sup> The  $[\text{Ag}_2\text{L}_2]$  dimers are further dimerized in compounds **32** and **33** (Fig. 21a and b), whereas the  $[\text{Ag}_2(\text{obpy})_2]$  molecules are associated into a trimer (Fig. 21c) in compound **34**. X-ray analyses show that the interdimer  $\text{Ag}-\text{Ag}$  separations in  $[\text{Ag}_2(\text{ophen})_2]_2$  ( $3.199$  Å) are remarkably shorter and, also, the face-to face  $\pi-\pi$  interactions hinder rather than sustain important interdimer  $\text{Ag}-\text{Ag}$  interactions. In the trimer-of-dimers structure in  $[\text{Ag}_2(\text{obpy})_2]_3$ , the ligand-unsupported  $\text{Ag}-\text{Ag}$  contact distances lie in the range of  $3.171$  to  $3.274$  Å. From the crystal structure, it is evident that the oligomerization process involving  $\text{Ag}_2\text{L}_2$  molecules is privileged due to stronger argentophilic and comparatively weaker face-to-face  $\pi-\pi$  interactions.

In 2005, Barbour reported an infinite 2D Borromean entanglement coordination framework  $[\text{Ag}_2(\text{BMIMB})_3](\text{BF}_4)_2$  (BMIMB:  $1,4\text{-bis}(2\text{-methylimidazol-1-ylmethyl})\text{benzene}$ ), **35**, which was obtained *via* the reaction of a flexible ligand with  $\text{AgBF}_4$  and stabilized *via* ligand-unsupported argentophilic interactions.<sup>28</sup> The coordination environment around the  $\text{Ag}^+$  ions is trigonal planar, and three imidazole rings are oriented in a propeller-like arrangement with their 2-methyl groups located on the same face of the plane. Each  $(\text{AgL}_3)$  motif is associated with an identical symmetry-related motif through an argentophilic interaction ( $\text{Ag}-\text{Ag} = 3.062(4)$  Å).

In the same year, Klausmeyer and coworkers reported the compound  $[\text{Ag}(2\text{-amp})_2(\text{tfa})]$  ( $2\text{-amp} = 2\text{-aminomethyl} \text{pyri}-$

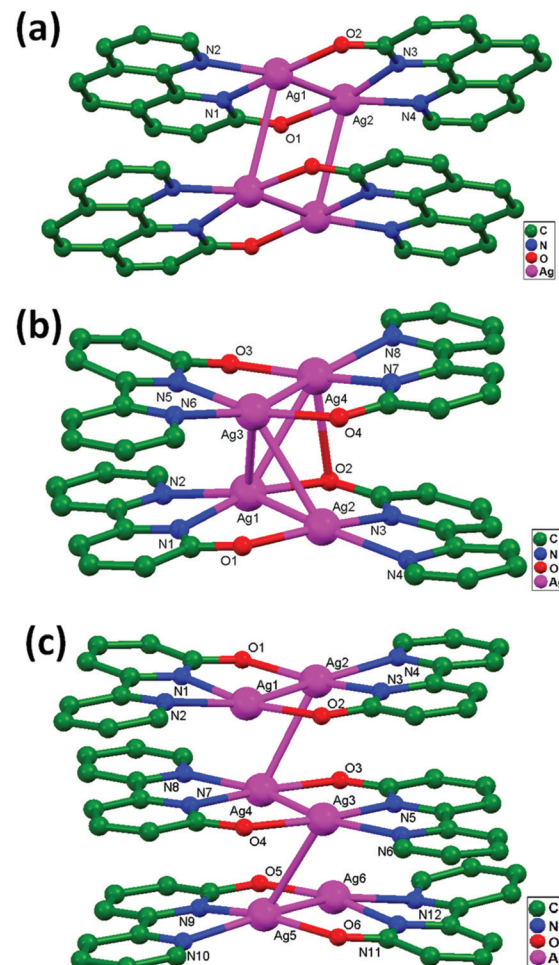


**Fig. 21** The molecular structures of (a)  $[\text{Ag}_2(\text{ophen})_2]_2 \cdot 6\text{H}_2\text{O}$ , **32**, (b)  $[\text{Ag}_2(\text{obpy})_2]_2 \cdot 4.5\text{H}_2\text{O} \cdot 0.5\text{DMF}$ , **33**, and (c)  $[\text{Ag}_2(\text{obpy})_2]_3 \cdot 18\text{H}_2\text{O}$ , **34**, showing ligand-unsupported argentophilic interactions.

dine, and  $\text{tfa}^- = \text{trifluoroacetate}$ ), **36**, in which both trigonal-bipyramidal and square-based pyramidal geometries are present in a single structure. The crystal structure of the compound displays short  $\text{Ag}-\text{Ag}$  contacts ( $3.007(4)$  Å) (Fig. 22) and shows similarity with metal-isolated counterparts. These species are held together by weaker  $\pi$ -stacking and H-bonding interactions with the lattice or coordinated anions.<sup>71</sup>

Englert and coworkers, in the year 2006, reported the compound  $[\text{Ag}(\text{rac-chxn})]\text{BF}_4$  ( $\text{rac-chxn} = \text{rac-1,2-diaminocyclohexane}$ ), **37**, in which  $\text{Ag}^+$  ions in neighboring strands are not separated by additional ligands but rather they remain di-coordinated<sup>72</sup> with additional ligand-unsupported short  $\text{Ag}-\text{Ag}$  ( $3.110$  Å) contacts (Fig. 23).

In 2006, Chen and coworkers structurally established two supramolecular isomers of  $\text{Ag}(\text{imidazolate})$  [**38** and **39**], exhibiting 2D (6,3) and (4,4) networks, respectively, through short interchain  $\text{Ag}-\text{Ag}$  contacts ( $3.159(5)$  Å for **38** and  $3.445(5)$  Å for **39**).<sup>4</sup> In fact, attributable to the different relative orientations between adjacent imd ligands, the crystal structure of **38** contains four crystallographically unique  $\text{Ag}(\text{imd})$  units, whereas

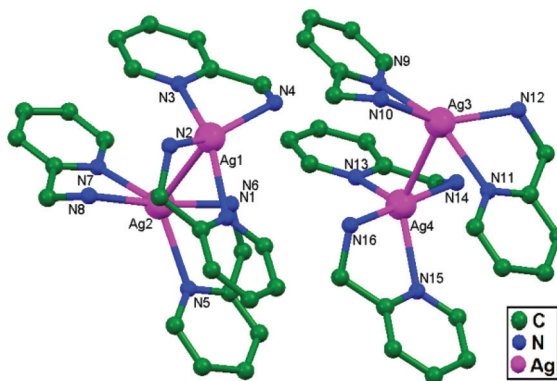


Fig. 22 The molecular structure showing ligand-unsupported Ag–Ag contacts in 36.

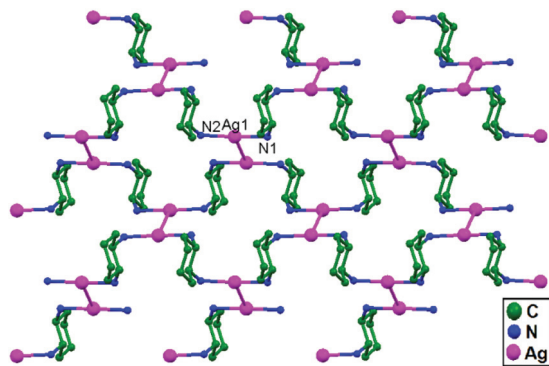


Fig. 23 The packing of  $\text{Ag}^+$  ions in 37 showing ligand-unsupported short Ag–Ag contacts; hydrogen atoms and anions are omitted.

that of 39 contains two crystallographically unique  $\text{Ag}(\text{im})$  units; also, because of different relative orientations, the associated Ag–Ag contacts are also different. In 38, there are two crystallographically unique  $\text{Ag}^+$  ions and short Ag–Ag contacts between adjacent chains ( $3.159(5)$  Å) have been shown. These chains extending along the  $[2\ 0\ 1]$  direction are inter-linked into a 2D network through short Ag–Ag contacts. Further, it can be simplified to a uninodal (6,3) net, with two unique  $\text{Ag}^+$  ions that have short Ag–Ag contacts acting as three-connected nodes and two other  $\text{Ag}^+$  ions and imd ligands also with short Ag–Ag contacts acting as linkers (Fig. 24a). In contrast, only one crystallographically unique  $\text{Ag}^+$  ion in 39 has short Ag–Ag contacts ( $3.445(5)$  Å, a value slightly longer than the sum of the van der Waals radii of silver atoms (3.40 Å) between adjacent chains). These chains are extended along the  $c$ -axis and are linked to each other through Ag–Ag contacts to construct a 2D (4,4) network (Fig. 24b).

Klausmeyer and coworkers, in 2005, synthesized a variety of silver(i) compounds,  $\text{Ag}(\text{3-amp})\text{OTf}$ , 40,  $\text{Ag}_2(\text{2,2'-bpy})_2\cdot\mu\text{-}(\text{3-amp})(\text{tfa})_2$ , 41, and  $\text{Ag}_2(\text{2,2'-bpy})_2\cdot\mu\text{-}(\text{3-amp})(\text{OTf})_2$ , 42, using the mixed-donor ligand 3-amp with  $\text{AgX}$  ( $\text{X} = \text{OTf}^-$  or  $\text{tfa}^-$ ; 3-amp = 3-(aminomethyl)pyridine;  $\text{OTf}$  = triflate;  $\text{tfa}$  = trifluoroacetate; and 2,2'-bpy = 2,2'-bipyridine). The structural fea-

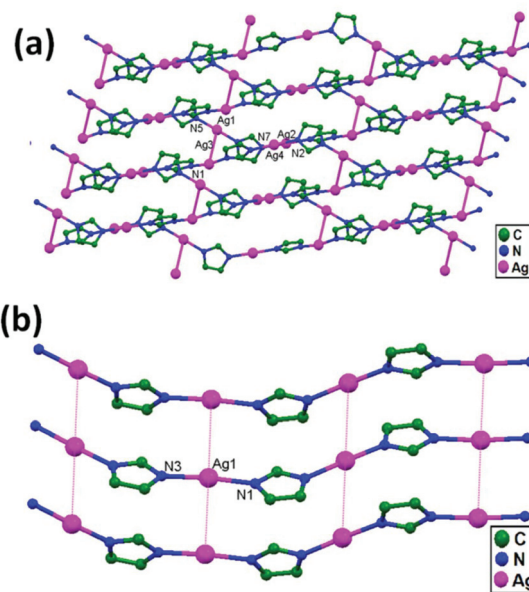


Fig. 24 The formation of a 2D network via short Ag–Ag contacts in (a) 38 and (b) 39.

tures, such as the dimensionality of the overall compound, coordination number, and coordination environment were controlled based on variations in the counter ion and ligand to metal ratio.<sup>73</sup> The 1D chain is connected to an identical one via Ag–Ag interactions (3.182(4) Å for 40, 3.058(3) Å for 41, and 3.085(3) and 3.040(3) Å for 42), such that the two 3-amp bridges are arranged head-to-tail with respect to one another. The effect of these Ag–Ag contacts is to join the isolated polymers into 1D zigzag chains or 2D sheets due to closed-shell Ag–Ag interactions involving the planar metals, holding the monomers together. In 40, the Ag–Ag interactions appear to be supported by the interpolymeric  $\pi$ -stacking of 2,2'-bpy rings, and the effect of this interaction is to join would-be isolated polymers into 2D sheets. The resulting sheets exhibit a staggered array of interlaced hexagons, similar to a chain-link fence (Fig. 25a). Similar to 40, the Ag–Ag interactions appear to be supported by the  $\pi$ -stacking of 2,2'-bpy rings, forming a 1D chain (Fig. 25b) in 41 and dimeric units (Fig. 25c) in 42.

In other work, Klausmeyer and coworkers, in the same year, managed to prepare another compound  $\text{Ag}_2(5,5'\text{-bm-2,2'-bpy})_2(\text{4-amp})(\text{BF}_4)_2$  (4-amp = 4-(aminomethyl)pyridine; and 5,5'-bm-2,2'-bpy = 5,5'-bismethyl-2,2'-bipyridine), 43. The typical Ag–Ag interaction lengths are 3.348(1) Å and appear to be supported by the  $\pi$ -stacking of pyridyl and bipyridyl rings bound to the silver metal. The unique and interesting feature of this structure is that it is actually a linear polymer that expands along the direction of the Ag–Ag interactions (3.348(1) Å) with an infinite Ag–Ag backbone. This backbone shows only a slight bend at each metal center, with a Ag–Ag–Ag angle of 174.85(2)°. Perpetuation of the polymer sees the molecular axis of each monomer shifted nearly perpendicular to the adjacent units, giving the overall polymer a saw-tooth appearance (Fig. 26).<sup>74</sup>

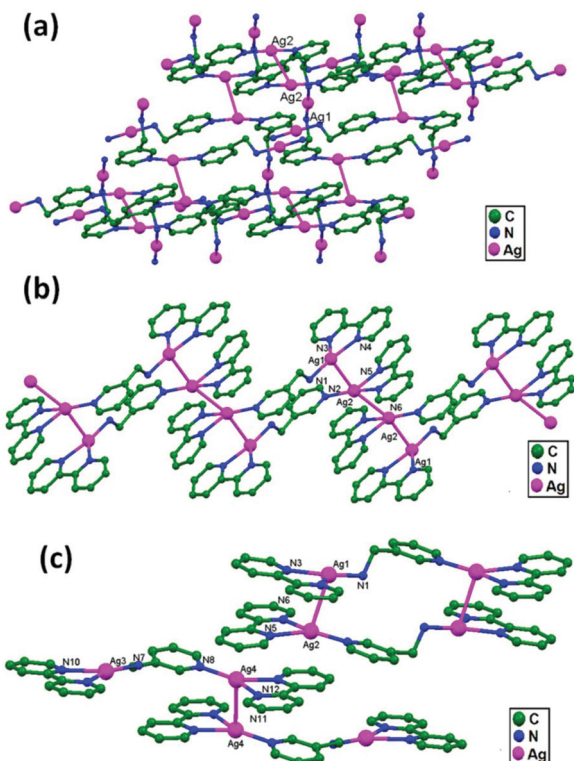


Fig. 25 Ligand-unsupported Ag–Ag contacts forming (a) a 2D network in **40**, (b) a 1D polymeric chain in **41**, and (c) dimeric units in **42**.

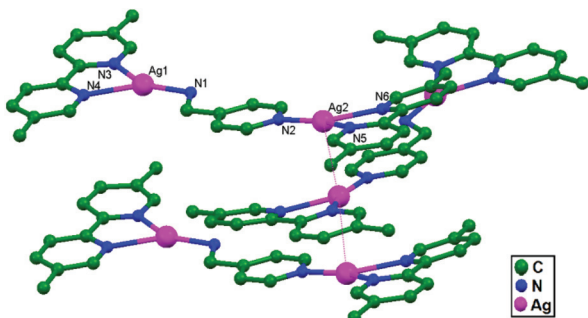


Fig. 26 The molecular structure of  $\text{Ag}_2(5,5'\text{-bm-}2,2'\text{-bpy})_2(4\text{-amp})(\text{BF}_4)_2$ , **43**, showing ligand-unsupported Ag–Ag contacts.

Klausmeyer and coworkers reported the compounds  $(\text{Ag}(3\text{-amp})\text{BF}_4)_n$ , **44**, and  $\text{Ag}_2(2,2'\text{-bpy})_2\mu\text{-}(3\text{-amp})(\text{BF}_4)_2$ , **45** ( $3\text{-amp} = 3\text{-aminomethylpyridine}$ ), in the year 2007. Depending upon the ratio of the reactants used and the crystallization temperature, asymmetric 3-amp with  $\text{AgBF}_4$  results in an array of structural motifs. With a 1:1 ratio of 3-amp to silver atoms, the linear coordination polymer **44** is formed, depending upon whether the crystals are grown at  $-35$  or  $5$   $^\circ\text{C}$ . The Ag–Ag distance herein is a bit lengthy at  $3.289(1)$   $\text{\AA}$ , but the contact appears to be completely unsupported with virtually no  $\pi$ -stacking occurring between the rings of the connected  $\text{Ag}^+$  ions in **44**. There do appear to be, however, substantial  $\pi$ -interactions between silver metal and the 2,2'-bipy rings of

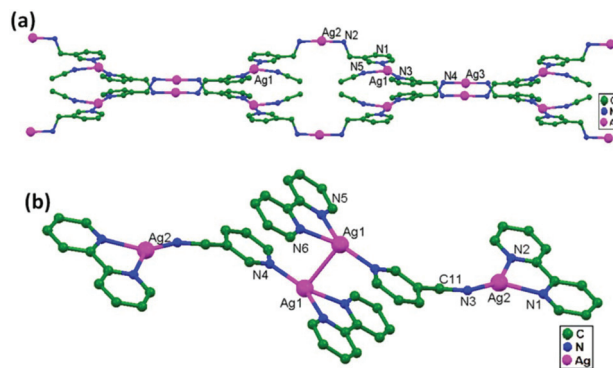


Fig. 27 The ligand-unsupported Ag–Ag contacts in (a) compound **44** and (b) compound **45**.

the polymer strands stacked above and below the silver atoms that hold the two halves of the polymer chain together. The  $\pi$ -clouds of the 2,2'-bipy rings approach to the silver atoms within the range of  $3.031(9)$  to  $4.176(9)$   $\text{\AA}$  (the distances between the silver and ring atoms), constructing a pseudo-double-metal sandwich arrangement (Fig. 27a). In **45**, symmetry-equivalent units are held close together *via* a Ag–Ag interaction distance of  $2.988(4)$   $\text{\AA}$  (Fig. 27b). This relatively short Ag–Ag interaction, which is over  $0.3$   $\text{\AA}$  closer than the others described herein, is held tightly together by the resonance stacking of the three coordinated rings connected to neighboring silver atoms. This interaction is not achievable with contrasting amine-bound silver atoms due to the projection of amine hydrogen atoms into the space required for ring stacking.<sup>30</sup>

Zhu and coworkers, in the year 2003, reported the coordination polymer  $[\text{Ag}(\text{dach})_n](\text{NO}_3)_n$  ( $\text{dach} = 1,2\text{-diaminocyclohexane}$ ), **46**, which has a 1D chain-like structure that is extended by ligand-unsupported Ag–Ag interactions ( $3.233(4)$   $\text{\AA}$ ), and hydrophobic and hydrogen-bonding interactions into a 2D supramolecular (Fig. 28) array.<sup>75</sup>

Guo and coworkers, in the year 2006, prepared two novel silver compounds, namely  $[\text{Ag}_5(\text{CN})_5(2,2'\text{-bpy})_2]_n$ , **47**, and  $[(\text{Me}_4\text{N})\text{Ag}_3(\text{CN})_4]_n$ , **48**, *via* a solvothermal technique.<sup>46</sup> In **47**, the 1D chains link with each other to form a 2D wavelike layer

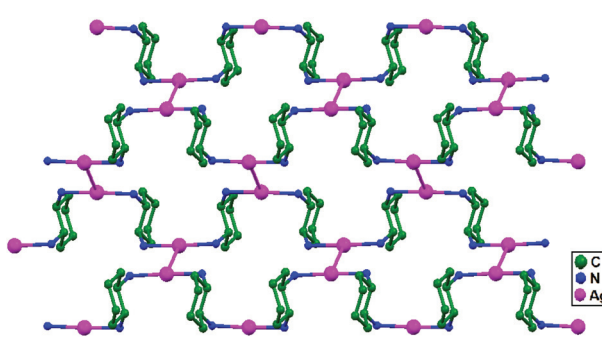


Fig. 28 Ligand-unsupported Ag–Ag interactions forming a 2D network in the compound **46**.

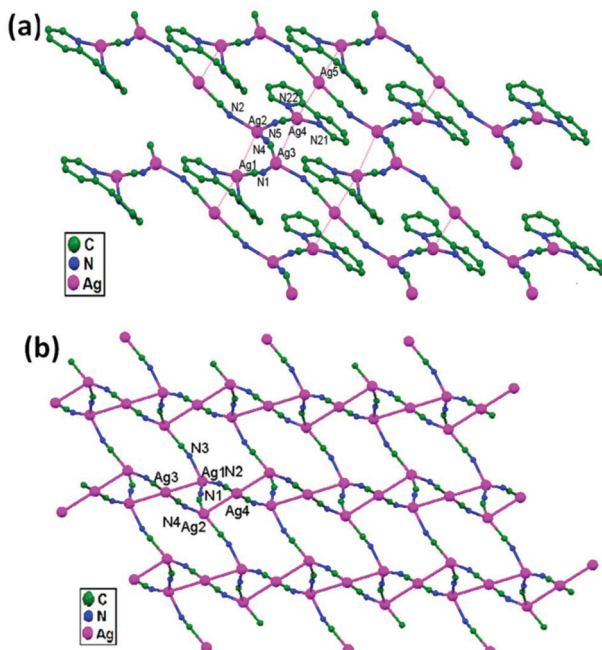


Fig. 29 Ligand-unsupported argentophilic interactions forming 2D networks in (a) compound 47 and (b) compound 48.

extending along the [0,1,0] and [1,0,1] directions through ligand-unsupported Ag1–Ag2 (3.276(2) Å) and Ag3–Ag4 (3.314(1) Å) interactions (Fig. 29a). These layers stack together tightly to form a 3D framework through ligand-unsupported Ag1–Ag5 (3.373(1) Å) and Ag4–Ag5 (3.342(2) Å) argentophilic interactions. In the adjacent 3-connected (10, 3)-g nets in 48, ligand-unsupported Ag1–Ag3 (3.073(5) Å) and Ag2–Ag4 (3.149(5) Å) argentophilic interactions exist, which play an important role in forming the stable framework (Fig. 29b).

Hong and coworkers, in the year 2006, prepared the novel coordination polymer  $[\text{Ag}(\text{pmtmb})]_n$ , 49, with a flexible asymmetrical bridging ligand, namely 4-(2-pyrimidylthiomethyl)benzoic acid (Hpmtmb).<sup>20</sup> The 2D layer of 49 consists of unusual zigzag silver chains based simultaneously on mixed ligand-supported and ligand-unsupported Ag–Ag interactions. However, the ligand-unsupported Ag–Ag interaction is weaker, with a distance of 3.336(11) Å. Li and coworkers, in 2007, prepared the compound  $\{[\text{Ag}_2(\text{C}_{10}\text{H}_{14}\text{N}_4)_2](\text{ClO}_4)_2\}_n$ , 50, which is a 1D coordination polymer formed from  $\text{Ag}^+$  ions linearly bridged by 1,10-(butane-1,4-diyl)diimidazole molecules. The chains have a double-helical arrangement (Fig. 30) and pairs of chains are held together by a rarely reported ligand-unsupported

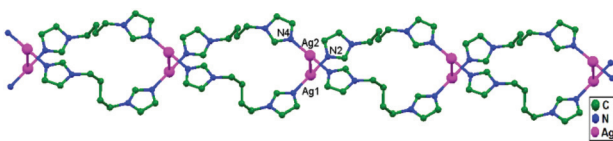


Fig. 30 The formation of a double-helical chain via ligand-unsupported Ag–Ag interactions in 50.

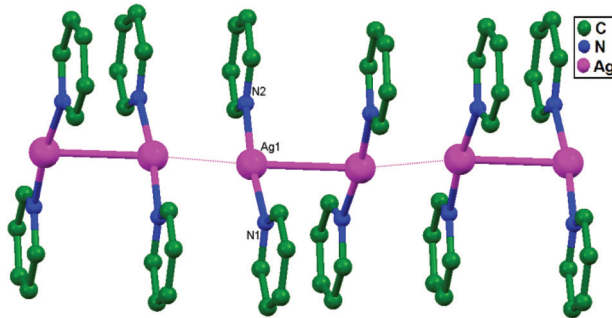


Fig. 31 A view of the zigzag chain of cations that is present in 51 and 52; the hydrogen atoms and counter-anions were omitted.

Ag–Ag interaction (2.966(1) Å). The double-helix consists of rotated 24-membered macrocyclic rings, in which four  $\text{Ag}^+$  ions (lying on a two-fold axis) and two pmtmb ligands are present in the crystal structure.<sup>76</sup>

Lee and coworkers, in the year 2007, synthesized and characterized three simple 1:2 silver(i)-pyridine adducts with different counter anions,  $[\text{Ag}(\text{py})_2]^+\cdot\text{X}^-$  ( $\text{X} = \text{ClO}_4^-$ : 51;  $\text{BF}_4^-$ : 52; and  $\text{PF}_6^-$ : 53).<sup>77</sup> Structural studies of 51–53 reveal the presence of strong ligand-unsupported argentophilic interactions ( $\text{Ag}–\text{Ag} = 2.96$ –3.00 Å) between  $[\text{Ag}(\text{py})_2]^+$  ions, forming pairs of  $[\text{Ag}(\text{py})_2]^{2+}$  ionic units. In 51 and 52, pairs of  $[\text{Ag}(\text{py})_2]^{2+}$  are further linked into 1D infinite chains *via* a combined set of multiple Ag–Ag close contact (3.34–3.37 Å), offset ‘head to head’  $\pi$ – $\pi$  stacking, and anion bridging interactions (Fig. 31). In contrast, 53 shows the presence of octahedral  $\text{PF}_6^-$  as a counter anion, and a couple of  $[\text{Ag}(\text{py})_2]^{2+}$  units are managed into a 3D framework with the collective help of a pair of Ag–F contacts, C(H)–F bonds, and ‘head to tail’  $\pi$ – $\pi$  stacking interactions. No extended 1D polymeric chains of  $\text{Ag}^+$  ions are present in 53.

Zhang and coworkers, in the year 2007, reported  $[\text{Ag}(\text{PCPA})(\text{PCPAH})(4,4'\text{-bpy})\text{H}_2\text{O}]_n$  ( $4,4'\text{-bpy} = 4,4'\text{-bipyridine}$ ; PCPA = *p*-chlorophenoxyacetate; and PCPAH = *p*-chlorophenoxyacetic acid), 54, with a 1D molecular ladder structure. This supramolecular framework is built *via* coordination bonds, weak interactions between  $\text{Ag}^+$  ions,  $\pi$ – $\pi$  stacking, and H-bonding interactions. It consists of molecular ladders with  $[\text{Ag}(4,4'\text{-bpy})]_n$  sidepieces, ligand-unsupported Ag–Ag rungs, PCPA counter anions, neutral PCPAH, and lattice water molecules. Two  $[\text{Ag}(4,4'\text{-bpy})]_n$  chains are linked into a 1D molecular ladder *via* ligand-unsupported Ag–Ag interactions (3.209(13) Å) (Fig. 32).<sup>78</sup>

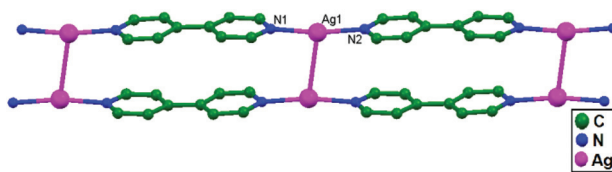
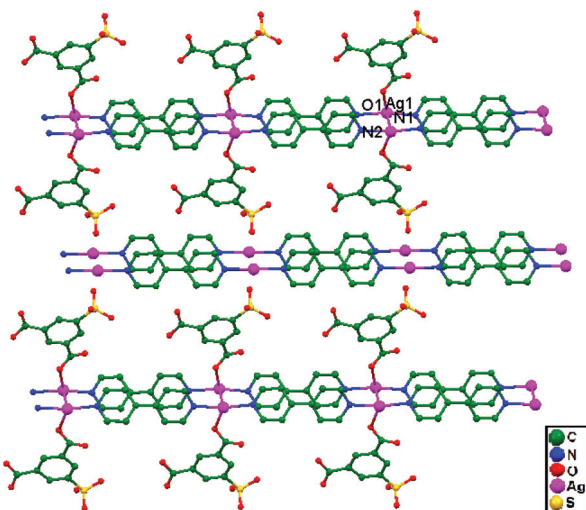


Fig. 32 The 1D molecular ladder made of  $[\text{Ag}(4,4'\text{-bpy})]_n$  sides and ligand-unsupported Ag–Ag interactions in 54.



**Fig. 33** A view of the 2D network and ligand-unsupported Ag–Ag interactions in compound 55.

Liu and coworkers, in 2008, produced a new silver(I) coordination polymer  $\{[\text{Ag}(4,4'\text{-bpy})][\text{Ag}(\text{HSIP})(4,4'\text{-bpy})](\text{H}_2\text{O})_2\}_n$ , 55, via the self-assembly of  $\text{Ag}(\text{NO}_3)_2$  with 5-sulfoisophthalic acid monosodium salt ( $\text{NaH}_2\text{SIP}$ ) in the presence of 4,4'-bipyridyl (4,4'-bpy). 4,4'-bpy bridges Ag1 atoms to form a 1D chain along the *b* axis, and the Ag–Ag distance is comparable to a value of 2.89 Å. Then, a 2D supramolecular network (Fig. 33) is formed from Ag-4,4'-bpy double chains and HSIP ligands through a combination of coordination bonds, ligand-unsupported Ag–Ag interactions (3.473 Å), and weak Ag–O coordinative interactions.<sup>79</sup>

Chen and coworkers, in 2008, prepared another dinuclear compound  $[\text{Ag}_2(\text{H}_2\text{L}_3)_2(\text{HL}_4)_2]$  ( $\text{H}_2\text{L}_3$  = 2,6-bis(5-phenyl-1*H*-pyrazol-3-yl)pyridine,  $\text{HL}_4$  = 6-(5-phenyl-1*H*-pyrazolyl-3-yl)picolinate), 56, in which ligand-unsupported Ag–Ag contacts are present between two  $\text{Ag}^+$  ions (3.040(1) Å) (Fig. 34). This distance is slightly longer than the Ag–Ag separation in metallic silver (2.889 Å), but shorter than the sum of the van der Waals radii (3.44 Å) reported in the literature.<sup>80</sup> Ghosh and coworkers, in the year 2008, synthesized the neutral dimeric silver compound  $\{[1\text{-}(benzyl)-3-(*N*-*tert*-butylacetamido)imid-$

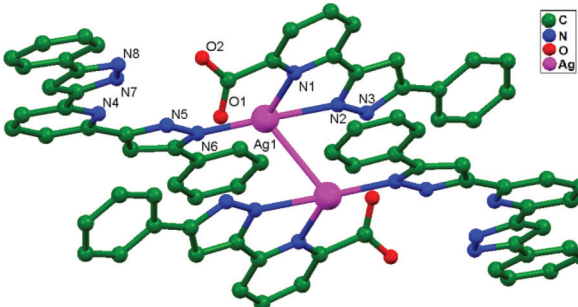


**Fig. 34** The molecular structure showing the ligand-unsupported argentophilic interactions in **56**.

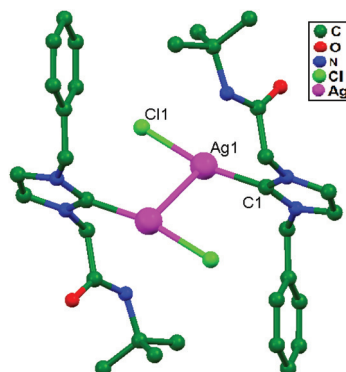


**Fig. 35** The molecular structure showing ligand-unsupported Ag–Ag contacts in dimeric **57**.

azol-2-ylidene]-AgCl<sub>2</sub>], 57, using a N/O-functionalized N-heterocyclic carbene ligand. It displayed attractive argento-philic interactions (Fig. 35) in the form of close ligand-unsupported Ag–Ag contact (3.197(12) Å), as observed from X-ray diffraction studies.<sup>81</sup>

Wang and coworkers, in the same year, reported a novel coordination polymer  $\{[\text{Ag}_2(\text{bpdc})(\text{bpp})(\text{H}_2\text{O})]\cdot 2\text{H}_2\text{O}\}_n$  ( $\text{H}_2\text{bpdc}$  = 2,2'-bipyridyl-4,4'-dicarboxylic acid,  $\text{bpp}$  = 1,3-bis(4-pyridyl)propane), **58**. The use of the multifunctional bpdc ligand with N- and O-donor sites in combination with the flexible ligand bpp presents a versatile approach for assembling multi-coordination silver(I) polymers. Analysis of the crystal structure indicates the existence of two kinds of ligand-unsupported  $\text{Ag}-\text{Ag}$  (3.08, 3.17 Å) contacts (Fig. 36), linking the  $\text{Ag}^+$  ions in tetra-nuclear 1D silver strings into a 2D network. The unusual coordination modes of bpdc provide potential supramolecular recognition sites to construct a 3D architecture.<sup>21</sup>

Yao and coworkers, in 2009, reported supramolecular chains of  $\{\text{Ag}_2(\text{dpa})(\text{H}_2\text{O})\}_2$  units in the compound  $\text{Ag}_2(4,4'\text{-bpy})_{1.5}(\text{dpa})(\text{H}_2\text{O})$  ( $\text{H}_2\text{dpa} = 1,1'\text{-biphenyl-2,2'-dicarboxylic acid}$ ; and  $4,4'\text{-bpy} = 4,4'\text{-bipyridine}$ ), 59. Two terminal  $\text{Ag}_2$  atoms from adjacent tetranuclear units are connected through ligand-unsupported argentophilic interactions (2.88 Å) (Fig. 37a) to extend these building units into a 1D supramolecular chain substructure. Another prominent feature related to

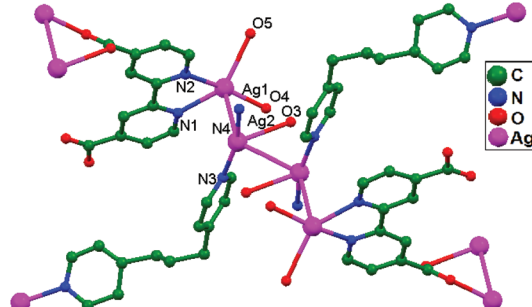


**Fig. 36** The coordination environment of  $\text{Ag}^+$  ions in **58**; free water molecules and hydrogen atoms have been omitted.

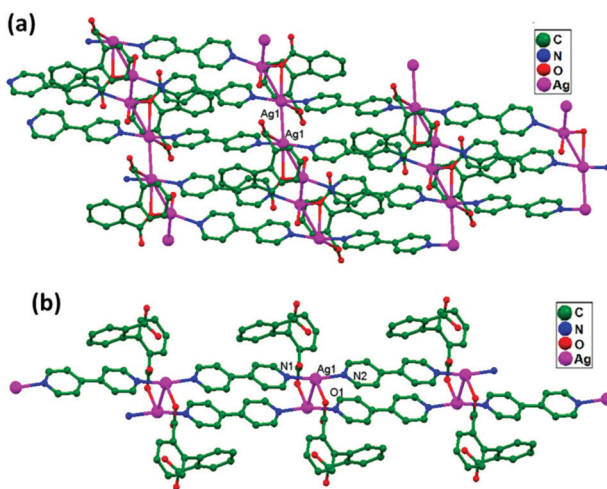


Fig. 37 The compounds (a)  $\text{Ag}_2(\text{bpy})_{15}(\text{dpa})(\text{H}_2\text{O})$ , **59**, and (b)  $\alpha\text{-}[\text{Ag}(\text{bpy})]_3(\text{Hdpa})$ , **60**, showing ligand-unsupported argentophilic interactions.

the 1D chain substructure is the coexistence of ligand-supported and ligand-unsupported argentophilic interactions. In another compound,  $\alpha\text{-}[\text{Ag}(4,4'\text{-bpy})]_3(\text{Hdpa})$ , **60**, two different  $[\text{Ag}(4,4'\text{-bpy})(\text{Hdpa})]$  1D supramolecular double chains are found (Fig. 37b), which are sustained by a combination of weak Ag–O interactions,  $\pi$ – $\pi$  stacking interactions, and argentophilic interactions.<sup>82</sup>

Englert and coworkers, in 2010, synthesized the compound  $[\text{Ag}(\text{SS-chxn})](\text{X}^-)\cdot 1.5\text{H}_2\text{O}$  (chxn = *trans*-1,2-diaminocyclohexane, and  $\text{X}^-$  = 4-methylbenzoate), **61**, in which Ag–Ag contacts increase the dimensionality of the solids from chain polymers (Fig. 38) to layer structures. The neighboring chains follow a perpendicular arrangement to create a layered network with short, ligand-unsupported argentophilic interactions (Ag–Ag = 3.002(8) Å).<sup>83</sup>

Huang and coworkers, in 2011, reported the compounds  $[\text{Ag}_2(\text{dmt})_2(\text{suc})\cdot \text{H}_2\text{O}]_n$ , **62**, and  $[\text{Ag}_2(\text{dmt})_2(\text{suc})(\text{H}_2\text{O})\cdot 0.5\text{H}_2\text{O}]$ , **63** (dmt = 2,4-diamino-6-methyl-1,3,5-triazine,  $\text{H}_2\text{suc}$  = succinic acid).<sup>84</sup> **62** exhibits a 2D sheet structure, having two  $\text{Ag}^+$  ions in an asymmetric unit (Fig. 39a); the two-fold axis passes

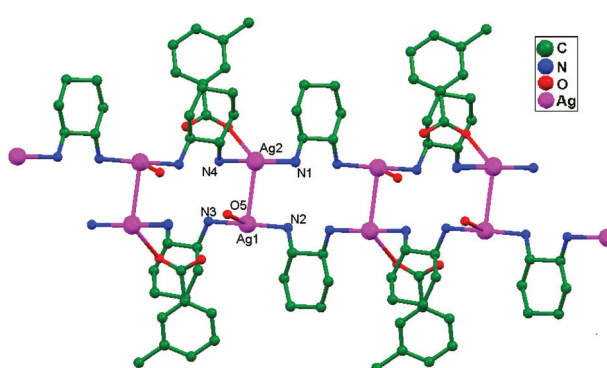


Fig. 38 The 1D polymeric structure of **61**, showing ligand-unsupported Ag–Ag contacts.

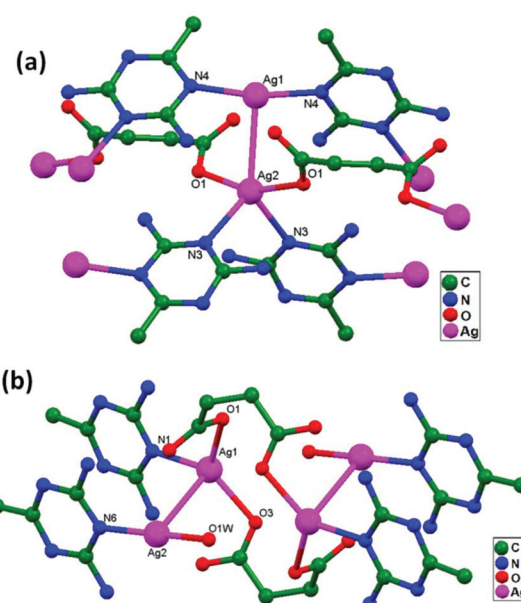
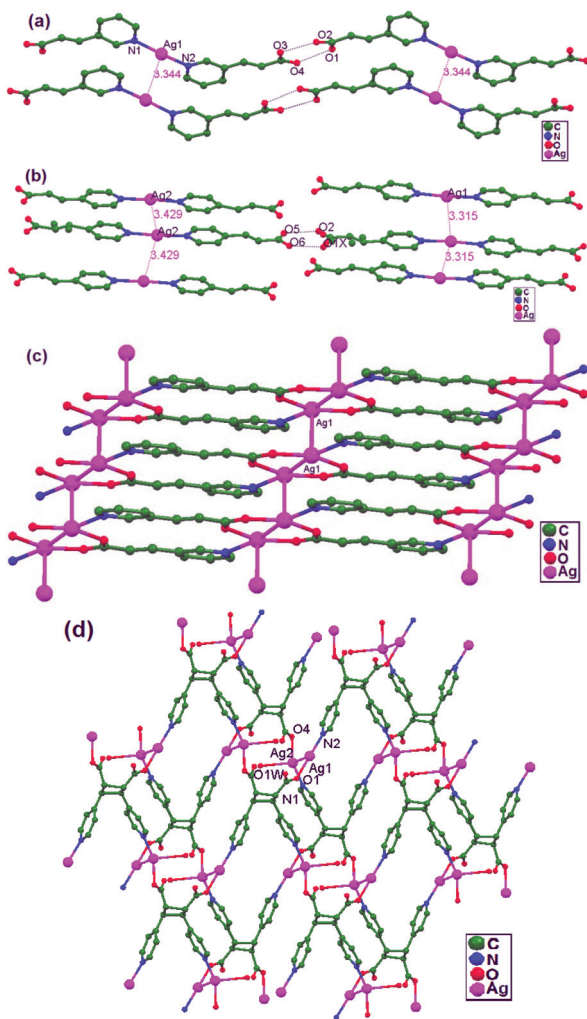


Fig. 39 The molecular structure of (a)  $[\text{Ag}_2(\text{dmt})_2(\text{suc})\cdot \text{H}_2\text{O}]_n$ , **62**, and (b)  $[\text{Ag}_2(\text{dmt})_2(\text{suc})(\text{H}_2\text{O})\cdot 0.5\text{H}_2\text{O}]$ , **63**, showing ligand-unsupported argentophilic interactions.

through Ag1 and Ag2, and, as a result, both Ag1 and Ag2 are half-occupied and the geometries of the Ag1 and Ag2 atoms are nearly square planar and seesaw, respectively. The Ag1–Ag2 contact distance is 3.106(15) Å, indicating the existence of argentophilicity, which promotes the aggregation of silver(I) centers. Tetranuclear **63** is composed of two suc-bridged symmetry-related dinuclear  $[\text{Ag}_2(\text{dmt})_2]$  subunits, in which a ligand-unsupported Ag–Ag separation distance of 3.146(16) Å was observed (Fig. 39b).

Vittal and coworkers, in 2011, attempted to orient the C=C bonds in *trans*-3-(3'-pyridyl)acrylic acid (3-PAH) in  $\text{Ag}^+$  ion coordination polymers,<sup>5</sup> utilizing Ag–Ag contacts. Both neutral and deprotonated ligands were employed to synthesize the compounds  $[\text{Ag}(3\text{-PAH})_2]\cdot (\text{BF}_4^-)$ , **64**,  $[\text{Ag}(3\text{-PAH})_2]\cdot (\text{ClO}_4^-)\cdot \text{H}_2\text{O}$ , **65**, and  $[\text{Ag}(3\text{-PA})\cdot 1.5\text{H}_2\text{O}]$ , **66**. Both **64** and **65** are isotypical hydrogen bonded polymers of  $\text{Ag}^+$ -based compounds, whereas **66** is a coordination polymer. Two  $[\text{Ag}(3\text{-PAH})_2]^+$  cations stack in a parallel orientation, which may be attributed to weak anion unsupported argentophilic interactions (Fig. 40a and b), with a Ag–Ag distance of 3.34 Å in both compounds **64** and **65**. In **66**, the pyridyl N atoms are bonded to neighboring  $[\text{Ag}(3\text{-PA})]$  repeating units to form a 1D ribbon-like polymer, which extends approximately along the [0 1 1] direction. These 1D ribbons (Fig. 40c) are further slip-stacked in a parallel arrangement (with a Ag–Ag–Ag angle of 34°) via ligand-unsupported argentophilic interactions, with a Ag–Ag distance of 3.61 Å. In the compound  $[\text{Ag}_2(\text{HH-4,4-BPCD})(\text{H}_2\text{O})]\cdot (2\text{H}_2\text{O})(0.5\text{MeOH})$  (HH-4,4-BPCD = 3,4-bis(4'-pyridyl)cyclobutane-1,2-dicarboxylic acid), **67**, each HH-4,4-BPCD ligand is bonded to four different  $\text{Ag}^+$  ions, giving rise to a 2D polymeric structure (Fig. 40d). The connectivity of the 2D polymeric sheets involves rhomboids, and these are commonly known as (4,4) grids, which further



**Fig. 40** Ligand-unsupported argentophilic interactions forming (a) a zigzag chain in **64**, (b) a polymeric chain in **65**, (c) a ribbon-like network in **66**, and (d) a 2D polymeric network in **67**.

accumulate through ligand-unsupported argentophilic interactions ( $\text{Ag1-Ag2} = 3.11 \text{ \AA}$ ). These  $\text{Ag-Ag}$  contacts lead to the construction of rare examples of 16-, 20-, and 24-membered argentophilic interaction assisted metallomacrocyclic rings.

Zhang and coworkers, in 2011, synthesized  $[\text{Ag}_2(\text{L1})_2 \cdot \text{AgNO}_3]_\infty$  ( $\text{L1} = 4\text{-C}_2\text{H}_4\text{CO}_2\text{CH}_3$ ), **68**, *via* reacting one ethynide group with three  $\text{Ag}^+$  ions to form a complex unit. These units aggregate *via* sharing  $\text{Ag}^+$  ions with the other three units to afford silver columns,<sup>6</sup> which are further linked through argentophilic interactions ( $\text{Ag2-Ag2C} = 3.173(11) \text{ \AA}$ ) to generate a 2D network (Fig. 41). Huang and coworkers, in 2011, prepared the compound  $[\text{Ag}_{1.5}(\text{apym})(\text{nta})_{0.5}]_n$  ( $\text{apym} = 2\text{-aminopyrimidine}$ , and  $\text{H}_3\text{nta} = \text{nitrilotriacetate}$ ), **69**, in which the  $\mu_2\text{-apym}$  ligands link  $\text{Ag}^+$  ions to form a 1D double-chain incorporating ligand-unsupported  $\text{Ag-Ag}$  interactions with a distance of  $3.020(3) \text{ \AA}$ . The  $\text{nta}_3^-$  ligands extend the 1D double-chains (Fig. 42) into a 3D framework.<sup>7</sup>

Yeşilel and coworkers, in 2012, reported a 3D framework  $[\{\text{Ag}_4(\mu_4\text{-pzdc})_2(\mu\text{-en})_2\} \cdot \text{H}_2\text{O}]_n$ , **70**, obtained *via* the reaction of

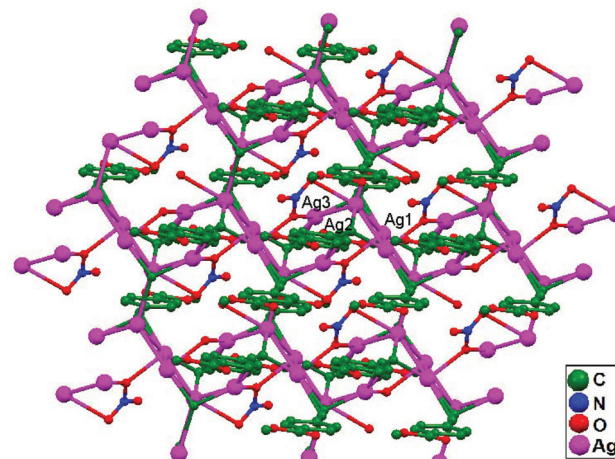


**Fig. 41** The formation of a 2D network *via* ligand-unsupported argentophilic interactions in **68**.

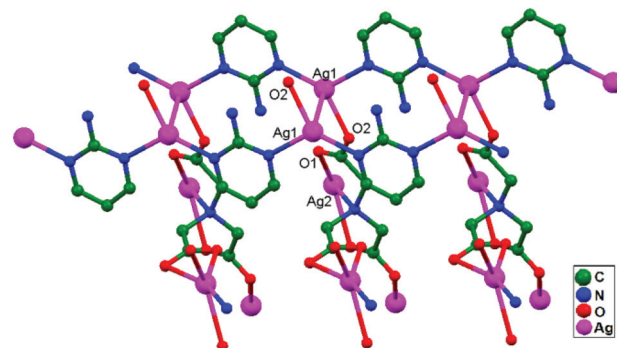


**Fig. 42** A view of the 1D double chain involving ligand-unsupported  $\text{Ag-Ag}$  contacts in **69**.

silver(I)-pyrazine-2,3-dicarboxylate (pzdc) with ethylenediamine (en). All four  $\text{Ag}^+$  ions show variable coordination geometries and are connected *via* the carboxylate oxygen atoms of pzdc to construct a 1D tetrานuclear building unit. The adjacent 1D blocks are connected through (en) ligands to form a 2D layer structure, which is further connected into a 3D framework *via* ligand-unsupported argentophilic interactions ( $\text{Ag1-Ag2} = 3.096 \text{ \AA}$  and  $\text{Ag3-Ag4} = 3.307 \text{ \AA}$ ). Thus, the presence of argentophilic interactions plays a vital role in the formation of the 3D coordination framework (Fig. 43). The presence of such useful interactions was also established on the basis of measured ( $2.36 \text{ kcal mol}^{-1}$ ) and calculated ( $1.74 \text{ kcal mol}^{-1}$ ) stabilization energies.<sup>8</sup>

Hardie and coworkers, in 2012, synthesized the compound  $\{[\text{Ag}_3(\text{NMP})_6(\text{L1})_2] \cdot 3(\text{ClO}_4)\}_\infty$  ( $\text{L1} = \text{tris(isonicotinoyl-}N\text{-oxide) cyclotri-guaiaicylene}$ , and  $\text{NMP} = N\text{-methylpyrrolidone}$ ), **71**. In the crystal structure, two crystallographically dissimilar  $\text{Ag}^+$  ions ( $\text{Ag1}$  and  $\text{Ag2}$ ) are present. Of these two,  $\text{Ag1}$  is positioned on a 3-fold inversion axis and  $\text{Ag2}$  is located on a 3-fold rotation axis. The geometry around  $\text{Ag1}$  is distorted octahedral and it is connected to one pyridyl-*N*-oxide group from six sym-

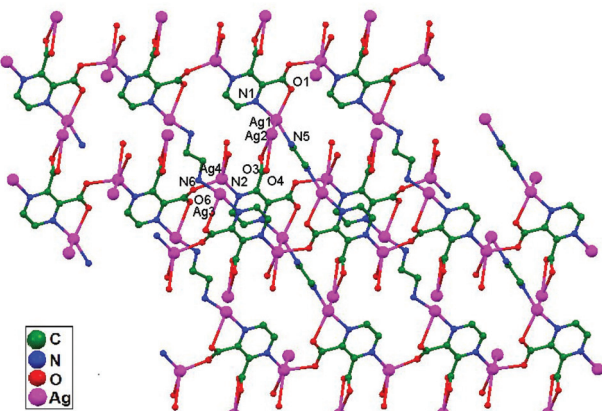


Fig. 43 The 3D metal–organic framework formed through ligand-unsupported argentophilic interactions in **70**.

metry equivalent ligands (L1). There are further interactions with two Ag<sub>2</sub> ions through ligand-unsupported argentophilic interactions with Ag–Ag separation (3.275(9) Å). The Ag<sub>3</sub> argentophilic trimer in **71** is centrosymmetric and exactly linear. The 3D coordination polymer formed between the Ag<sup>+</sup> ions and L1 has 3,6-connectivity with a pyrite-like (**pyr**) network.<sup>9</sup>

In 2012, Sun, Huang, and coworkers reported a novel silver (i) wire sustained *via* 4-*tert*-butylbenzoate and ligand-unsupported Ag–Ag interactions. This compound, [Ag<sub>3</sub>(tbb)<sub>3</sub>(NH<sub>3</sub>)<sub>2</sub>]<sub>n</sub> (Htbb = 4-*tert*-butylbenzoic acid), **72**, has three tbb ligands coordinated with three Ag<sup>+</sup> ions to form a trinuclear subunit. The inversion-related subunits are further extended into an infinite 1D zigzag silver(i) wire through ligand-unsupported Ag–Ag contacts (3.028(14)–3.091(17) Å) (Fig. 44), which play an important role in forming the infinite silver(i) wire.<sup>22</sup>

In 2012, Song, Zhang, and coworkers synthesized a novel coordination polymer Ag<sub>4</sub>L<sub>2</sub>(4,4'-bpy)(H<sub>2</sub>O)<sub>2</sub>·6H<sub>2</sub>O (H<sub>2</sub>L = bicyclo[2.2.2]oct-7-ene-2,3,5,6-tetracarboxydiimide, and 4,4'-bpy = 4,4'-bipyridine), **73**, which exhibits a two-fold interpenetrated array. Remarkably, adjacent sets of 2D interpenetrating sheets are ultimately cross-linked into an unusual 3D self-

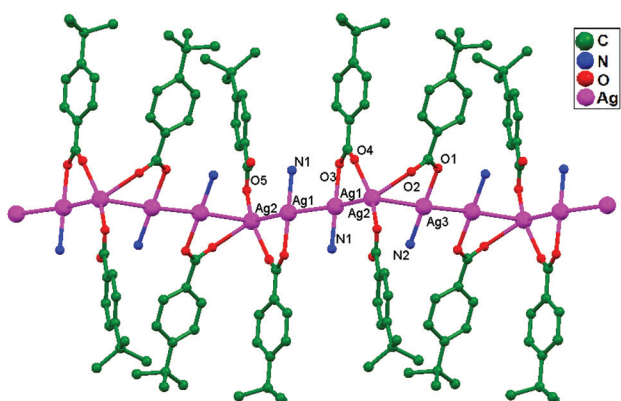


Fig. 44 The 1D silver wire incorporating ligand-supported and unsupported Ag–Ag contacts in **72**.

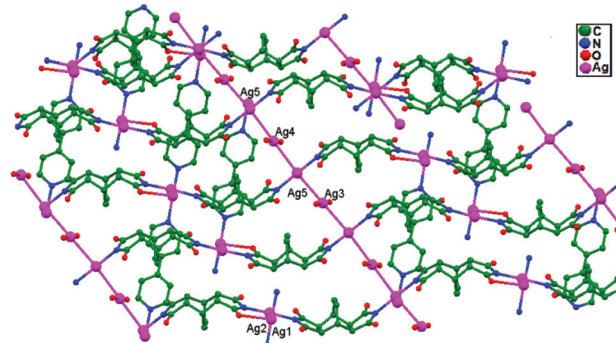


Fig. 45 The 3D structure, in which adjacent sets of parallel interpenetrating (4,4) nets are joined together through ligand-unsupported Ag–Ag bonds, of compound **73**.

penetrating network (Fig. 45) with **mbc** topology when ligand-unsupported Ag–Ag bonds (3.087 Å for Ag<sub>3</sub>–Ag<sub>5</sub> and 3.114 Å for Ag<sub>4</sub>–Ag<sub>5</sub>) are taken into account.<sup>49</sup>

In 2013, Manzano and coworkers synthesized two dimeric compounds [Ag(HL1)(OTf)]<sub>2</sub>, **74**, and [Ag(HL2)(OTf)]<sub>2</sub>, **75** (HL1 = *N,N*-diethyl-4,6-bis(3,5-dimethyl-1*H*-pyrazol-1-yl)-1,3,5-triazin-2-amine, and HL2 = 2-methoxy-4,6-bis(3,5-dimethyl-1*H*-pyrazol-1-yl)-1,3,5-triazine). The monomeric units are situated in a parallel and head-to-tail fashion to form dimers (Fig. 46a and b) that are apparently connected *via* unsupported argentophilic interactions.<sup>39</sup> The distances of these Ag–Ag contacts are

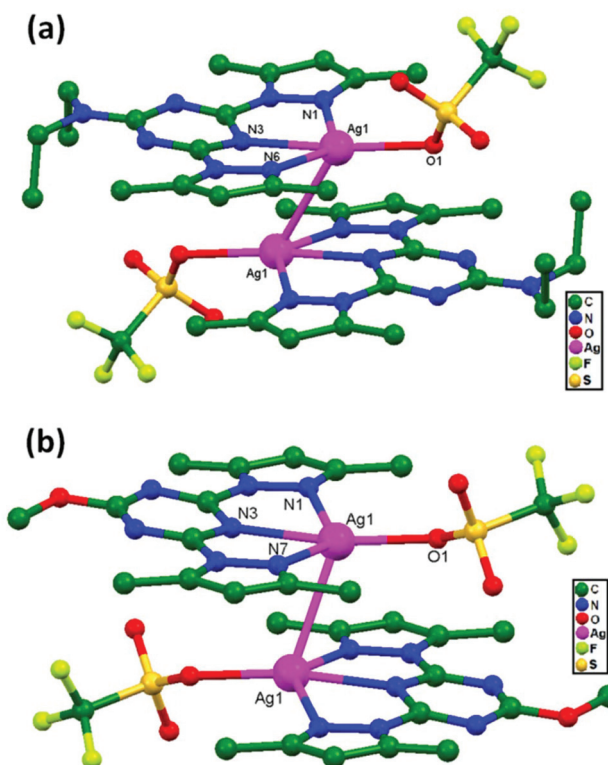


Fig. 46 The molecular structures of (a) [Ag(HL1)(OTf)]<sub>2</sub>, **74**, and (b) [Ag(HL2)(OTf)]<sub>2</sub>, **75**, showing ligand-unsupported argentophilic interactions.

3.194(7) and 3.263(7) Å for **74** and 3.132(4) Å for **75**, which are comparatively shorter than the summation of van der Waals radii for silver atoms. In addition to the Ag–Ag contacts, other supramolecular interactions, such as hydrogen bond, anion–π, CH–π contact, and π–π stacking interactions, are also present in the dimers.

In 2014, Wu and coworkers synthesized an infinite silver(I) coordinated 4<sub>1</sub>-helical chain,  $[\text{Ag}(\text{Hdpma})](\text{NO}_3)_2 \cdot \text{H}_2\text{O}$ , **76**, *via* the self-assembly of  $\text{AgNO}_3$  and dpma (di(3-pyridylmethyl) amine). This helix is interwoven 5-fold and has a topologically diamondoid-like net (Fig. 47a) that is extended *via* ligand-unsupported helix-to-helix argentophilic interactions (3.068(6) Å) into a 3D framework. Distinctive anion–exchange reactions result in a significant single-crystal-to-single-crystal structural conversion from the 1D helix structure of **76** to the 0D molecular loop  $[\text{Ag}(\text{dpma-NO})(\text{NO}_2)]_2$ , **77**, which is an *N*-nitroso compound (Fig. 47b). Compound **77** forms a chair-like  $\text{Ag}_2\text{L}_2$  molecular loop structure, and these molecular loops stack well along the crystallographic *a* axis, with an intermolecular argentophilic interaction distance of 3.094(5) Å, and create an infinite chain-like array with the appearance of a strip of fused loops. Afterward, this chain interacts with another chain *via* π–π interactions (3.62 Å) between the closed pyridine rings, forming a 2D supramolecular layer array.<sup>50</sup>

Miguel and coworkers, in 2014, first isolated the precursor  $[\text{H}_2\text{bisMeOEtIm}]_2$  ( $\text{bisMeOEtIm}$  = methylenebis(*N*-2-methoxyethyl)-imidazole-2-ylidene) as a crystalline material. After that, a solution of this precursor in acetonitrile was treated with  $\text{AgNO}_3$  to achieve anion exchange and, subsequently, with  $\text{Ag}_2\text{O}$  to yield  $[\text{Ag}_2(\text{bisMeOEtIm})_2](\text{NO}_3)_2$ , **78**. From the solid-state characterization of compound **78**, Ag–Ag contacts are the

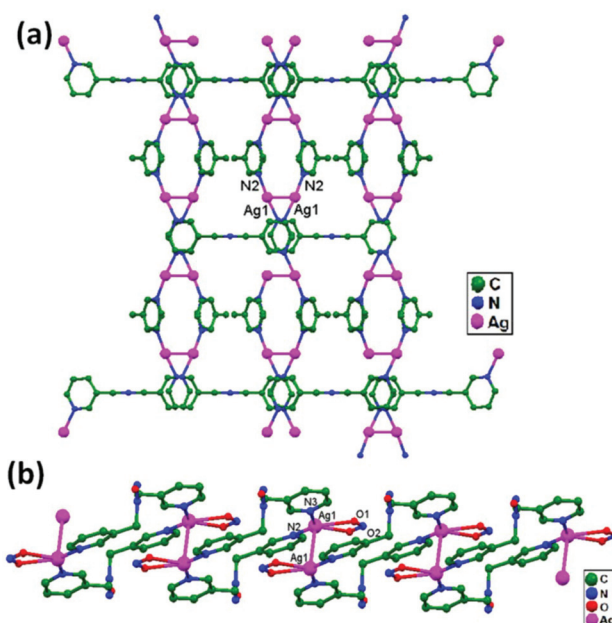


Fig. 47 (a) The diamondoid-like network extended *via* ligand-unsupported helix-to-helix argentophilic interactions in **76**, and (b) the ligand-unsupported argentophilic interactions forming polymeric chains in **77**.

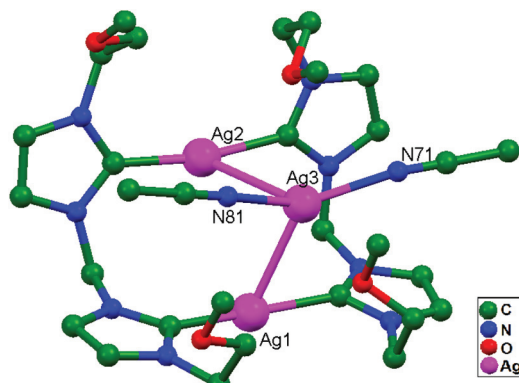


Fig. 48 The molecular structure of **79**, showing ligand-unsupported argentophilic interactions.

only bonding interactions between the host and guest, overcoming their inherent electrostatic repulsion. The Ag1–Ag2 distance (3.451(5) Å) slightly exceeds two times the silver-atom van der Waals radius (3.44 Å). However, considering the absence of additional remarkable interactions of  $\text{Ag}^+$  ions with surrounding atoms, despite this long Ag1–Ag2 distance, the existence of Ag–Ag interactions should not be fully discarded here.<sup>85</sup> After the addition of  $\text{LiBF}_4$  to a solution mixture of **78** and  $\text{AgNO}_3$ , suitable crystals for X-ray analysis were isolated as  $[\text{Ag}(\text{CH}_3\text{CN})_2 \subset \text{Ag}_2(\text{bis-MeOEtIm})_2](\text{NO}_3)_2(\text{BF}_4)_2$ , **79**. The Ag–Ag host–guest distances are relatively short, 2.823(4) Å (Ag1–Ag3) and 2.995(4) Å (Ag2–Ag3), and this robustly suggests the existence of Ag–Ag contacts between Ag3 (guest atom) and both Ag1 and Ag2 (hosting atoms) (Fig. 48). Thus, it represents a clear example of ligand-unsupported argentophilicity. The existence of same kind of Ag–Ag interactions has been established in the solution state; this might be identified as a preliminary step in a transmetalation mechanism using closed-shell metal centers as transferring agents.

Liu, Cui, and coworkers, in 2014, synthesized the compounds  $[(\text{AgL})\text{ClO}_4]$ , **80**, and  $[(\text{AgL})\text{BF}_4]$ , **81** (L: a *C*<sub>2</sub>-symmetric 1,1'-biphenyl-type ligand with *ortho* positions functionalized with pyridyl Schiff-base groups), *via* layering a solution of  $\text{AgClO}_4$  in  $\text{CH}_3\text{CN}$ -isopropyl alcohol and a solution of  $\text{AgBF}_4$  in  $\text{CH}_3\text{CN}$ -THF, respectively. In **80**, a chiral 2D lamellar network is assembled from interlinked 1D polymeric chains *via* argentophilic interactions (Ag–Ag = 3.167(2) and 3.195(2) Å) are sustained by mono- or bidentate  $\text{ClO}_4^-$  ions *via* weak Ag–O contacts with distances in the range of 2.436(11)–2.748(11) Å, directing the pack of parallel 1D chains into a 2D network in the *ab* plane. Compound **81** is also a 2D chiral framework built from intertwined polymeric chains (Fig. 49b). Adjacent  $\text{Ag}^+$  ions are thus linked *via* the biphenyl backbones of the ligands to give an infinite zigzag chain along the [1 0 1] direction. These 1D strands are interlinked *via* ligand-unsupported short argentophilic interactions, with Ag–Ag separation of 3.098(13) Å (significantly shorter than the van der Waals contact distance of 3.44 Å), to form 2D lamellar frameworks, which stack on top of

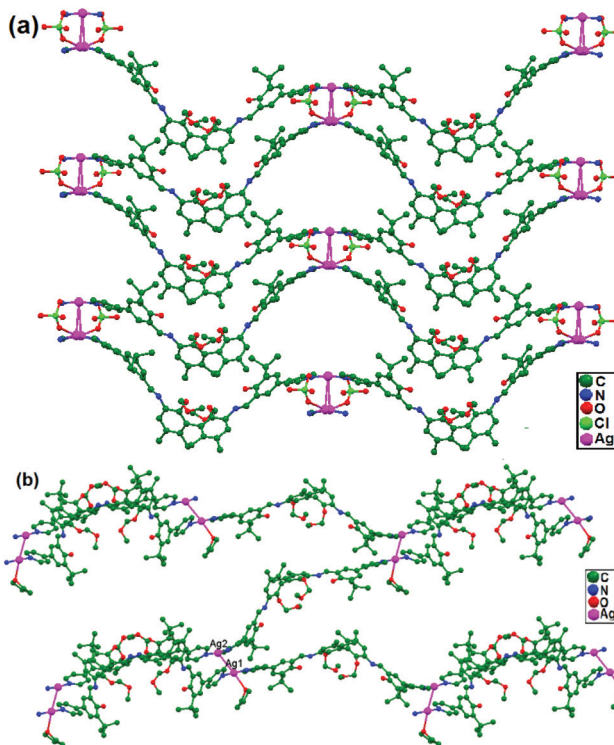


Fig. 49 (a) The chiral 2D lamellar network in **80**, and (b) the 2D chiral framework built from intertwined polymeric chains in **81**.

each other along the *a* axis in a staggered fashion to generate a 3D supramolecular structure.<sup>86</sup>

Yeşilel and coworkers, in 2014, reported the compound  $[\text{Ag}_2(\text{Hssa})(\text{daoc})]_n$  (Hssa = 5-sulfosalicylate, and daoc = 1,8-diaminoctane), **82**, in which zigzag polymeric chains assemble from alternating  $\text{Ag}^+$  ions and ligands (Hssa and daoc) linked *via* unsupported Ag–Ag interactions. The  $[\text{Ag}_2(\text{Hssa})_2]$  metallo-ligands produce a 1D coordination polymer running parallel to the [1 0 0] direction (Fig. 50), with  $\text{Ag1–Ag1}$  separation of 7.722 Å. These 1D polymeric chains are connected *via* ligand-unsupported argentophilic interactions to form a 3D coordination polymer, with an  $\text{Ag1–Ag2}$  distance of 3.131(11) Å.<sup>34</sup>

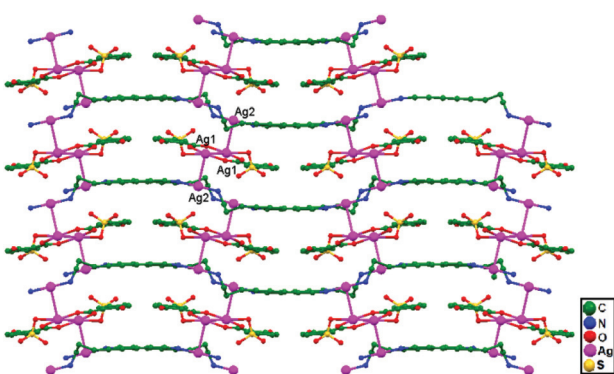


Fig. 50 Zigzag polymeric chains assembled via ligand-unsupported argentophilic interactions in compound **82**.

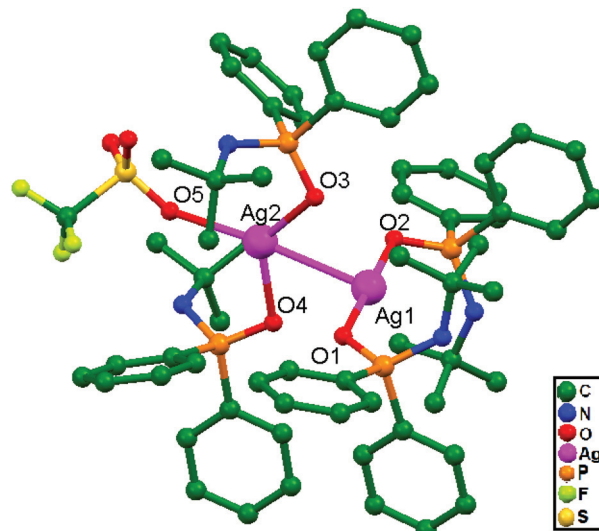


Fig. 51 The molecular structure of compound **83** showing ligand-unsupported argentophilic interactions; hydrogen atoms are excluded for clarity.

Zyl and coworkers, in 2015, prepared a rare silver(I) dinuclear compound,  $[\text{Ag}(\text{CF}_3\text{SO}_3)\{\text{OPPh}_2\text{N}(\text{H})\text{CMe}_3\}_2\{\text{Ag}(\text{OPPh}_2\text{N}(\text{H})\text{CMe}_3)_2\}]\text{SO}_3\text{CF}_3$ , **83**, with *N*-*tert*-butyl-1,1-diphenylphosphinamine ( $\text{Ph}_2\text{P}(\text{N}(\text{H})\text{CMe}_3)_2$ ), which was subsequently treated with solid  $\text{AgSO}_3\text{CF}_3$  in THF. The compound consists of ligand-unsupported Ag–Ag interactions at a distance of 2.897(3) Å, coordinating through two oxygen donor atoms from the two separate silver units (A & B) (Fig. 51). The silver unit A consists of a three-coordinate silver center that is twisted considerably from linear geometry because of coordination with the triflate oxygen donor atom, but unit B remained effectively as a two-coordinate system with linear geometry.<sup>35</sup>

Englert and coworkers, 2016, prepared the compounds  $[\text{Ag}_6(\text{HacacPz})_6]\cdot 2\text{EtOH}$ , **84**,  $[\text{Ag}_6(\text{HacacPz})_6]\cdot 4\text{EtOH}$ , **85**, and  $[\text{Ag}_6(\text{HacacPz})_6]\cdot 0.5\text{CH}_2\text{Cl}_2\cdot 1.5\text{C}_4\text{H}_{10}\text{O}$ , **86**, from  $\text{H}_2\text{acacPz}$  (3-(3,5-dimethylpyrazol-4-yl)pentane-2,4-dione) with  $\text{Ag}(\text{PhCO}_2)$  in different solvent systems. The ligand  $\text{H}_2\text{acacPz}$  may be deprotonated at either the N or O donor site in the presence of  $\text{Ag}^+$  ions. Silver benzoates are adequately basic to deprotonate the pyrazolyl component. The deprotonated  $\text{HacacPz}^-$  then bridges two  $\text{Ag}^+$  ions, and this type of coordination approach results in analogous distinct  $[\text{Ag}_6(\text{HacacPz})_6]$  molecules in compounds **84**, **85**, and **86**. In all independent  $[\text{Ag}_6(\text{HacacPz})_6]$  molecules, pairs of  $\text{Ag}_3$  triangles are formed; their Ag–Ag edge distances range between 3.3 and 3.5 Å. The accumulation of  $\text{Ag}_3$  triangles into a hexanuclear moiety is accomplished *via* considerably shorter Ag–Ag contacts (2.9 Å), which arise undeviatingly in addition to the absence of any bridging ligand. Due to the concomitant presence of ligand-supported and ligand-unsupported contacts (Fig. 52), the more general expression “aggregate” is preferred. In the solids **84**, **85**, and **86**, solvent molecules fill the voids between the large  $[\text{Ag}_6(\text{HacacPz})_6]$  aggregates. **84** contains two molecules of ethanol per unit cell or hexanuclear aggregate. In **85**, eight

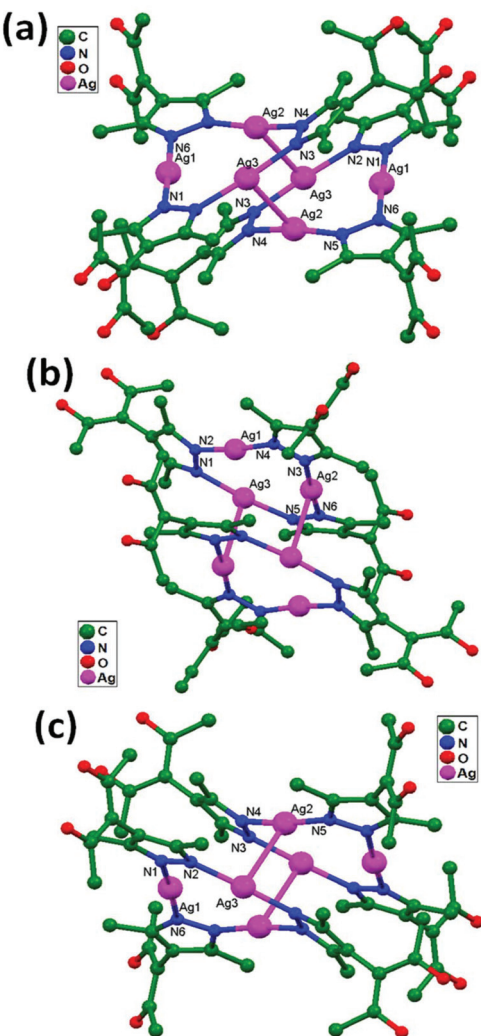


Fig. 52  $\text{Ag}_6(\text{HacacPz})_6$  cores in compounds (a) 84, (b) 85, and (c) 86, showing ligand-unsupported argentophilic interactions.

molecules of ethanol per unit cell occupy two voids. A more complex situation is encountered in the case of 86. The compound contains well-localized  $\text{CH}_2\text{Cl}_2$  with half-occupied atom sites in general positions, *i.e.*, one  $\text{CH}_2\text{Cl}_2$  per unit cell and three strongly disordered molecules of 2-butanol in two voids per unit cell.<sup>36</sup>

In 2017, Omondi, Nyamori, and coworkers, synthesized novel  $[(\text{AgO}_2\text{C}_2\text{F}_3)_2 \cdot \text{L}_2]$  compounds (where  $\text{L} = (\text{E})\text{-N}\text{-}(1\text{-pyridin-2-yl})\text{ethylidene}\text{-aniline}$  for compound 87, and  $\text{L} = (\text{E})\text{-N}\text{-}(1\text{-pyridin-2-ylmethylene})\text{-aniline}$  for compound 88) *via* the reaction of  $\text{AgO}_2\text{C}_2\text{F}_3$  with 2-pyridinyl Schiff base ligands. From structural studies of compounds 87 and 88, they were shown to be dinuclear, with each  $\text{Ag}^+$  ion chelated by a ligand in a bidentate manner *via* pyridinyl and imine nitrogen atoms. The geometries of 87 and 88 allow for strong unsupported argentophilic interactions, where the  $\text{Ag}\text{-Ag}$  bond distances are 2.943 (2) Å in 87 and 3.173(13) Å in 88 (Fig. 53), both shorter than the sum of the van der Waals radii (3.44 Å) of two silver atoms. The difference between the  $\text{Ag}\text{-Ag}$  bond distances in 87 and 88

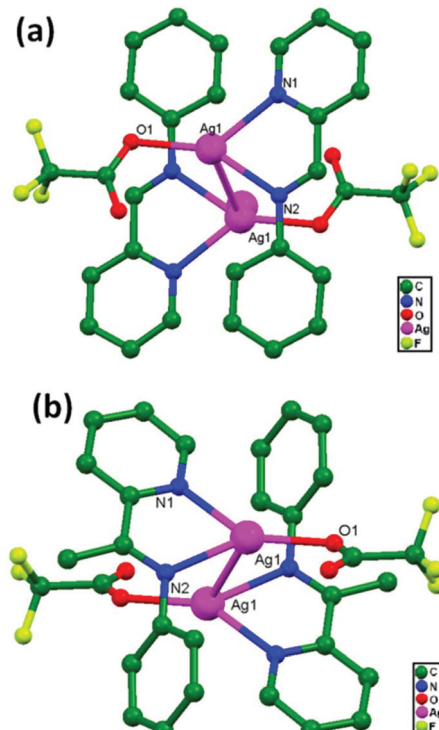


Fig. 53 The molecular structures of (a) 87 and (b) 88, showing ligand-unsupported  $\text{Ag}\text{-Ag}$  contacts.

can be attributed to the presence of imine carbon, which plays a crucial role in stabilizing closed-shell  $\text{d}^{10}\text{-d}^{10}$  interactions. The fact that these  $\text{Ag}\text{-Ag}$  interactions are not ligand-supported points towards the presence of a real bond.<sup>37</sup>

## Ligand-unsupported argentophilic interactions in bimetallic compounds

Leznoff and coworkers, in 2002, reported the compound  $[\text{Cu}(\text{en})_2][\text{Ag}_2(\text{CN})_3][\text{Ag}(\text{CN})_2]$  (en = ethylenediamine), 89, which forms 1D chains of alternating  $[\text{Ag}(\text{CN})_2]^-$  and  $[\text{Ag}_2(\text{CN})_3]^-$  units *via* argentophilic interactions at a distance of 3.102(1) Å (Fig. 54). These 1D chains are further united into a 2D arrangement *via* strong Ag-cyano(N) (2.572(3) Å) interactions. Another reported compound,  $[\text{Cu}(\text{dien})\text{Ag}(\text{CN})_2]_2[\text{Ag}_2(\text{CN})_3][\text{Ag}(\text{CN})_2]$  (dien = diethylenetriamine), 90, also forms 1D chains of alternating  $[\text{Cu}(\text{dien})]^{2+}$  and  $[\text{Ag}(\text{CN})_2]^-$  units with  $\text{Cu}^{2+}$  ions connected in an apical/equatorial fashion. These chains are cross-linked through the  $[\text{Ag}_2(\text{CN})_3]^-$  units *via* argentophilic interactions (3.172(8) Å) and held weakly in a 3D array *via* argentophilic interactions (3.289(5) Å) between  $[\text{Ag}(\text{CN})_2]^-$  in the 2D array. The influence of argentophilic interactions on the structures of 89 and 90 is apparent, with  $\text{Ag}\text{-Ag}$  bond lengths ranging from 3.102(1) to 3.289(5) Å. An increase in dimensionality from zero to one in  $[\text{Cu}(\text{en})_2][\text{Ag}_2(\text{CN})_3][\text{Ag}(\text{CN})_2]$ , 89, is assisted by  $\text{Ag}\text{-Ag}$  contacts. The dimensionality of  $[\text{Cu}(\text{dien})\text{Ag}(\text{CN})_2]_2[\text{Ag}_2(\text{CN})_3][\text{Ag}(\text{CN})_2]$ , 90, is raised from 1D chains to a

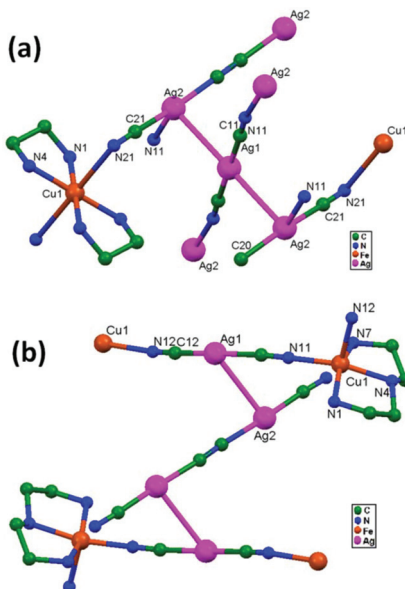


Fig. 54 The molecular structures of (a)  $[\text{Cu}(\text{en})_2][\text{Ag}_2(\text{CN})_3][\text{Ag}(\text{CN})_2]$ , 89, and (b)  $[\text{Cu}(\text{dien})\text{Ag}(\text{CN})_2]_2[\text{Ag}_2(\text{CN})_3][\text{Ag}(\text{CN})_2]$ , 90, showing the ligand-unsupported Ag–Ag contacts.

3D network as a sole result of Ag–Ag contacts, exhibiting their use as an element in crystal engineering design, the same as  $\text{Au}^+–\text{Au}^+$  interactions.<sup>33</sup>

In 2003, Chaudhuri and coworkers prepared a heterometallic 3D coordination polymer  $[\text{AgNa}(\text{C}_5\text{O}_5)(\text{H}_2\text{O})_2]_n$  ( $\text{C}_5\text{O}_5^{2-}$  = the croconate dianion), 91, in which croconate dianions interweave alternately aligned and layered  $-\text{Na}-(\mu-\text{H}_2\text{O})_2-\text{Na}-(\mu-\text{H}_2\text{O})_2-$  and  $-\text{Ag}-\text{Ag}-\text{Ag}-$  chains along the *b* direction. The infinite  $-\text{Ag}-\text{Ag}-\text{Ag}-$  zigzag chains have a Ag–Ag distance of 3.170 (2) Å, which is shorter than twice the van der Waals radius (3.44 Å), indicating the presence of argentophilic interactions. The Ag–Ag contacts are unsupported by bridging ligands, and the distances lie within the range observed for other argentophilic bonds in the literature.<sup>51</sup> The  $-\text{Ag}-\text{Ag}-\text{Ag}-$  and  $-\text{Na}-(\mu-\text{H}_2\text{O})_2-\text{Na}-(\mu-\text{H}_2\text{O})_2-$  chains line up alternately and strictly in the *ab* plane (Fig. 55).

In 2005, Goeta and coworkers reported the compound  $\{\text{Fe}(\text{pmd})[\text{Ag}(\text{CN})_2][\text{Ag}_2(\text{CN})_3]\}$  (pmd = pyrimidine), 92, which has five  $[\text{FeN}_6]$  pseudo-octahedral sites linked *via* pmd,  $[\text{Ag}(\text{CN})_2]^-$ , and  $[\text{Ag}_2(\text{CN})_3]^-$  bridging ligands to form unprecedented 3D (6,6) topology (Fig. 56). The iron layers are associated through  $[\text{Ag}(\text{CN})_2]^-$  and  $[\text{Ag}_2(\text{CN})_3]^-$ , and the separation of such layers occurs *via* dense layers of silver atoms with the help of observed strong argentophilic interactions. These ligand-unsupported Ag–Ag interactions define linear trinuclear, angular trinuclear, and hexanuclear moieties. The shortest Ag–Ag distances between  $[\text{Ag}(\text{CN})_2]^-$  and  $[\text{Ag}_2(\text{CN})_3]^-$  are in the range of 2.98–3.02, only slightly longer than the silver metal distance (2.89 Å).<sup>52</sup>

In 2008, Jiang, Lu, and coworkers reported a 1D helical chain of  $\{[\text{Ni}(\text{f-}R\text{-L})][\text{Ag}(\text{CN})_2]_2\}_n$ , 93, and one trimer of  $[\text{Ni}(\text{f-}R\text{-L})\text{Ag}(\text{CN})_2]_3[\text{ClO}_4]_3$ , 94, which were prepared from the

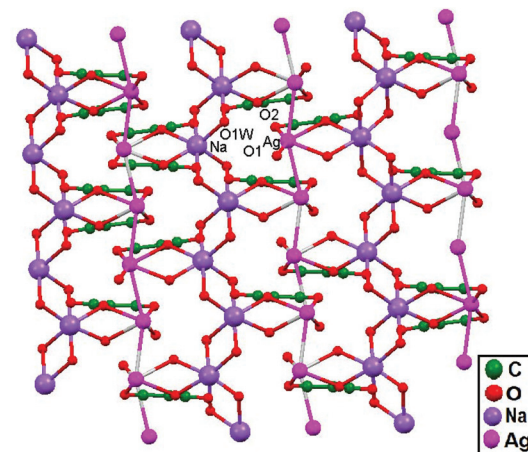


Fig. 55 A perspective view showing the connectivity of  $-\text{Ag}-\text{Ag}-\text{Ag}-$  and  $-\text{Na}-(\mu-\text{H}_2\text{O})_2-\text{Na}-(\mu-\text{H}_2\text{O})_2-$  chains in the *ab* plane in compound 91.

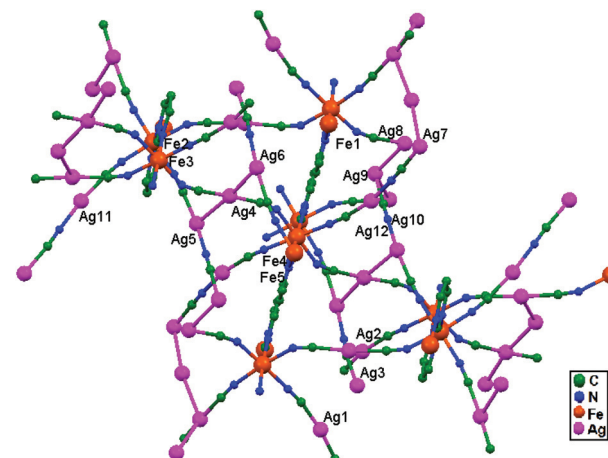


Fig. 56 The coordination environments around crystallographically inequivalent iron and silver atoms and the ligand-unsupported argentophilic interactions in  $\{\text{Fe}(\text{pmd})[\text{Ag}(\text{CN})_2][\text{Ag}_2(\text{CN})_3]\}$ , 92.

racemic and enantiopure macrocyclic compounds  $[\text{Ni}(\text{R-}R\text{-L})](\text{ClO}_4)_2$  and  $\text{K}[\text{Ag}(\text{CN})_2]$ . In 93,  $[\text{Ni}(\text{f-}RR\text{-L})][\text{Ag}(\text{CN})_2]_2$  enantiomers alternately coordinate with  $[\text{Ni}(\text{f-}SS\text{-L})][\text{Ag}(\text{CN})_2]_2$  enantiomers to form a 1D meso-helical chain (Fig. 57a) *via* ligand-unsupported Ag–Ag interactions (3.048(1) Å). These 1D chains are further connected through interchain H-bonds to generate a 2D network.<sup>53</sup> In compound 94, three  $\mu_2^+[\text{Ag}(\text{CN})_2]^-$  units alternately bridge three  $[\text{Ni}]^{2+}$  cations to generate a trimer (Fig. 57b). Three macrocycles within a trimer adopt unsymmetrical *RR/RR/SS* or *RR/SS/SS* configurations and, thus, each trimer is chiral; the whole compound of 94 crystallizes in the space group  $P\bar{1}$ , is achiral, and shows closest intra- and intermolecular Ag–Ag interactions calculated at distances of 5.764(6) and 8.117(20) Å, respectively.

Zhang and coworkers, in 2006, reported a heterobimetallic  $(\text{Zn}^{2+}-\text{Ag}^+)$  cyano-bridged coordination compound,  $[\text{Ag}_5\text{Zn}_2(\text{tren})_2(\text{CN})_9]$  (tren = tris(2-aminoethyl)amine), 95, fea-

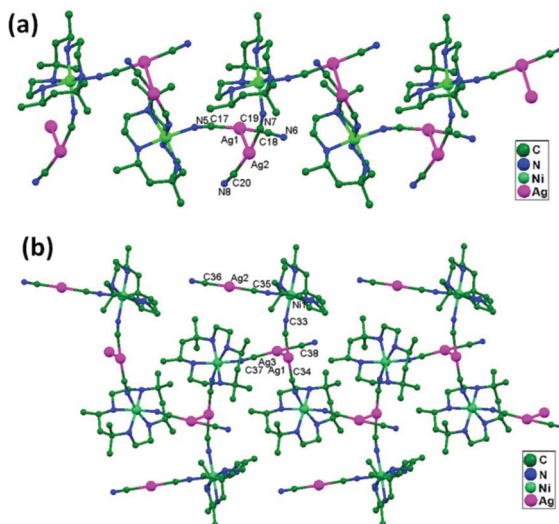


Fig. 57 Ligand-unsupported argentophilic interactions supporting the polymeric structures in (a) compound 93 and (b) compound 94.

turing rare linear pentameric units with dicyanoargentate( $\text{i}$ ) ions as building blocks, assembled *via* ligand-unsupported  $\text{d}^{10}-\text{d}^{10}$  interactions. Remarkably, five  $[\text{Ag}(\text{CN})_2]^-$  ions are assembled into unusual pentameric strings, and pentanuclear silver cords are further knotted through  $\text{CN}^-$  bridges between adjacent  $[\text{Ag}(\text{CN})_2]^-$  groups, forming one unique zigzag 1D framework (Fig. 58) with ligand-unsupported  $\text{Ag}-\text{Ag}$  distances of 3.335(6) to 3.376(7) Å.<sup>54</sup>

In 2002, Černák and coworkers reported the compound  $[\text{CuAg}(\text{CN})_2(\text{dien})_2][\text{Ag}(\text{CN})_2][\text{Ag}_2(\text{CN})_3]$ , 96, which was isolated from  $[\text{Cu}(\text{dien})_2](\text{NO}_3)_2$  and  $\text{K}[\text{Ag}(\text{CN})_2]$  (dien = diethylenetriamine) in distilled water. This structure is fashioned from  $[-\text{Cu}(\text{dien})-\text{NC}-\text{Ag}-\text{CN}-]_n^{n+}$  chains with two isolated centrosymmetric  $[\text{Ag}(\text{CN})_2]^-$  and  $[\text{Ag}_2(\text{CN})_3]^-$  ions (Fig. 59), in which short ligand-unsupported argentophilic interactions ( $\text{Ag}-\text{Ag} = 3.16-3.30$  Å) are present in the crystal structure.<sup>87</sup>

In 2014, Liu and coworkers reported the doping of potassium ions into a silver cyanide compound, which further led to

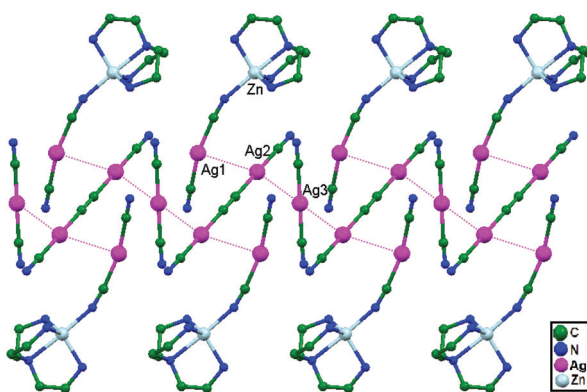


Fig. 58 Ligand-unsupported  $\text{d}^{10}-\text{d}^{10}$  interactions forming a unique zigzag 1D framework in 95.

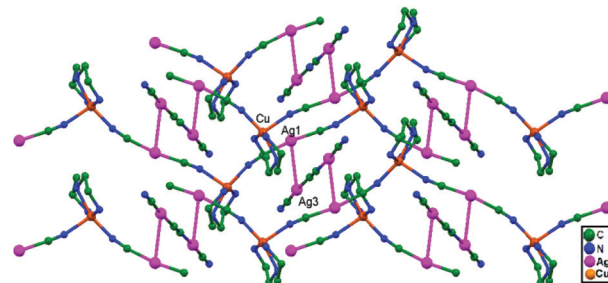


Fig. 59 Short ligand-unsupported argentophilic interactions in the polymeric compound 96.

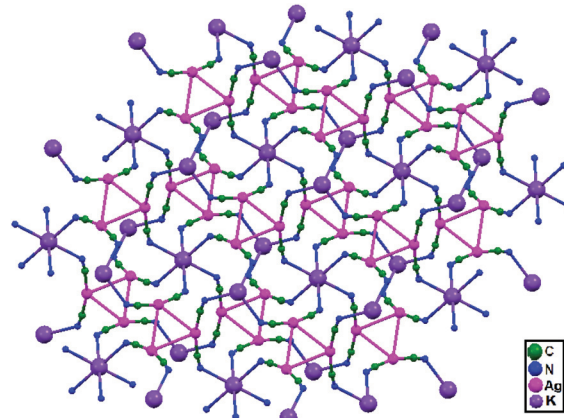


Fig. 60 The polymeric compound  $[\text{Me}_4\text{N}]_2[\text{KAg}_3(\text{CN})_6]$ , 97, showing ligand-unsupported argentophilic interactions.

a heterometallic silver-potassium cyanide compound, *i.e.*  $[\text{Me}_4\text{N}]_2[\text{KAg}_3(\text{CN})_6]$ , 97. This compound consists of a typical  $\text{NaCl}$ -type framework<sup>88</sup> with distinct ligand-unsupported argentophilic interactions ( $\text{Ag}-\text{Ag} = 3.201(9)$  Å) between three adjacent  $[\text{Ag}(\text{CN})_2]^-$  subunits (Fig. 60).

## Ligand-unsupported argentophilic interactions in polyoxometalate-based compounds

In 2013, Peng, Li, and coworkers hydrothermally synthesized the unusual  $\alpha$ -Keggin-based compound  $\{[\text{Ag}_7(\text{H}_2\text{biim})_5]\text{[PW}_{11}\text{O}_{39}\} \cdot \text{Cl}\cdot \text{H}_2\text{O}$  ( $\text{H}_2\text{biim} = 2,2'\text{-biimidazole}$ ), 98, with multinuclear silver clusters. It displays a 2D network featuring dimerized monolacunary Keggin anions  $\{\text{PW}_{11}\text{O}_{39}\}_2^-$ , which are connected through hexanuclear silver clusters. Interestingly, besides the  $\{\text{Ag}_5\}^{5+}$  clusters, other kinds of ligand-unsupported argentophilic  $\{\text{Ag}_4\}^{4+}$  clusters coexist. The  $\{\text{Ag}_4\}^{4+}$  cluster is approximately square, with four crystallographically unique silver atoms, and it is constructed *via* bridging  $\text{H}_2\text{biim}$  ligands and ligand-unsupported argentophilic interactions between  $\text{Ag}_2$  and  $\text{Ag}_4$ , having a distance of 3.131 Å and  $\text{Ag}_2-\text{Ag}_4-\text{Ag}_4\text{A}$  bond angle of 166.315° (Fig. 61). The spatial

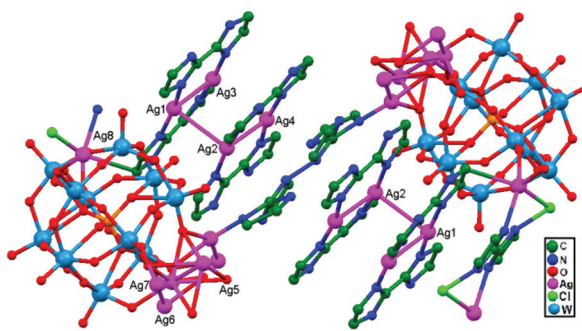


Fig. 61 The molecular structure of **98**, showing ligand-unsupported argentophilic interactions.

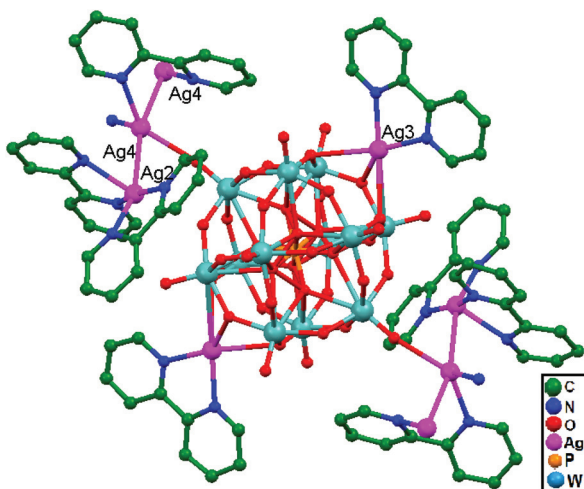


Fig. 62 The molecular structure of **99**, showing ligand-unsupported argentophilic interactions.

arrangement also allows a high degree of orbital overlap between the two silver centers and results in short Ag–Ag distances ( $\text{Ag1–Ag2} = 3.184(4)$  Å), suggesting short argentophilic interactions.<sup>55</sup>

In 2009, You, Su, and coworkers reported a novel  $\alpha$ -Keggin anion-based coordination polymer,  $[\{\text{Ag}(2,2'\text{-bpy})\}_2\{\text{Ag}_4(2,2'\text{-bpy})_6\}\{\text{PMo}_{11}\text{VO}_{40}\}]$   $[\{\text{Ag}(2,2'\text{-bpy})\}_2\{\text{PMo}_{11}\text{VO}_{40}\}]$  ( $2,2'\text{-bpy} = 2,2'\text{-bipyridine}$ ]), **99**, with argentophilic  $\{\text{Ag}_3\}^{3+}/\{\text{Ag}_4\}^{4+}$  clusters. It consists of isolated bisupporting  $[\{\text{Ag}(2,2'\text{-bpy})\}_2\{\text{PMo}_{11}\text{VO}_{40}\}]^{2-}$  anions and infinite 1D cationic chains of  $[\{\text{Ag}(2,2'\text{-bpy})\}_2\{\text{Ag}_4(2,2'\text{-bpy})_6\}\{\text{PMo}_{11}\text{VO}_{40}\}]^{2+}$  constructed from  $[\{\text{Ag}(2,2'\text{-bpy})\}_2\{\text{PMo}_{11}\text{VO}_{40}\}]^{2-}$  anions bridged via  $\{\text{Ag}_4(2,2'\text{-bpy})_6\}^{4+}$  clusters (Fig. 62), and ligand-unsupported argentophilic ( $\{\text{Ag}_3\}^{3+}$  and  $\{\text{Ag}_4\}^{4+}$ ) interactions do exist in this polymer.<sup>56</sup>

## Synthetic approaches and reticular design

The combination of various processes or systems (mixing and stirring; grinding; precipitation; and hydro-/solvothermal

methods) for synthesis, the types of ligands and metal salts that are used as starting materials, and the types of solvents and environmental conditions (temperature of the reaction mixture and pH of solution<sup>19,82</sup>) are all factors that can affect the desired final compound. To obtain the expected product with the desired molecular/crystal structure and reticular design, learning about or better understanding the whole system is necessary. Since before the year 2000, researchers have used different procedures for the synthesis of compounds, such as the simple mixing of two reagents and slow evaporation at room temperature,<sup>30,33,65,67,69,74,83</sup> precipitation methods,<sup>3,10–12,32,38</sup> refluxing the reaction mixture,<sup>25</sup> the layering of solutions of reagents,<sup>18,26,86</sup> and diffusion processes.<sup>27,31,52,70,73,75,76</sup> Imidazol-based<sup>1</sup>, mono/di/tri-substituted aromatic carboxylates,<sup>11,17,19–22,79,82,83</sup> N-heterocyclic carbene,<sup>81,85</sup> cyanide,<sup>14,46,54,87,88</sup> triazine-based,<sup>39,84</sup> biphenyl-type,<sup>46,82,86</sup> and pyrazolyl ligands<sup>10,13,36,69,80</sup> are important ligands for the preparation of silver compounds with supramolecular networks. Pyrazolyl ligands are a kind of multifunctional organic ligand that often display an *exo*-bidentate coordination mode, and bipyridyl<sup>32,49,56</sup> can be used as a ligand or co-ligand.  $C_2$ -Symmetric 1,1'-biphenyl-type ligands are excellent candidates for making helical polymers.<sup>86</sup> For the synthesis of compounds with aromatic carboxylate ligands, the pH of the reaction mixture is an important factor for controlling the deprotonation of different labile hydrogen atoms attached to the oxygen or nitrogen atoms of the ligand.<sup>19</sup> The crystal structure of the compound produced by reacting isonicotinic acid with  $\text{Ag}^+$  ions in the low pH medium shows no  $\mu_3$ -bridging mode between the isonicotinate anion and  $\text{Ag}^+$  ion. Ligand-unsupported argentophilic interactions involving compounds **27** and **28** are produced upon adjusting the solution acidity to a high pH value. The diversification in the structures of compounds **59** and **60** reveals that the use of controlled synthetic experiments, *via* regulating the molar ratios of reactants or the pH value of the solution mixture, presents an effective synthetic approach for the design and construction of novel supramolecular assemblies with unique structural traits.<sup>82</sup> It is worth mentioning that envisaging and organizing the final structures of supramolecular compounds is an immense challenge. Relevant structural features, such as Ag–Ag contacts, not only depend on the choice of counteranion but also reflect the influence of the chirality of the bridging ligand.<sup>72</sup> To obtain possible supramolecular structures, researchers have switched to hydro(solvothermal methods<sup>4,21,46,55,56,88</sup> for the preparation of compounds, *e.g.*, the synthesis of silver(I) imidazolates,<sup>4</sup> in contrast to previously utilized conventional solution methods.<sup>1</sup> In racemic compounds<sup>53,72</sup> with heterochiral strings, argentophilic interactions may arise between two adjoining polymer chains.<sup>72</sup> In homochiral structures,<sup>86</sup> the diaminocyclohexane ligand adopts a new conformation, which allows for short Ag–Ag distances within the chain.<sup>73,75,83</sup> Both the chirality of the *trans*-1,2-diaminocyclohexane ligand and the substitution pattern of the benzoate anion have a strong impact on the nature of secondary interactions perpendicular to the polymer strands. Ag–Ag interactions can increase the

dimensionality of solids from chain polymers to layer structures.<sup>83</sup> To make fluorescent coordination polymers, a conjugated and semiflexible 1,1'-biphenol ligand with *ortho* positions functionalized *via* pyridyl Schiff-base groups was chosen. N-Heterocyclic carbene behaves as a strong  $\sigma$ -donor entity in terms of the stabilization of compounds **78** and **79**. Both compounds are widely employed as transfer agents with transmetalation mechanisms that are relatively unexplored.<sup>85</sup> Assemblies of **17** and **18** involve novel and distinct cationic networks, and the irreversible conversion of **17** into **18** upon treatment with NaPF<sub>6</sub> has been carried out. This conversion is unique in that it is driven by the formation of more and stronger Ag–Ag bonds in the polymeric unit; no such transformations have been previously reported for other silver compounds to date.<sup>26</sup> It is observed from the extended structures of **17** and **18** that the latter is more stable than the former, primarily because of the greater number and strength of Ag–Ag contacts. This rationale encourages the study of the possibility of transforming **17** into **18** *via* anion exchange.<sup>26</sup>

Ligand-unsupported argentophilic interactions also affect the orientations of ligands and metal ions within the molecular structures of compounds and give rise to a variety of architectures, *e.g.*, hexamers (**1**), rhombohedral units (**7**), ladders (**12**, **54**), zigzag chains (**13**, **31**, **72**), brick-wall networks (**16**), sinusoidal chains (**17** & **18**),  $\beta$ -sheets (**20**), cyclic structures (**23**–**26**), layered structures (**29**), uninodal (6,3) (**38**) and (4,4) (**39**) networks, saw-tooth appearances (**43**), pseudo-double-metal sandwiches (**44**), wavelike layers (**47**), double-helical chains (**50**), 1D ribbons (**67**), pyrite-like (**pyr**) networks (**71**), diamondoids (**76**), and chiral lamellar networks (**80**).

## Experimental evidence for argentophilic effects

Patterson and co-workers reported that the temperature dependence of the very low energy part of Raman spectra provides more direct evidence for the significance of Ag–Ag contacts in Tl[Ag(CN)<sub>2</sub>].<sup>14</sup> However, Raman spectra at room-temperature are not well-resolved and for better resolution, spectra should be recorded under low-temperature conditions (*e.g.*, 10 and 80 K). It has been observed that the relative intensity of the broad band at  $\sim$ 100 cm<sup>−1</sup> increases in comparison to the band at  $\sim$ 50 cm<sup>−1</sup> at a temperature of 10 K because the phonon or lattice bands turn out to be less important at low temperature. Therefore, it is believed that the band at  $\sim$ 100 cm<sup>−1</sup> is not due to lattice vibrations but, instead, is due to Ag–Ag bonding gaining additional strength. The position of the peak at  $\sim$ 88 cm<sup>−1</sup> at room temperature is in the range where bands usually assigned to metal–metal stretching frequencies are observed.

The Raman-active bands at 120 and 83 cm<sup>−1</sup> for [Ag<sub>2</sub>(bsdab)<sub>3</sub>]<sub>n</sub>[NO<sub>3</sub>]<sub>2n</sub>, **7**, and 121 and 82 cm<sup>−1</sup> for [Ag<sub>2</sub>(bsdab)<sub>3</sub>]<sub>n</sub>[ClO<sub>4</sub>]<sub>2n</sub>, **8**, (where bsdab = *N,N'*-bis(salicylidene)-1,4-diaminobutane) may be assigned to Ag–Ag vibrations and are comparable to those found in related compounds.<sup>14,89</sup> In

[Ag<sub>2</sub>( $\mu$ -dcpm)<sub>2</sub>]X<sub>2</sub> compounds (X = CF<sub>3</sub>SO<sub>3</sub>: **14**, PF<sub>6</sub>: **15**; dcpm = bis(dicyclohexyl-phosphino)methane), due to the optical transparency of the phosphine ligands, the UV-vis absorption band at 261 nm in acetonitrile is assigned to the 4dσ\* → 5pσ transition derived from Ag–Ag bonding interactions. The argentophilicity of this absorption band is authenticated based on Raman spectroscopy at an excitation value of 273.9 nm, where effectively all of the Raman intensities appear as fundamental Ag–Ag stretches with a value of 80 cm<sup>−1</sup> and as overtone bands.<sup>12</sup>

ESR studies were carried out by Russell, Symons, and co-workers<sup>1</sup> on crystals of bis(imidazole)silver perchlorate, **1**, after exposure to <sup>60</sup>Co X-rays at 77 K. It should be noted that in this compound, all six Ag–Ag contacts are unsupported, and silver atoms are engaged in two (peripheral) and three argentophilic bonds. The radical generated upon irradiation shows an ESR signal with hyperfine coupling to three <sup>107</sup>Ag/<sup>109</sup>Ag and six <sup>14</sup>N nuclei, suggesting delocalization of the extra electron over the Ag<sub>3</sub> center in an orbital primarily of 5s character.

## Theoretical approaches

Besides experimental evidence based on short Ag–Ag distances in crystal structures, the presence of significant Ag–Ag interactions in Tl[Ag(CN)<sub>2</sub>], **5**, is also supported theoretically.<sup>14</sup> Extended Hückel calculations from the literature indicate the thermodynamically constructive propensity of Ag(CN)<sub>2</sub><sup>−</sup> units to accumulate. This is concluded from the decreasing total energy and increasing binding energy as one proceeds from a monomer to a dimer, and then to a trimer and a pentamer. The formation of potential wells for dimer, trimer, and pentamer units of Ag(CN)<sub>2</sub><sup>−</sup> at relatively short Ag–Ag distances provides further support for the existence of Ag–Ag bonding. The dimer {[H<sub>3</sub>PAgCl]<sub>2</sub>} with staggered conformation was selected for theoretical studies and *ab initio* calculations (MP2, MP2 (CP), LMP2, and LMP2(CP)). The results gave Ag–Ag distances in the range of 2.866–2.921 Å. The Ag–Ag interaction energies are in the range of  $-30.70$  to  $-38.90$  kJ mol<sup>−1</sup>, indicating significant bonding interactions.<sup>90</sup> In some cases when DFT calculations were conducted, it was realized that this approach may not be reliable for van der Waals-like attractions (dispersion forces).<sup>91</sup>

The compound {[1-(benzyl)-3-(*N*-*tert*-butylacetamido)-imidazol-2-ylidene]AgCl}<sub>2</sub>, **57**, is isomorphous and contains dimers in staggered conformation, with a Ag–Ag contact distance of 3.197(12) Å. The bonding in these dimers has been analyzed *via* DFT methods, and the interaction energy is calculated to be 12.8 kcal mol<sup>−1</sup>.<sup>81</sup>

## Other supporting interactions

The pyridyl rings of 4,4'-bpy in [Ag(4,4'-bpy)]<sub>n</sub>[H<sub>2</sub>PO<sub>4</sub>]<sub>n</sub>·[H<sub>3</sub>PO<sub>4</sub>]<sub>n</sub>, **12**, are virtually coplanar with each other, only with smaller twisting angles from 3.6(1)<sup>o</sup> to 7.4(2)<sup>o</sup>.

The sides of adjacent ladders are separated by *ca.* 3.44 Å in **12**, suggesting significant  $\pi$ - $\pi$  stacking interactions. Each pair of  $[\text{Ag}(4,4'\text{-bpy})]_{\infty}$  chains is linked into a 1D molecular ladder *via* ligand-supported Ag–Ag interactions with a separation of 3.286(2) Å. It is to be noted that the Ag–Ag distances are considerably shorter than the face-to-face distances of the intra-ladder pyridyl rings. In a sense, the Ag–Ag distances presented here provide further experimental evidence for the existence of argentophilic attraction without any weak supporting ligands.<sup>47</sup> Face-to-face  $\pi$ - $\pi$  interactions are important non-covalent intermolecular forces in  $d^{10}$  compounds, which may be denoted as “ $\pi$ - $\pi$  stacking supported metallophilic interactions”.

The ophen ligand in the compound  $[\text{Ag}_2(\text{ophen})]_2 \cdot 6\text{H}_2\text{O}$ , **32**, should undergo more significant  $\pi$ - $\pi$  interactions than obpy in the compounds  $[\text{Ag}_2(\text{obpy})]_2 \cdot 4.5\text{H}_2\text{O} \cdot 0.5\text{DMF}$ , **33**, and  $[\text{Ag}_2(\text{obpy})]_3 \cdot 18\text{H}_2\text{O}$ , **34**, due to differences in conjugation size and rigidity, similar to phen *versus* 4,4'-bpy.<sup>70</sup> In the compounds  $\text{Ag}(\text{3-amp})\text{OTf}$ , **40**,  $\text{Ag}_2(2,2'\text{-bpy})_2 \cdot \mu\text{-}(3\text{-amp})(\text{tfa})_2$ , **41**, and  $\text{Ag}_2(2,2'\text{-bpy})_2 \cdot \mu\text{-}(3\text{-amp})(\text{OTf})_2$ , **42**, the Ag–Ag interactions are supported by the interpolymeric  $\pi$ -stacking of 2,2'-bpy rings, and the effect of this interaction is to join would-be isolated polymers into 2D sheets in **40**, 1D chains in **41**, and dimeric units in **42**.<sup>73</sup> In the same category of interactions,  $\text{Ag}_2(5,5'\text{-bm-2,2'-bpy})_2(4\text{-amp})(\text{BF}_4)_2$ , **43**, also shows Ag–Ag interactions, supported by the  $\pi$ -stacking of bipyridyl rings and H-bonding from the amine groups of the 4-amp ligands, resulting in an infinite polymer with a saw-tooth appearance.<sup>74</sup>

$[\text{Ag}(\text{py})_2]^+ \cdot \text{X}^-$  compounds (X =  $\text{ClO}_4$ : **51**,  $\text{BF}_4$ : **52**;  $\text{PF}_6$ : **53**) are perfect examples showing the importance of  $\pi$ - $\pi$  stacking interactions. In **51** and **52**, pairs of  $[\text{Ag}(\text{py})_2]^{2+}$  ions are linked into 1D infinite chains *via* multiple Ag–Ag contacts, supported by offset ‘head-to-head’  $\pi$ - $\pi$  stacking in addition to anion bridging interactions. In the case of **53**, pairs of  $[\text{Ag}(\text{py})_2]^{2+}$  ions are organized into a 3D network *via* a combined set of Ag–F and C(H)–F contacts, and ‘head-to-tail’  $\pi$ - $\pi$  stacking interactions.<sup>77</sup>

## The properties of silver compounds containing ligand-unsupported argentophilic interactions

Metal compounds with ligand-unsupported argentophilic interactions have drawn a lot of interest because of their distinctive properties in the fields of magnetism,<sup>33</sup> cytotoxicity,<sup>75</sup> luminescence,<sup>6–8,17–22,53–55,71,79–81,82–88</sup> gas storage,<sup>8</sup> antimicrobial activity,<sup>8,83</sup> and electrocatalysis,<sup>55,56</sup> and because they can behave as catalytic reagents for ring-opening polymerization reactions.<sup>37</sup> The high cytotoxicity of **46** implies that it is a potential candidate for use in antitumor agents.<sup>75</sup> Luminescence properties have been exhibited by compounds **7–11**, **16**, **36**, **47–48**, **55–60**, **62–63**, **68–73**, **80–82**, **87–88**, **93–95**, and **97–99**; compound **97** also demonstrates a relationship between structure and photoluminescence, and amendable

luminescence effects *via*  $\text{K}^+$  ion doping, which were well investigated *via* density functional theory analysis.<sup>88</sup> Electrochemical and electrocatalytic behavior has been exhibited by compound **98**.<sup>55</sup> Compound **70** is an important candidate for gas storage applications and it also showed good antimicrobial activity (36–63  $\mu\text{g mL}^{-1}$ ) against the studied microorganisms.<sup>8</sup> Compounds **64–67** show photodimerization in head-to-head fashion in the solid state.<sup>5</sup> In the case of compound **99**, the electrochemical behavior of a polymer-modified carbon paste electrode and its use in the electrocatalytic reduction of nitrite were investigated.<sup>56</sup> Compounds **87** and **88** were studied for the ring-opening polymerization of  $\epsilon$ -caprolactone, where  $\epsilon$ -polycaprolactone polymers were obtained with average molecular weights and good polydispersity indexes.<sup>37</sup>

## Conclusions

In this review, the role of ligand-unsupported argentophilic interactions in the design and synthesis of coordination polymers has been summarized. The indagation about argentophilic interactions in crystal engineering is in the middle of a period of inundation with respect to experimental data, being accrued in relation to the production of new supramolecular compounds involving various interactions (such as  $\pi$ - $\pi$  stacking, H-bonding, van der Waals forces, *etc.*). A major goal of these studies is to establish the correlations between supramolecular interactions and the structural characteristics of these compounds.

Widespread interest has centered on attractive interactions between formally closed-shell metal centers; these relatively weak Ag–Ag interactions are defined as argentophilic. In this review, using knowledge relating to  $\text{Ag}^+$ -based coordination polymers, a preliminary attempt at the analysis of this kind of interaction has been done. From earlier literature reports based on argentophilic interactions, most of them are ligand-supported, and merely a handful are divulged to be ligand-unsupported examples. Ligand-unsupported closed-shell Ag–Ag attractive interactions are established to be prospective sources for the establishment of enthralling structures.

There are numerous reports of silver-metal and mixed-metal compounds in which silver atoms connect with other silver atoms in a variety of geometries leading to the construction of discrete dimers or oligomers, 1D chains or rings, or 3D polymeric structures, with the help of ligand-unsupported argentophilic interactions. A three-fold interpenetrating net derived from the cross-linking of chains, 2–3–4-connected self-penetrating species, and a class of 1-D to 3-D supramolecular architectures, all assembled *via* the assistance of ligand-unsupported Ag–Ag interactions, have been successfully reported by Yaghi's group, Chen's research lab, and Guo and coworkers, respectively.

Many of these interactions have characteristics (Ag–Ag bond lengths, Ag–Ag–Ag angles, low binding energies, *etc.*) similar to those of ligand-supported argentophilic Ag–Ag contacts. However, mixed-metal (between two metal ions other than  $\text{Ag}^+$ )

ions) metallophilic bonding has not been included here, even though it certainly is one of the most interesting, intriguing, and quickly emerging areas in the field of metal–metal bonding interactions.

The existence of ligand-unsupported Ag–Ag aggregating interactions in compounds has been confirmed *via* various spectroscopic techniques, *e.g.*, IR, Raman, and UV/vis spectral studies. These evaluations have also been authenticated by the outcomes of density functional theory (DFT) calculations and quantum chemical calculations. From these studies, ligand-unsupported argentophilic interactions can be considered as weak forces, and these are closest in energy value to H-bonding.

It is worth mentioning that the examples of metal compounds with ligand-unsupported argentophilic interactions are few, and this has led many researchers in solid-state chemistry to postulate the existence of “weak Ag–Ag interactions” between silver centers. This is not only true for simple halides and chalcogenides, but also for carboxylate-, phosphonate-, and sulfonate-based ligands and a few other systems involving polyoxometalates.

## Conflicts of interest

There are no conflicts to declare.

## Acknowledgements

AKJ is grateful to DST, India for a fellowship under the scheme Women Scientist A. This work was supported by the Department of Science and Technology, India, and Technion Israel Institute of Technology, Haifa, Israel for Post-Doctoral fellowships.

## Notes and references

- 1 G. W. Eastland, M. A. Mazid, D. R. Russell and M. C. R. Symons, Silver(i) Imidazole Perchlorate. An  $(\text{Ag}^+)_6$  Cluster and its Radiolytically Produced One-electron Adduct studied by X-Ray Diffraction and Electron Spin Resonance Spectroscopy, *J. Chem. Soc., Dalton Trans.*, 1980, 1682–1687.
- 2 O. M. Yaghi and H. Li, T-Shaped, Molecular Building Units in the Porous Structure of  $\text{Ag}(4,4'\text{-bpy})\text{-NO}_3$ , *J. Am. Chem. Soc.*, 1996, **118**, 295–296.
- 3 M. L. Tong, Y. M. Wu, J. Ru, X. M. Chen, H. C. Chang and S. Kitagawa, Pseudo-Polyrotaxane and  $\beta$ -Sheet Layer-Based Three-Dimensional Coordination Polymers Constructed with Silver Salts and Flexible Pyridyl-Type Ligands, *Inorg. Chem.*, 2002, **41**, 4846–4848.
- 4 X. C. Huang, J. P. Zhang and X. M. Chen, One-Dimensional Supramolecular Isomerism of Copper(i) and Silver(i) Imidazolates Based on the Ligand Orientations, *Cryst. Growth Des.*, 2006, **6**, 1194–1198.
- 5 G. K. Kole, G. K. Tan and J. J. Vittal, Photoreactivity of Ag(i) Complexes and Coordination Polymers of Pyridyl Acrylic Acids, *Cryst. Growth Des.*, 2012, **12**, 326–332.
- 6 Y. Zhao, P. Zhang, B. Li, X. Meng and T. Zhang, Photoreactivity of Ag(i) Complexes and Coordination Polymers of Pyridyl Acrylic Acids, *Inorg. Chem.*, 2011, **50**, 9097–9105.
- 7 D. Sun, N. Zhang, Q. J. Xu, Z. H. Wei, R. B. Huang and L. S. Zheng, Assembly of 1D, 2D and 3D silver(i) coordination polymers with nitrilotriacetate and 2-aminopyrimidyl mixed ligands, *Inorg. Chim. Acta*, 2011, **368**, 67–73.
- 8 O. Z. Yeşilel, G. Günay, C. Darcan, M. S. Soylu, S. Keskin and S. W. Ng, An unusual 3D metal–organic framework,  $[\text{Ag}(\mu_4\text{-pzdc})_2(\mu\text{-en})_2]\text{H}_2\text{O}_n$ : C–H…Ag, N–H…Ag and (O–H)…Ag interactions and an unprecedented coordination mode for pyrazine-2,3-dicarboxylate, *CrystEngComm*, 2012, **14**, 2817–2825.
- 9 J. J. Henkelis, S. A. Barnett, L. P. Harding and M. J. Hardie, Coordination Polymers Utilizing N-Oxide Functionalized Host Ligands, *Inorg. Chem.*, 2012, **51**, 10657–10674.
- 10 N. Masciocchi, M. Moret, P. Cairati, A. Sironi, G. A. Ardizzoia and G. L. Monica, The Multiphase Nature of the Cu(pz) and Ag(pz) (Hpz = Pyrazole) Systems: Selective Syntheses and *ab initio*, X-ray Powder Diffraction Structural Characterization of Copper(i) and Silver(i) Pyrazolates, *J. Am. Chem. Soc.*, 1994, **116**, 7668–7676.
- 11 A. D. Burrows, M. F. Mahon and M. T. Palmer, Synthesis and structure of a co-ordination polymer based on silver(i) triangles linked by isonicotinate anions, *J. Chem. Soc., Dalton Trans.*, 1998, 1941–1942.
- 12 C. M. Che, M. C. Tse, M. C. W. Chan, K. K. Cheung, D. L. Phillips and K. H. Leung, Spectroscopic Evidence for Argentophilicity in Structurally Characterized Luminescent Binuclear Silver(i) Complexes, *J. Am. Chem. Soc.*, 2000, **122**, 2464–2468.
- 13 K. Singh, J. R. Long and P. Stavropoulos, Ligand-Unsupported Metal-Metal (M = Cu, Ag) Interactions between Closed-Shell  $d^{10}$  Trinuclear Systems, *J. Am. Chem. Soc.*, 1997, **119**, 2942–2943.
- 14 M. A. Omary, T. R. Webb, Z. Assefa, G. E. Shankle and H. H. Patterson, Crystal Structure, Electronic Structure, and, Temperature-Dependent Raman Spectra of  $\text{Ti}[\text{Ag}(\text{CN})_2]$ : Evidence for Ligand-Unsupported Argentophilic Interactions, *Inorg. Chem.*, 1998, **37**, 1380–1386.
- 15 A. Bondi, van der Waals Volumes and Radii, *J. Phys. Chem.*, 1964, **68**, 441–451.
- 16 M. Veronelli, N. Kindermann, S. Dechert, S. Meyer and F. Meyer, Crowning of Coinage Metal Pyrazolates: Double-Decker Homo- and Heteronuclear Complexes with Synergic Emissive Properties, *Inorg. Chem.*, 2014, **53**, 2333–2341.
- 17 D. Sun, F. J. Liu, R. B. Huang and L. S. Zheng, Structural diversity of Ag/3-nitrophthalate coordination polymers controlled by solvent and induction agent, *CrystEngComm*, 2013, **15**, 1185–1193.
- 18 D. Sun, R. Cao, J. Weng, M. Hong and Y. Liang, A novel luminescent 3D polymer containing silver chains formed

by ligand unsupported Ag–Ag interactions and organic spacers, *J. Chem. Soc., Dalton Trans.*, 2002, 291–292.

19 Z. Liu, P. Liu, Y. Chen, J. Wang and M. Huang, Synthesis, structures, and photoluminescent properties of two ligand unsupported silver(i) coordination polymers from isonicotinate anions, *New J. Chem.*, 2005, **29**, 474–478.

20 L. Han, D. Yuan, B. Wu, C. Liu and M. Hong, Syntheses, structures and properties of three novel coordination polymers with a flexible asymmetrical bridging ligand, *Inorg. Chim. Acta*, 2006, **359**, 2232–2240.

21 C. J. Wang, Y. Y. Wang, H. Wang, G. P. Yang, G. L. Wen, M. Zhang and Q. Z. Shi, A novel silver(i) coordination polymer based on mixed ligands bpp and 2,2'-bipyridine-4,4'-dicarboxylate, *Inorg. Chem. Commun.*, 2008, **11**, 843–846.

22 F. J. Liu, D. Sun, H. J. Hao, R. B. Huang and L. S. Zheng, A novel photoluminescent silver(i) wire supported by 4-tert-butylbenzoate and ligand-unsupported Ag···Ag interactions, *Inorg. Chem. Commun.*, 2012, **15**, 136–139.

23 F. Robinson and M. J. Zaworotko, Triple interpenetration in  $[\text{Ag}(4,4'\text{-bipyridine})]\text{[NO}_3]$ , a cationic polymer with a three-dimensional motif generated by self-assembly of 'T-shaped' building blocks, *J. Chem. Soc., Chem. Commun.*, 1995, 2413–2414.

24 R. Villanneau, A. Proust, F. Robert and P. Gouzerh, Synthesis and characterization of  $[\text{NBu}_4]_4[\text{Ag}_2\{\text{Mo}_5\text{O}_{13}(\text{OMe})_4(\text{NO})\}_2]$ , a novel polyoxomolybdate complex with a short  $\text{Ag}^{\text{I}}\cdots\text{Ag}^{\text{I}}$  distance, *Chem. Commun.*, 1998, 1491–1492.

25 M. L. Tong, X. M. Chen, B. H. Ye and L. N. Ji, Self-Assembled Three-Dimensional Coordination Polymers with Unusual Ligand-Unsupported Ag···Ag Bonds: Syntheses, Structures, and Luminescent Properties, *Angew. Chem., Int. Ed.*, 1999, **38**, 2237–2240.

26 L. Pan, E. B. Woodlock, X. Wang, K. C. Lamb and A. L. Rheingold, Novel silver(i)-organic coordination polymers: conversion of extended structures in the solid state as driven by argentophilic interactions, *Chem. Commun.*, 2001, 1762–1763.

27 O. S. Jung, Y. J. Kim, Y. A. Lee, S. W. Kang and S. N. Choi, Tunable Transannular Silver–Silver Interaction in Molecular Rectangles, *Cryst. Growth Des.*, 2004, **4**, 23–24.

28 L. Dobrzańska, H. G. Raubenheimer and L. J. Barbour, Borromean sheets assembled by self-supporting argentophilic interactions, *Chem. Commun.*, 2005, 5050–5052.

29 G. Mezei, C. M. Zaleski and V. L. Pecoraro, Structural and Functional Evolution of Metallacrowns, *Chem. Rev.*, 2007, **107**, 4933–5003.

30 R. P. Feazell, C. E. Carson and K. K. Klausmeyer, Silver(i) 3-Aminomethylpyridine Complexes, Part 1: Effect of Ligand Ratio,  $\pi$ -Stacking, and Temperature with a Noninteracting Anion, *Inorg. Chem.*, 2006, **45**, 2627–2634.

31 J. W. Lee, E. A. Kim, Y. J. Kim, Y. A. Lee, Y. Pak and O. S. Jung, Relationship between the Ratio of Ligand to Metal and the Coordinating Ability of Anions. Synthesis and Structural Properties of  $\text{AgX}$ -Bearing Bis(4-pyridyl)dimethylsilane ( $\text{X}^- = \text{NO}_2^-$ ,  $\text{NO}_3^-$ ,  $\text{CF}_3\text{SO}_3^-$ , and  $\text{PF}_6^-$ ), *Inorg. Chem.*, 2005, **44**, 3151–3155.

32 M. L. Tong, X. M. Chen and B. H. Ye, Helical Silver(i)-2,4'-Bipyridine Chains Organized into 2-D Networks by Metal-Counterion or Metal–Metal Bonding. Structures of  $[\text{Ag}(2,4'\text{-bipyridine})]\text{X}$  ( $\text{X}^- = \text{NO}_3^-$  or  $\text{ClO}_4^-$ ), *Inorg. Chem.*, 1998, **37**, 5278–5281.

33 C. J. Shorrock, B. Y. Xue, P. B. Kim, R. J. Batchelor, B. O. Patrick and D. B. Leznoff, Heterobimetallic Coordination Polymers Incorporating  $[\text{M}(\text{CN})_2]^-$  ( $\text{M} = \text{Cu}$ ,  $\text{Ag}$ ) and  $[\text{Ag}_2(\text{CN})_3]^-$  Units: Increasing Structural Dimensionality via M–M' and M···NC Interactions, *Inorg. Chem.*, 2002, **41**, 6743–6753.

34 M. Arıcı, O. Z. Yeşilel, Y. Yeşilöz and O. Şahin, One- and three-dimensional silver(i)-5-sulfosalicylate coordination polymers having ligand-supported and unsupported argentophilic interactions, *J. Solid State Chem.*, 2014, **220**, 70–78.

35 V. Moodley, L. Mthethwa, M. N. Pillay, B. Omondi and W. E. V. Zyl, The silver(i) coordination polymer  $[\text{AgO}_2\text{PPh}_2]_n$  and unsupported Ag···Ag interactions derived from amino-phosphinate and phosphinic acid, *Polyhedron*, 2015, **99**, 87–95.

36 Q. Guo and U. Englert, An Acetylacetone or a Pyrazole? Both! 3-(3,5-Dimethyl-pyrazol-4-yl)pentane-2,4-dione as a Ditopic Ligand, *Cryst. Growth Des.*, 2016, **16**, 5127–5135.

37 E. M. Njogu, B. Omondi and V. O. Nyamori, Silver(i)-pyridinyl Schiff base complexes: Synthesis, structural characterization and reactivity in ring-opening polymerization of  $\epsilon$ -caprolactone, *Inorg. Chim. Acta*, 2017, **457**, 160–170.

38 O. Kristiansson, Unusual Manifestation of Closed-Shell Interactions in Silver(i) Complexes: Crystal Structure of Catena-bis(4-aminobenzoato)disilver(i) Acetone Solvate with Ligand Unsupported Chains of Repeated Rhombohedral  $\text{Ag}_4$  Units, *Inorg. Chem.*, 2001, **40**, 5058–5059.

39 M. P. Carranza, B. R. Manzano, F. A. Jalón, A. M. Rodríguez, L. Santosc and M. Moreno, Experimental and theoretical evidence of unsupported Ag–Ag interactions in complexes with triazine-based ligands. Subtle effects of the symmetry of the triazine substituents, *New J. Chem.*, 2013, **37**, 3183–3194.

40 T. C. W. Mak, X.-L. Zhao, Q.-M. Wang and G.-C. Guo, Synthesis and structural characterization of silver(i) double and multiple salts containing the acetylenediide dianion, *Coord. Chem. Rev.*, 2007, **251**, 2311–2333.

41 O. Fuhr, S. Dehnen and D. Fenske, Chalcogenide clusters of copper and silver from silylated chalcogenide sources, *Chem. Soc. Rev.*, 2013, **42**, 1871–1906.

42 Q. M. Wang, Y.-M. Lin and K.-G. Liu, Role of Anions Associated with the Formation and Properties of Silver Clusters, *Acc. Chem. Res.*, 2015, **48**, 1570–1579.

43 Y.-P. Xie and T. C. W. Mak, Synthetic and Structural Studies on High-Nuclearity Silver Ethynide Cluster Systems, *J. Cluster Sci.*, 2014, **25**, 189–204.

44 Y.-P. Xie, J.-L. Jin, X. Lu and T. C. W. Mak, High-Nuclearity Silver Thiolate Clusters Constructed with Phosphonates, *Angew. Chem., Int. Ed.*, 2015, **54**, 15176–15180.

45 Y.-P. Xie, J.-L. Jin, G.-X. Duan, X. Lu and T. C. W. Mak, High-nuclearity silver(I) chalcogenide clusters: A novel class of supramolecular assembly, *Coord. Chem. Rev.*, 2017, **331**, 54–72.

46 X. Liu, G. C. Guo, M. L. Fu, X. H. Liu, M. S. Wang and J. S. Huang, Three Novel Silver Complexes with Ligand-Unsupported Argentophilic Interactions and Their Luminescent Properties, *Inorg. Chem.*, 2006, **45**, 3679–3685.

47 M. L. Tong, X. M. Chen and S. W. Ng, Synthesis and crystal structures of two infinite molecular ladders  $\text{Ag}(4,4'\text{-bpy})\text{X}$  ( $\text{X} = \text{MeCO}_2\cdot 3\text{H}_2\text{O}$  or  $\text{H}_2\text{PO}_4\cdot \text{H}_3\text{PO}_4$ ): function of hydrogen-bonding interaction, *Inorg. Chem. Commun.*, 2000, **3**, 436–441.

48 Q. M. Wang and T. C. W. Mak, Argentophilicity and Solvent-Induced Structural Diversity in Double Salts of Silver Acetylide with Silver Perfluoroalkyl Carboxylates, *J. Am. Chem. Soc.*, 2001, **123**, 7594–7600.

49 X. Z. Song, C. Qin, W. Guan, S. Y. Song and H. J. Zhang, An unusual three-dimensional self-penetrating network derived from cross-linking of two-fold interpenetrating nets via ligand-unsupported Ag–Ag bonds: synthesis, structure, luminescence, and theoretical study, *New J. Chem.*, 2012, **36**, 877–882.

50 J. Y. Wu, Y. C. Liu and T. C. Chao, From 1D Helix to 0D Loop: Nitrite Anion Induced Structural Transformation Associated with Unexpected *N*-Nitrosation of Amine Ligand, *Inorg. Chem.*, 2014, **53**, 5581–5588.

51 T. K. Maji, S. Konar, G. Mostafa, E. Zangrandi, T. H. Lu and N. R. Chaudhuri, Self-assembly of new three-dimensional molecular architectures of Cd(II) and Ag(I)–Na(I) using croconate as a building block, *Dalton Trans.*, 2003, 171–175.

52 V. Niel, A. L. Thompson, A. E. Goeta, C. Enachescu, A. Hauser, A. Galet, M. C. MuÇoz and J. A. Real, Thermal- and Photoinduced Spin-State Switching in an Unprecedented Three-Dimensional Bimetallic Coordination Polymer, *Chem. – Eur. J.*, 2005, **11**, 2047–2060.

53 X. D. Zheng, L. Jiang, X. L. Feng and T. B. Lu, The Supramolecular Isomerism Based on Argentophilic Interactions: The Construction of Helical Chains with Defined Right-Handed and Left-Handed Helicity, *Inorg. Chem.*, 2008, **47**, 10858–10865.

54 H. Zhang, Y. Zhang, C. Wang, L. Cai, Y. Xie and G. Xue, Synthesis, crystal structure, and photoluminescent property of a novel heterobimetallic  $\text{Zn}(\text{II})\text{-Ag}(\text{I})$  cyano-bridged coordination polymer incorporating a pentameric unit  $[\text{Ag}(\text{CN})_2]_5$  assembled by argentophilic interaction, *Inorg. Chem. Commun.*, 2006, **9**, 555–558.

55 Z. Shi, J. Peng, Y. Li, Z. Zhang, X. Yu, K. Alimaje and X. Wang, Assembly of multinuclear Ag complexes and Keggin polyoxometalates adjusted by organic ligands: syntheses, structures and luminescence, *CrystEngComm*, 2013, **15**, 7583–7588.

56 L. Dai, W. You, E. Wang, S. Wu, Z. Su, Q. Du, Y. Zhao and Y. Fang, Two Novel One-Dimensional  $\alpha$ -Keggin-Based Coordination Polymers with Argentophilic  $\{\text{Ag}_3\}^{3+}/\{\text{Ag}_4\}^{4+}$  Clusters, *Cryst. Growth Des.*, 2009, **9**, 2110–2116.

57 S. P. Yang, H. L. Zhu, X. H. Yin, X. M. Chen and L. N. Ji, Polymeric and tetranuclear silver(I) chains encapsulated by a scorpion-like ligand. Synthesis and structures of  $[\text{Ag}_2(\text{tren}(\text{mim})_3)]_n(\text{NO}_3)_{2n}\cdot n\text{H}_2\text{O}$  and  $[\text{Ag}_4(\text{tren}(\text{mim})_3)_2]\cdot (\text{CF}_3\text{SO}_3)_4\cdot 2\text{H}_2\text{O}$  ( $\text{tren}(\text{mim})_3 = \text{tris}\{2\text{-[2-(1-methyl imidazolyl]-methyl-iminoethyl}]\text{amine}$ ), *Polyhedron*, 2000, **19**, 2237–2242.

58 A. F. Wells, *Structural Inorganic Chemistry*, Oxford [Oxfordshire], Clarendon Press Oxford University Press, New York, 1984, ©1975.

59 M. Jansen, Homoatomic  $d^{10}\text{-}d^{10}$  Interactions: Their Effects on Structure and Chemical and Physical Properties, *Angew. Chem., Int. Ed. Engl.*, 1987, **26**, 1098–1110.

60 P. Pykkö, J. Li and N. Runeberg, Predicted ligand dependence of the  $\text{Au}(\text{I})\cdots\text{Au}(\text{I})$  attraction in  $(\text{X}\text{AuPH}_3)_2$ , *Chem. Phys. Lett.*, 1994, **218**, 133–138.

61 P. Pykkö, Strong Closed-Shell Interactions in Inorganic Chemistry, *Chem. Rev.*, 1997, **97**, 597–636.

62 P. Pykkö, Relativistic Effects in Structural Chemistry, *Chem. Rev.*, 1988, **88**, 563–594.

63 P. Pykkö, N. Runeberg and F. Mendizabal, Theory of the  $d^{10}\text{-}d^{10}$  Closed-Shell Attraction: Dimers Near Equilibrium, *Chem. – Cur. J.*, 1997, **3**, 1451–1457.

64 W. Meng and F. Kraus, Crystal Structures of  $\text{Ag}_2\text{ZrF}_6\cdot 8\text{NH}_3$  and  $\text{Ag}_2\text{HfF}_6\cdot 8\text{NH}_3$  and Their Synthesis by the “Reactive Fluoride Route” in Liquid Ammonia, *Eur. J. Inorg. Chem.*, 2008, 3068–3074.

65 B. L. Fei, W. Y. Sun, T. Okamura, W. X. Tanga and N. Ueyama, Synthesis and crystal structure of a luminescent infinite 2D brick-wall network with two- and three-coordinate silver(I) atoms and ligand-unsupported silver–silver interactions, *New J. Chem.*, 2001, **25**, 210–212.

66 N. Masciocchi, M. Moret, P. Cairati, A. Sironi, G. A. Ardizioia and G. La Monica, Powder route to crystal structures: X-ray powder diffraction determination of polymeric silver imidazolate, *J. Chem. Soc., Dalton Trans.*, 1995, 1671–1675.

67 P. Lin, R. A. Henderson, R. W. Harrington, W. Clegg, C. D. Wu and X. T. Wu, New 1- and 2-Dimensional Polymeric Structures of Cyanopyridine Complexes of  $\text{Ag}^{\text{I}}$  and  $\text{Cu}^{\text{I}}$ , *Inorg. Chem.*, 2004, **43**, 181–188.

68 X. Y. Qiu, J. L. Ma, L. Sun, S. Yang and H. L. Zhu, Synthesis and Characterization of Diaquatetra(3,5-dinitrobenzoato) tetrasilver(I) and Polymeric (Ethylenediaminesilver(I) Di (3,5-dinitrobenzoato)silver(I)Dihydrate), *Synth. React. Inorg., Met.-Org., Nano-Met. Chem.*, 2005, **35**, 189–192.

69 A. A. Mohamed, L. M. Pérez and J. P. Fackler Jr., Unsupported intermolecular argentophilic interaction in the dimer of trinuclear silver(I) 3,5-diphenylpyrazolates, *Inorg. Chim. Acta*, 2005, **358**, 1657–1662.

70 J. P. Zhang, Y. B. Wang, X. C. Huang, Y. Y. Lin and X. M. Chen, Metallophilicity versus p–p Interactions: Ligand-Unsupported Argentophilicity/Cuprophilicity in Oligomers-of-Dimers  $[\text{M}_2\text{L}_2]_n$ , ( $\text{M} = \text{Cu}^{\text{I}}$  or  $\text{Ag}^{\text{I}}$ ,  $\text{L} = \text{tridentate ligand}$ ), *Chem. – Eur. J.*, 2005, **11**, 552–561.

71 R. P. Feazell, C. E. Carson and K. K. Klausmeyer, Variability in the Structures of Luminescent [2-(Aminomethyl) pyridine]silver(i) Complexes: Effect of Ligand Ratio, Anion, Hydrogen Bonding, and  $\pi$ -Stacking, *Eur. J. Inorg. Chem.*, 2005, 3287–3297.

72 I. Kalf, M. Braun, Y. Wang and U. Englert, Homo- and heterochiral coordination polymers of silver with diaminocyclohexane as bridging ligand: The effect of chirality on argentophilic interactions, *CrystEngComm*, 2006, **8**, 916–922.

73 R. P. Feazell, C. E. Carson and K. K. Klausmeyer, Silver(i) 3-Aminomethylpyridine Complexes, Part 2: Effect of Ligand Ratio, Hydrogen Bonding, and  $\pi$ -Stacking with an Interacting Anion, *Inorg. Chem.*, 2006, **45**, 2635–2643.

74 R. P. Feazell, C. E. Carson and K. K. Klausmeyer, Variability in the Structures of [4-(Aminomethyl)pyridine]silver(i) Complexes through Effects of Ligand Ratio, Anion, Hydrogen Bonding, and  $\pi$ -Stacking, *Inorg. Chem.*, 2006, **45**, 935–944.

75 H. L. Zhua, X. M. Zhangb, G. F. Liua and D. Q. Wang, Syntheses, Crystal Structures, and Cytotoxicity Evaluation of two Chain-like and Diamond-like Silver(i) Complexes, *Z. Anorg. Allg. Chem.*, 2003, **629**, 1059–1062.

76 Y. F. Li, Z. H. Pan and T. J. Lou, catena-Poly[[disilver(i)(Ag–Ag)-bis- $\mu$ -1,1'-(butane-1,4-diyl)diimidazole- $\kappa^2$ N<sup>3</sup>:N<sup>3</sup>']bis-(perchlorate)]: a double helix stabilized by ligand-unsupported argentophilic interactions, *Acta Crystallogr., Sect. C: Cryst. Struct. Commun.*, 2007, **63**, m516–m518.

77 C. Y. Chen, J. Y. Zeng and H. M. Lee, Argentophilic interaction and anionic control of supramolecular structures in simple silver pyridine complexes, *Inorg. Chim. Acta*, 2007, **360**, 21–30.

78 Y. Sun, Z. Wang, H. Zhang, Y. Cao, S. Zhang, Y. Chen, C. Huang and X. Yu, Self-assembly of three novel mixed-ligand coordination polymers: Formation of 2-D grids, 1-D chains and ladders and crystal band structure, *Inorg. Chim. Acta*, 2007, **360**, 2565–2572.

79 Y. L. Wang, Q. Y. Liu and L. Xu, Two novel luminescent silver(i) coordination polymers containing octanuclear silver cluster units or ligand unsupported Ag–Ag interactions constructed from 5-sulfoisophthalic acid (H<sub>3</sub>SIP) and organic amine, *CrystEngComm*, 2008, **10**, 1667–1673.

80 Y. Zhou, W. Chen and D. Wang, Mononuclear, dinuclear, hexanuclear, and one-dimensional polymeric silver complexes having ligand-supported and unsupported argentophilic interactions stabilized by pincer-like 2,6-bis(5-pyrazolyl)pyridine ligands, *Dalton Trans.*, 2008, 1444–1453.

81 L. Ray, M. M. Shaikh and P. Ghosh, Shorter Argentophilic Interaction than Auophilic Interaction in a Pair of Dimeric  $\{(NHC)MCl\}_2$  (M = Ag, Au) Complexes Supported over a N/O-Functionalized N-Heterocyclic Carbene (NHC) Ligand, *Inorg. Chem.*, 2008, **47**, 230–240.

82 P. X. Yin, J. Zhang, Z. J. Li, Y. Y. Qin, J. K. Cheng, L. Zhang, Q. P. Lin and Y. G. Yao, Supramolecular Isomerism and Various Chain/Layer Substructures in Silver(i) Compounds: Syntheses, Structures, and Luminescent Properties, *Cryst. Growth Des.*, 2009, **9**, 4884–4896.

83 Y. Wang and U. Englert, Homo- and heterochiral coordination polymers of silver with diaminocyclohexane as bridging ligand: Trends in alkylbenzoates, *Inorg. Chim. Acta*, 2010, **363**, 2539–2545.

84 D. Sun, Y. H. Li, H. J. Hao, F. J. Liu, Y. Zhao, R. B. Huang and L. S. Zheng, Syntheses, structures and photoluminescent properties of a series of Ag(i) coordination architectures based on 2,4-diamino-6-methyl-1,3,5-triazine and dicarboxylates: from a 0D discrete molecule to a 3D infinite network, *CrystEngComm*, 2011, **13**, 6431–6441.

85 A. Vellé, A. Cebollada, M. Iglesias and P. J. S. Miguel, Argentophilicity as Essential Driving Force for a Dynamic Cation–Cation Host–Guest System: [Ag(acetonitrile)<sub>2</sub>]<sup>+</sup>C[Ag<sub>2</sub>(bis-NHC)<sub>2</sub>]<sup>2+</sup> (NHC=N-Heterocyclic Carbene), *Inorg. Chem.*, 2014, **53**, 10654–10659.

86 X. Xi, Y. Liu and Y. Cui, Homochiral Silver-Based Coordination Polymers Exhibiting Temperature-Dependent Photoluminescence Behavior, *Inorg. Chem.*, 2014, **53**, 2352–2354.

87 J. Černák, J. Chomič and W. Massa, Cu<sub>2</sub>(dien)<sub>2</sub>Ag<sub>5</sub>(CN)<sub>9</sub> containing the one-dimensional polymeric cation [Cu(dien)Ag(CN)<sub>2</sub>]<sub>n</sub><sup>n+</sup> and the unusual [Ag<sub>2</sub>(CN)<sub>3</sub>]<sup>–</sup> anion (dien is diethylene-triamine), *Acta Crystallogr., Sect. C: Cryst. Struct. Commun.*, 2002, **58**, m490–m493.

88 X. Liu, L. Li, Y. Z. Yang and K. L. Huang, Doping potassium ions in silver cyanide complexes for green luminescence, *Dalton Trans.*, 2014, **43**, 4086–4092.

89 P. D. Harvey, Reparameterized Herschbach-Laurie empirical relationships between metal–metal distances and force constants applied to homonuclear bi- and polynuclear complexes (M = Cr, Mo, Rh, Pd, Ag, W, Re, Ir, Pt, Au, Hg), *Coord. Chem. Rev.*, 1996, **153**, 175–201.

90 L. Magnko, M. Schweizer, G. Rauhut, M. Schuetz, H. Stoll and H. J. Werner, A comparison of metallophilic attraction in (X–M–PH<sub>3</sub>)<sub>2</sub> (M = Cu, Ag, Au; X = H, Cl), *Phys. Chem. Chem. Phys.*, 2002, **4**, 1006–1013.

91 E. O'Grady and N. Kaltsosyannis, Does metallophilicity increase or decrease down group 11? Computational investigations of [Cl–M–PH<sub>3</sub>]<sub>2</sub> (M = Cu, Ag, Au, [111]), *Phys. Chem. Chem. Phys.*, 2004, **6**, 680–687.